MOUNTAIN-PLAINS CONSORTIUM

MPC 17-336 | F. Ting, R. Larsen, and R. Rossell

Analysis of Compound Channel Flow with Two-Dimensional Models

MOUNTAIN-PLAINS CONSORTIUM REGION 8

A University Transportation Center sponsored by the U.S. Department of Transportation serving the Mountain-Plains Region. Consortium members:

Colorado State University
North Dakota State University
South Dakota State University
University of Colorado Denver
University of Denver
University of Utah
Utah State University
University of Wyoming

Analysis of Compound Channel Flow with Two-Dimensional Models

Francis C. K. Ting
Ryan J. Larsen
Ryan P. Rossell

Department of Civil and Environmental Engineering
South Dakota State University
Brookings, South Dakota

October 2017

Acknowledgements

Funding for the work presented in this report was provided by the United States Department of Transportation to the Mountain-Plains Consortium (MPC). Matching funds were provided by the South Dakota Department of Transportation (SDDOT). We would like to acknowledge the technical support provided by SDDOT and the South Dakota District of the United States Geological Survey (USGS). We would like to specially thank Ryan Thompson at USGS for conducting the topography and bathymetry survey at the bridge sites; Dan Vockrodt at SDDOT for conducting the subsurface exploration; Mary O'Neill at South Dakota State University (SDSU) for her help with geographical information systems (GIS) data processing; and Allen Jones at SDSU for his assistance with soil analysis and classification. LiDAR data for the James River at the Highway 13 bridges were provided by Paul Boyd with the United States Army Corps of Engineers (USACE) Omaha District. David Mueller with the USGS has assisted with retrieving achieved data from the National Bridge Scour Database. Their assistance is greatly appreciated.

Disclaimer

ABSTRACT

The South Dakota Department of Transportation (SDDOT) currently has a Finite-Element Surface-Water Modeling System for Two-Dimensional Flow (FESWMS-2DH) and Research Management Associates 2 (RMA2) Both programs have the capability to model two-dimensional (2D) flow around structures. The department must identify settings in which a 2D model would be beneficial, and to determine what degree of effort needs to be invested in data collection to produce an effective model. Once these factors are understood, site-specific 2D models can be utilized to properly analyze structures subject to compound channel flow and to design the structure to minimize damage caused by scour. The research began with a literature review and a survey of current practices used by other state DOTs. The SD 13 Bridge over the Big Sioux River near Flandreau and the SD 37 bridges over the James River near Mitchell were selected to conduct a 2D flow analysis. Two-dimensional flow models were created for each bridge site and validated using field measurements. A sensitivity analysis was conducted to determine the critical input parameters to develop an effective model. Modeling results were used to investigate the site conditions producing 2D flow effects and to predict pier and contraction scour. This report recommends that SDDOT does the following: (1) develops a formal decision-making process for selecting hydraulic models, (2) coordinates with other agencies to collect LiDAR data in South Dakota, (3) conducts a department needs assessment to establish a continuing education program for SDDOT engineers, (4) conducts additional case studies to develop improved design guidelines, (5) measures soil erodibility when evaluating scour at bridges, (6) initiates a research project to collect flow and scour data at selected bridge sites during high flow events, and (7) supports research to develop long-term hydrograph for use in scour predictions in cohesive soils.

TABLE OF CONTENTS

LIST OF FIGURES

LIST OF TABLES

ACRONYMS AND ABBREVIATIONS

ADCIRC	Coastal Circulation and Storm Surge Model
DENR	Department of Environmental and Natural Resources
DOT	Department of Transportation
FESWMS	Finite-Element Surface-Water Modeling System
FEMA	Federal Emergency Management Agency
FHWA	Federal Highway Administration
HEC-RAS	Hydrologic Engineering Centers River Analysis System
HEC-8	Culvert Hydraulic Analysis Program
LiDAR	Light Detection and Ranging
NHI	National Highway Institute
RMA2	Resource Management Associates: 2
SDDOT	South Dakota Department of Transportation
SRH-2D	Sedimentation and River Hydraulics –Two-Dimensional Model
SMS	Surface-Water Modeling System
TUFLOW	Two-Dimensional Unsteady Flow
USGS	United States Geological Survey

EXECUTIVE SUMMARY

PROBLEM DESCRIPTION

The South Dakota Department of Transportation (SDDOT) research study SD2006-08 recommended evaluating two-dimensional (2D) flow effects at bridges. Study SD2006-08 demonstrated that a one-dimensional (1D) river model such as the Hydrologic Engineering Centers River Analysis System (HEC-RAS) may not predict velocity distributions at bridge crossings accurately in some channel configurations. Compound channel flow can cause HEC-RAS to under-predict measured approach flow velocity because the 1D model distributes flow based on conveyance. This could result in under-estimation of scour depth when the Scour Rate in Cohesive Soils (SRICOS) method is used to predict scour.

Compound channel flow can cause sizeable differences in flow magnitude and direction in the main channel and floodplain. Two-dimensional analysis defines the magnitude and direction of flow along with detailed geometry of the water surface profile around a structure. The need to predict 2D flow effects at bridges becomes even more important when predicting contraction scour where the results may be very sensitive to how the width of the approach flow is defined. Another particular advantage of 2D models is their capability to describe the contraction of floodplain flow into a channel and through a bridge opening.

SDDOT has structures that have compound channel flow. At some locations it occurs during normal flow events, while at others it occurs only during flooding. Structures added to minimize bank erosion or even scour around structures sometimes simply move the effect to another area or increase the erosion effect, rather than mitigate the erosion.

The department currently has a Finite-Element Surface-Water Modeling System for Two-Dimensional Flow (FESWMS-2DH) and a Resources Management Associates 2 (RMA2). Both programs have the capability to model 2D flow around structures. The department must identify settings in which a 2D model would be beneficial, and to determine what degree of effort needs to be invested in data collection to produce an effective model. Department personnel also need training in the use of the programs. Once these factors are understood, site-specific 2D models can be utilized to properly analyze structures subjected to compound channel flow and design the structure to minimize damage caused from scour.

OBJECTIVES AND SCOPE OF RESEARCH PROJECT

This research project has three main objectives. The first is to determine if the computed stream flow velocities of 2D river models and resulting scour predictions are comparable with field measurements at the SD 13 Bridge near Flandreau. The second objective is to conduct a sensitivity analysis to determine the critical input parameters for the 2D flow models, with an emphasis on the optimal density of channel and overbank topography data. The third objective is to determine the applicability of 2D flow models for use on streams and rivers with compound channel flow around a structure and identify cost effective ways to utilize these models.

CONTRIBUTIONS/POTENTIAL APPLICATIONS OF RESEARCH

SDDOT needs to define the types of channel configurations that produce compound channel flow and also determine the degree of data collection effort required to produce adequate 2D models. The potential benefits of this project would be new procedures and guidelines for bridge hydraulic analysis. SDDOT has both FESWMS and RMA2, which were developed to model 2D flows. Once the capabilities and data requirements of these models are understood, they can be utilized where warranted to assist in the design of new structures and to determine the locations for scour countermeasures. Therefore, the sooner this

method can be verified in South Dakota the sooner the potential foundation cost savings can be realized. The case studies in this report would serve as detailed examples on creating and using 2D flow models for bridge hydraulic analysis, including field data collection, mesh generation, model calibration, and analysis and interpretation of modeling results.

THE APPROACH

Current practices in bridge scour evaluation and bridge hydraulic analysis were reviewed. A list of specific questions on bridge hydraulics and hydraulic modeling was developed to form a questionnaire. Eight state DOTs were called and asked the questions on the questionnaire. A summary of the state DOTs' research, experiences, and current practices was compiled in this report.

A compound channel comprises a central deeper portion (main channel) flanked by left and right overbanks (floodplain). Complex flow interactions often occur between floodplain and main channel at river crossings. The resulting flow field is often far from one-dimensional. Case studies were conducted to determine the types of channel configurations that would produce compound channel flow and to develop guidelines to create an effective 2D model. Two bridge sites in South Dakota were selected to perform detailed flow and scour analysis. The sites are the SD 13 bridge (structure number 51-150-099) over the Big Sioux River near Flandreau and the SD 37 bridges (structure numbers 56-149-176 and 56-150-176) over the James River near Mitchell. Both sites have flow conditions that are known to create problems with 1D river models. These site characteristics include bridges on river bends (SD 13 Bridge), bridges with significant constrictions (SD 37 bridges), embankment skew (SD 37 bridges), bridges over meandering rivers with asymmetric floodplains (SD 13 and SD 37 bridges), changes in position of thalweg in vicinity of bridge crossings (SD 13 Bridge), and skewed bridges (SD 37 bridges). Additionally, an 8.5-ft. deep scour hole was observed at the northern-most pier at the SD 13 Bridge during the floods of June and July 1993; and the wide floodplain at the SD 37 bridges suggests that this site has a large potential for contraction scour.

Bathymetry and topography data were collected on the ground at the SD 13 Bridge. High-resolution Light Detection and Ranging (LiDAR) data and coarse-resolution National Elevation Dataset (NED) data are available at the SD 37 bridges. These data sets allowed the researchers to evaluate the effectiveness of different types of survey data for creating 2D flow models. 1D and 2D models of the bridge sites were created in the HEC-RAS and Finite-Element Surface-Water Modeling System (FESWMS), respectively. The 2D model for the SD 13 bridge was calibrated using flow measurements collected at the bridge crossing during the floods of March and July 1993. The SD 37 bridges have extensive flow measurements from the flood of April 2001, which was a 25-year event. The 2001 flow data were collected over a large area extending from the upstream meander loop through the bridge crossing to the downstream meander loop, which provides a comprehensive data set for validating 2D models for prediction of compound channel flow. In each case study, a sensitivity analysis was conducted to examine the sensitivity of the modeling results to the inputs to develop an effective model. Modeling results were also used to determine the critical parameters that influence the hydraulic conditions at each bridge site.

Pier scour and contraction scour were evaluated at the SD 13 Bridge and SD 37 bridges, respectively. The scour calculations were conducted using the scour equations in HEC-18 (Arneson et al. 2012), the SRICOS method (Briaud et al. 1999, 2001a, and 2005), and an energy method originally proposed by Güven et al. (2002) but modified in this study for unsteady flow calculations. Thin wall tube samples were collected at foundation depth at each bridge site. The soil samples were tested in the laboratory to determine the soil erodibility. Curves of measured erosion rate versus shear stress were used with rating curves derived from the 2D flow models to calculate scour.

Results from the two case studies and findings from the literature review and telephone survey were summarized to provide a knowledge base for the development of procedures and guidelines for selecting hydraulic models and for creating an effective 2D model. Detailed instructions for creating a 2D river model in the Surface-Water Modeling System (SMS) are documented in two master of science theses (Larsen 2010; Rossell 2012) completed under this research project.

FINDINGS AND RECOMMENDATIONS

Two published reports that are directly related to this project are discussed in the literature review. The final report for NCHRP Project 24-24 (*Criteria for Selecting Hydraulic Models*; Gosselin et al. 2006) describes the most commonly used 1D and 2D numerical models for hydraulic analysis of bridge waterways. The report identifies the site characteristics that produce compound channel flow at a bridge site and presents modeling results from 1D and 2D models for a wide range of idealized site conditions. A decision matrix was included in the report to guide the engineer in selecting hydraulic models. The final report for NCHRP project 24-14 (*Scour at Contracted Bridges*; Wagner et al. 2006) identifies additional hydraulic and geomorphic factors affecting scour magnitude at contracted bridges.

The telephone survey found that the FESWMS is the most commonly used 2D flow model for bridge hydraulic analysis in inland waterways by state DOTs. The decision to use 2D models is made primarily based on needs, information available, and time frame rather than costs. Training and motivation of the modeler and support from management are the key factors in determining whether 2D flow models are used regularly in a state DOT office.

The case studies showed that a 2D flow model provided substantial improvements in hydraulic analysis compared with a 1D model. 2D models correctly predicted the flow velocity distributions at both bridge sites. The benefits of a 2D model become apparent when modeling results are used with more advanced methodologies to predict bridge scour. When rating curves derived from a 2D flow model were used with the SRICOS method to predict pier scour at the SD 13 Bridge, the computed scour depths were reasonably close to the observed scour. At the SD 37 bridges, modeling results from the 2D model produced a more realistic estimation of live-bed contraction scour and predicted a clear-water contraction scour that was consistent with the measured channel cross sections. A sensitivity analysis showed that better estimates of critical shear stress and slope of the curve of erosion rate versus shear stress would improve the accuracy of scour predictions.

The project found that the density of topographic data in the floodplain can be reduced considerably at the SD 13 Bridge without affecting the results of the 2D model. The project also found that LiDAR data can be used to create an accurate 2D flow model. At the SD 37 bridges, a 2D flow model created using coarse-resolution NED data also produced results that matched the field measurements better than the 1D model created in HEC-RAS.

The use of different software tools in the Surface-Water Modeling System (SMS) for creating 2D river models was demonstrated for the SD 13 and SD 37 bridges. Detailed instructions for creating an effective 2D river model are given in Larsen (2010) and Rossell (2012).

This report recommends that SDOT does the following: (1) develops a formal decision process for selecting 1D and 2D hydraulic models, (2) coordinates with other agencies in the state to collect LiDAR data for the entire South Dakota and make the data available to the users, (3) conducts a department needs assessment and establish a continuing education program for SDDOT engineers with clearly identified training goals, (4) conducts additional case studies to provide the knowledge base for the development of improved design procedures and guidelines for bridge hydraulic analysis and evaluating scour at bridges, (5) measures soil erodibility when evaluating scour at bridges, (6) initiates a research project to collect

flow and scour data at selected bridge sites across the state during high flow events, and (7) supports research to understand the time effect of scour and to develop a long-term hydrograph for use in scour computations in cohesive soils.

1. INTRODUCTION

1.1 Problem Description

Reliable flow and soil data are crucial for accurate prediction of bridge scour depths. Hydraulic analysis of bridge waterways is commonly conducted using one-dimensional (1D) river models. One-dimensional models may not predict the velocity distributions at bridge crossings accurately when two-dimensional (2D) flow effects are important. Typical examples include compound channels, skewed bridges, and bridges located on river bends. In a hydraulic study of the Highway 13 Bridge over the Big Sioux River near Flandreau, South Dakota, Ting et al. (2010) found that the approach flow velocities were under-predicted by almost a factor of two for the floods of March and July 1993 by using the 1D model Hydrologic Engineering Center's River Analysis System (HEC-RAS, 2017). The floods produced a scour hole 8.5-ft. deep at the northern-most pier. However, when the computed flow velocities from HEC-RAS were used as inputs to the Scour Rate in Cohesive Soils (SRICOS) method to predict scour, the predicted scour depth was zero because the computed initial bed shear stress was less than the critical shear stress. Because the soil erosion rate depends critically on flow velocity, the latter needs to be calculated accurately when the time rate of scour is considered.

A compound channel comprises a central deeper portion (main channel) flanked by left and right overbanks (floodplain). A change in flow alignment due to bends, lateral migration of channel, or other obstructions can produce complex flow patterns. In addition, complex flow interactions often occur between the floodplain and the main channel of a compound channel at river crossings. Exchange of flow between the two portions arises as the approach flow contracts into the channel and through the bridge opening, and then expands to re-establish across the floodplain. This process leads to the formation of large eddies in the shear layer in the flow region between the channel and floodplain, and creates ineffective flow areas upstream and downstream of the bridge crossing. The resulting flow field is often far from 1D. Two-dimensional flow analysis can define the magnitude and direction of shear stress along with detailed geometry of streamlines around a structure. The need to predict 2D flow effects at bridge crossings becomes even more evident when predicting live-bed contraction scour since the results are very sensitive to how the width of the approach flow is defined and the flow in the upstream channel transporting sediment.

The South Dakota Department of Transportation (SDDOT) currently has Finite-Element Surface-Water Modeling System (FESWMS) and Resource Management Associates 2 (RMA2). Both are programs with the capability to model 2D flows around highway structures. However, little is known about the improvements that may be expected from the use of 2D models, and there are few guidelines on what the most cost-effective ways are to apply these models. SDDOT must identify settings in which a 2D model would be beneficial and determine what degree of effort needs to be invested in data collection to produce an effective model. Once these factors are understood, site-specific 2D models can be utilized to properly analyze structures subjected to compound channel flows and to design the structures to minimize damage caused by scour.

1.2 Objectives

The following are the objectives of this research project:

1. Determine if the modeled stream velocities (and resultant scour predictions) of two-dimensional channel flow models are comparable with the velocity and scour measurements from existing scour studies at the SD 13 Bridge site near Flandreau.

This objective was accomplished by creating a 2D river model of the bridge site using FESWMS in the Surface Water Modeling System (SMS). The model was calibrated using flow measurements collected by the United States Geological Survey (USGS). Rating curves of flow velocity and flow depth were generated by running the 2D model over a wide range of discharges from low flow to the 500-year event. The rating curves were used with the recorded hydrograph for the floods of March and July 1993 to calculate flow velocities for scour prediction. The SRICOS method was used to predict the scour history at the northern-most pier. The predicted final scour depth was compared with the observed scour depth. This study provided an overall assessment of the state-of-the-art in estimation of bridge hydraulics and prediction of pier scour.

2. Evaluate sensitivity and determine critical input parameters for the two-dimensional models, with an emphasis on the optimal density of channel and overbank topography data.

The sensitivity of flow velocity and depth computed using a 2D flow model to the input parameters was examined for the SD 13 Bridge. The sources of uncertainty and critical input parameters were identified. Numerical testing was conducted to quantify the effects of uncertainty in the input parameters on the outputs. The effects of changing the Manning's roughness coefficient, eddy viscosity, downstream water surface elevation, and density of channel and overbank topography data on the numerical results were investigated. The findings were used to determine what degree of effort needs to be invested in field data collection to produce an effective 2D model.

3. Determine the applicability of a two-dimensional flow model for use on streams and rivers with compound channel flow around a structure.

The key element of this objective was to understand the hydraulics of compound channel flows at contracted bridges over meandering rivers. The SD 37 bridges over the James River north of Mitchell, SD, were chosen to conduct a 2D flow analysis. When the river rises above flood stage, complex flow interactions occur between the meandering channel and asymmetric floodplain due to severe flow constriction at the skewed, parallel bridges. Two separate 2D models of the bridge site were created using Light Detection and Ranging (LiDAR) and National Elevation Dataset (NED) data. A 1D model was also created in HEC-RAS using cross sections extracted from the LiDAR 2D model. The computed results were compared with field measurements to evaluate the models. Numerical simulations were conducted to identify site characteristics producing the 2D flow effects classified as compound channel flow by systematically varying the model input parameters. A contraction scour analysis was conducted for a 100-year flood event using the scour equations in Hydraulic Engineering Circular No. 18 (HEC-18, Arneson et al. 2012) and a method that accounts for the time rate of scour in cohesive soils.

1.3 Research Tasks

The following tasks were completed in this project:

1.3.1 Literature Review and Telephone Survey

Current practices in bridge scour evaluation and bridge hydraulic analysis were reviewed. A list of specific questions was developed to form a questionnaire for the project. Eight state Department of Transportation (DOT) offices (California, Florida, Illinois, Iowa, Maryland, Minnesota, Nebraska, and Texas) were called and asked the questions on the questionnaire. The review of current practices and background for the bridge site selection is presented in Section 2. The questionnaire and a summary of the telephone survey are presented in Section 3.

1.3.2 Hydraulic and Scour Analysis, SD 13 Bridge Over Big Sioux River Near Flandreau, SD

Working with the USGS district office in Huron, SD, bathymetric and topographic survey data were collected at the SD 13 Bridge site in August 2009 to establish the ground elevation and channel geometry for creating a 2D flow model. The survey was conducted using a global positioning system (GPS) topographic survey system. The area surveyed covered approximately 1.5 miles of main channel and extended into the floodplain to the elevation of the 100-year flow. A 2D model of the bridge site was created in SMS using the depth-averaged model FESWMS. The model was calibrated using flow data collected at the bridge crossing by the USGS on March 30 and July 7, 1993. The calibrated model was run for a range of discharges up to the 100-year flow to determine how the hydraulic conditions at the site change with stage and to identify the site characteristics that produced the concentrated flow observed at the northern-most pier. A 1D model was created in HEC-RAS for comparison. A sensitivity analysis was conducted to determine the critical input parameters for the 2D model. The 2D model was run at two different mesh resolutions to identify the most effective field data collection effort. Rating curves for flow depth, approach flow velocity, and flow angle of attack were derived from the 2D model. These results were used as inputs to the SRICOS model to predict scour at the northern-most pier. The results of hydraulic and scour analysis for the SD 13 Bridge are presented in Section 4.

1.3.3 Hydraulic and Scour Analysis, SD 37 Bridges Over the James River Near Mitchell, SD

A 2D flow model of the SD 37 bridges was created using a bathymetry survey and LiDAR data collected by the United States Army Corps of Engineers (USACE) in fall of 2002. A second 2D flow model was created using NED data for comparison. The LiDAR 2D model was validated using flow measurements collected by the USGS during three high-flow events. The most detailed measurements were obtained on April 15, 2001, during a 25-year event. Flow velocities and bed elevations were measured over a large area at the bridge site by using an Acoustic Doppler Current Profiler (ADCP). The channel cross sections at the parallel bridges were most recently surveyed on November 17, 2011, by the USGS and researchers. The researchers also collected two thin wall tube samples in the low flow channel near the southbound bridge. SDDOT personnel collected two additional thin wall tube samples at the foundation level under the north abutment between the northbound and southbound bridges on March 8, 2012. These samples were tested at SDSU to determine the soil erodibility. The results of 2D flow modeling and soil erosion tests were employed to evaluate contraction scour at the bridge site by using the scour equations in HEC-18 and a method that takes into account the scour rate of cohesive soils. The results of hydraulic and scour analysis for the SD 37 bridges are presented in Section 5.

1.4 Findings and Conclusions

Major findings and conclusions of this project are summarized in Section 6. The summary focuses on lessons learned from the project that will aid the engineer in selecting hydraulic models and creating an effective 2D flow model for evaluating scour at bridges.

1.5 Implementation Recommendations

Implementation recommendations are presented in Section 7. This section describes the recommended actions and outlines the tasks required to implement these actions.

2. BACKGROUND AND LITERATURE REVIEW

2.1 Evaluating Scour at Bridges

The majority of bridge failures were caused by the scouring of bed material around the bridge foundations (Arneson et al. 2012). Therefore, scour evaluation is required in the design of bridges over waterways by the American Association of State Highway and Transportation Officials (AASHTO). AASHTO recommends that the Federal Highway Administration (FHWA) Hydraulic Engineering Circular No. 18 (HEC-18) be used to evaluate scour at bridges. The basic procedure consists of seven steps as outlined below:

1. Determine the flood event(s) that will produce severe scour conditions.
2. Develop a hydraulic model that can accurately model the flood flows determined in Step 1. For 1D flow conditions, the USACE HEC-RAS may be used. For more complex bridge structures or hydraulic conditions, a 2D model such as the FHWA's FESWMS may be used. (FESWMS-2DH, 2017)
3. Estimate the total scour from the results of the hydraulic model created in Step 2. The total scour includes long-term aggradation/degradation, contraction scour, and local scour around the piers and abutments.
4. Plot total scour depths obtained in Step 3 on a cross section of the stream channel and floodplain at the bridge site.
5. Critically evaluate the results from Steps 3 and 4 and ensure they are reasonable based on the judgment from a multi-disciplinary team that includes hydraulic, geotechnical, and structural engineers. All factors that will affect the scour depth should be considered, including storm duration, erodibility of channel materials, flow conditions, ice and debris, and many others.
6. Examine the proposed bridge size, configuration, and foundation elements based upon the scour analysis performed in Steps 3 through 5.
7. Analyze the bridge foundation with the assumption that all the streambed material has been removed down to the total scour depth, ensuring that the foundations are in accordance with the AASHTO Standard Specifications for Highway Bridges.

In Step 3, long-term aggradation is the accumulation of sediment in the bridge crossing, and long-term degradation is the scouring or lowering of the bed elevation in the bridge crossing. Both of these can be human-induced or naturally occurring. Contraction scour is the result of the increased flow velocities in the main channel due to the flow contracting near the bridge crossing during a flood. This in turn increases the bed shear stress, which results in the lowering of the bed elevation. Local scour is caused by the piers or abutments obstructing the flow, which produces turbulence around the structures that can remove bed material. Additionally, there are two different regimes, clear-water and live-bed scour, in terms of sediment transport for scour. Clear-water scour occurs when there is no inflow of sediment into the bridge crossing, and live-bed scour occurs when there is an inflow of sediment from upstream of the bridge crossing (Arneson et al. 2012). Live-bed scour typically involves non-cohesive sediments. When the rate of scour is high, the general practice is to assume that the equilibrium scour depth will be reached during a single design flood. Scouring in cohesive soils is considered clear-water scour since the bed material transported from the upstream reach will be mostly in suspension and may wash through the bridge site. In addition, several major flood events may be required to generate equilibrium scour in cohesive soils. For bridges founded on highly scour resistant cohesive soils, substantial construction cost savings may be realized by taking into account soil erodibility in scour calculations.

For the two case studies investigated in this project, only pier scour and contraction scour were evaluated because the bridge abutments at both sites are protected by riprap. The scour calculations were performed using the equations in HEC-18 and two different methods that account for the scour rate of cohesive soils.

The detailed hydraulic and scour analyses are presented in Sections 4 and 5. To provide the background for these case studies the pertinent literature is briefly reviewed in this section.

2.2 Scour Analysis

Pier scour was evaluated for the SD 13 Bridge over the Big Sioux River near Flandreau in Chapter 4. The pier scour equation in HEC-18 can be written as (Arneson et al. 2012):

$$\frac{y_s}{a} = 2.0K_1 \cdot K_2 \cdot K_3 \cdot K_4 \cdot \left(\frac{y_1}{a}\right)^{0.35} \left(\frac{V_1}{\sqrt{gy_1}}\right)^{0.43} \tag{2.1}$$

where y_s is equilibrium scour depth; a is pier width; V_1 is approach flow velocity; g is gravity; and K_1, K_2, K_3 and K_4 are correction factors for pier nose shape, flow angle of attack, bed condition, and armoring by bed material size, respectively. Eq. (2.1) was developed from flume tests in sands, but has been used for all types of soils in the field. This equation shows that the equilibrium scour depth is a function of flow velocity to the 0.43 and water depth to the 0.135. Therefore, equilibrium scour depth is somewhat sensitive to flow velocity but relatively insensitive to flow depth.

The SRICOS method has been proposed as an alternative design methodology for predicting bridge scour at cohesive soil sites in HEC-18. While Eq. (2.1) would produce the same scour depth for all soil types, SRICOS uses site-specific measurements to quantify the soil erosion rate. Thus, this new technique was developed to predict the curve of scour depth versus time associated with a hydrograph (Briaud et al. 1999, 2001a). Unlike the equilibrium scour depth, however, the rate of scour is very sensitive to flow velocity. The rate of scour is a function of the bed shear stress. Briaud et al. (2004) proposed a general equation for calculating the maximum initial bed shear stress, τ_{max}, around a complex pier:

$$\tau_{max} = k_w \cdot k_{sp} \cdot k_{sh} \cdot k_a \times 0.094\rho V_1^2 \left[\frac{1}{\log\left(\frac{BV_1}{\nu}\right)} - \frac{1}{10}\right] \tag{2.2}$$

where B is pier width (= D or pier diameter for circular piers); V_1 is approach flow velocity; ρ is fluid density; ν is kinematic viscosity; and k_w, k_{sp}, $k_{sh,}$ and k_a are correction factors for shallow water effect, pier spacing, pier shape, and flow angle of attack. Thus, a 100% change in flow velocity would produce roughly a 400% change in bed shear stress. Since soil erosion rate increases with bed shear stress, it is apparent that flow velocity needs to be estimated much more accurately when the rate of scour is considered. Thus, using more advanced scour models also require more accurate hydraulic results as input. A detailed review of the SRICOS method for pier scour and contraction scour can be found in Ting et al. (2010).

Contraction scour is evaluated for the SD 37 bridges over the James River near Mitchell in Chapter 5. The equations in HEC-18 for calculating the live-bed contraction scour depth, y_s, can be written as (Arneson et al. 2012):

$$y_s = y_2 - y_0 \quad \text{and} \tag{2.3}$$

$$\frac{y_2}{y_1} = \left[\frac{Q_2}{Q_1}\right]^{6/7} \left[\frac{W_1}{W_2}\right]^{k_1} \tag{2.4}$$

where y_1 is average depth in the upstream main channel; y_2 is average depth in the contracted section; y_0 is existing depth in the contracted section before scour; Q_1 is flow in the upstream channel transporting sediment; Q_2 is flow in the contracted channel; W_1 is bottom width of the upstream main channel; W_2 is bottom width of main channel in the contracted section less pier width(s); and k_1 is exponent determined by the mode of bed material transport. Eq. (2.4) was derived for non-cohesive sediment by applying a simplified sediment transport equation to a long contraction with uniform reaches where the flow is essentially one-dimensional (1D). It is not uncommon to encounter a bridge site where it is difficult to relate the input parameters in Eq. (2.4) to the field conditions. In such situations, a two-dimensional (2D) flow model may improve scour predictions by providing more accurate flow information for the scour equations (e.g., Q_1 and W_1) and/or advanced modeling of the scouring process.

The clear-water scour equation in HEC-18 only predicts the equilibrium scour depth. Briaud et al. (2005) extended the SRICOS method, which was originally developed for pier scour to include contraction scour. The equations in Briaud et al. (2005) were developed based on flume tests in a rectangular channel. These equations are difficult to apply to a complex site like the SD 37 bridges. In this study, a more general method developed by Güven et al. (2002) was modified to predict clear-water scour in unsteady flow using rating curves of average unit discharge and flow depth derived from the 2D flow analysis.

2.3 Flow Analysis

The U.S. Army Corps of Engineers' HEC-RAS is commonly used for analyzing hydraulics of bridge waterways. HEC-RAS is a 1D river model. One-dimensional models solve the energy equation for the water surface profile and distribute flow in a cross section based on conveyance. Typically, this means that larger discharge (and velocity) is apportioned to the deeper portion of the channel, which is not necessarily true in reality. Furthermore, ineffective flow areas are often difficult to define in a 1D model, although they are critical for accurate calculations of flow velocities and energy losses through the bridge opening. Thus, 1D river models may not predict velocity distribution at bridge crossing correctly when 2D flow effects are important. Typical examples include compound channels, skewed bridges, and bridges located on river bends. Two-dimensional river models overcome the limitations of 1D models by computing water surface elevations and depth-averaged velocities in the two horizontal directions, but require more time, data, and experience to develop, so they are used only occasionally by engineers.

The Federal Highway Administration's FESWMS and U. S. Army Corps of Engineers' RMA2 are commonly used in the United States for 2D flow analysis. Both models operate under the hydrostatic assumption (i.e., accelerations in the vertical direction are negligible). The models compute water surface elevations and depth-averaged velocities in the two horizontal directions. FESWMS was developed specifically for modeling highway river crossings and includes specific features for modeling bridge hydraulics, such as pressure flow under bridge decks and flow over roadway embankments. Both FESWMS and RMA2 have been interfaced with the SMS, which is a comprehensive environment for hydrodynamic modeling, with powerful pre- and post-processing tools for importing and manipulating topographic/bathymetric data, automatic grid generation, and data visualization, analysis, and plotting.

Although advances in the development of graphical user interfaces (GUI) have made 2D models much easier to apply today, they are still only used occasionally in the design of highway structures. There are several reasons for this. First, additional field data are required to construct and calibrate 2D models. Second, little documented information is available that describes the refinement that may be expected from the application of 2D models, including the situations in which 2D models are more appropriate and

more cost-effective than 1D models. Third, considerably more training and experience are required to use 2D models. This includes not only creating and running the models but also analyzing and interpreting the results. Thus, additional training is required. As part of the literature survey, eight DOT offices were contacted via telephone and asked a list of questions related to bridge hydraulic analysis, including the type of river models they have used. Results from this survey are summarized in Chapter 3.

A recent study (Gosselin et al. 2006) completed under NCHRP Project 24-24 has compared numerical results obtained using HEC-RAS and FESWMS on a number of test cases, including bridges located on river bends, bridges near confluences, skewed bridges, and bridges with multiple openings. The model setup used idealized compound channels consisting of a trapezoidal main channel with gently sloping floodplains. A decision matrix (see Table 2.1) was developed to guide the engineer in determining whether a 1D or 2D model is more appropriate in situations similar to those encountered in the test cases. Since there were no measured flow data for comparison, it was assumed that the computed velocities from the 2D model were more accurate. Thus, if both models produce similar results, the 1D model was considered to be adequate in that situation. An important step in the decision was the design requirements. In Gosselin et al. (2006), the equations in HEC-18 were used to predict scour. It is well known that the HEC-18 equations generally over-predict scour, sometimes significantly, because the equations do not account for the slower rate of scour in cohesive soils. Hence, using more accurate hydraulic input does not by itself improve scour predictions. Indeed, the predicted scour would be more conservative (greater) if larger velocities are computed by the 2D model than by the 1D model, even though the flow velocities from the 2D model may be more accurate. As demonstrated by the case studies in this report, the benefits of using 2D flow models in evaluating scour at bridges become apparent only when they are used in conjunction with more accurate methodologies for prediction of scour.

Although the study by Gosselin et al. (2006) has provided useful design guides to the engineer, the geometries used in their test cases are highly simplified compared with the field conditions at most bridge sites. Change in flow alignment due to bends, lateral migration of channel or other obstructions can produce complex flow patterns in compound channels, with important effects on bridge scour. Ettema et al. (2004) described the range of scour types that may occur at bridge abutments in compound channels. Wagner et al. (2006) discussed the hydraulic and geomorphic factors affecting scour at contracted bridges. However, few documented case studies that use field data and 2D flow models to improve and verify numerical predictions of hydraulic conditions and bridge scour are available. Presently, the effects of many site characteristics on bridge hydraulics and scour are still not well understood. Wagner (2007) simulated the water surface elevations and velocity distributions at the U. S. Highway 13 Bridge over the Tar River at Greenville, North Carolina, using 1D and 2D flow models. He found that the 2D model more accurately simulates the water surface profile in the study reach and the flow velocity magnitude and direction through the bridge opening. He commented that case studies that combine detailed field data sets with 2D flow modeling will be extremely useful for establishing the knowledge base for the development of modeling guidelines for hydraulic analysis of bridge waterways.

2.4 Case Studies

Two bridge sites were investigated in this project. In Section 4, the 2D depth-averaged model FESWMS was employed to conduct a hydraulic and scour analysis for the SD 13 Bridge over the Big Sioux River near Flandreau, South Dakota. The Flandreau site has complex channel and floodplain geometry. The river crossing is located at the sharp bend of a compound channel with asymmetric floodplains (see Figure 4.1). Concentrated channel flow develops at the right bank as the river flows parallel to the highway and then abruptly crosses underneath it. The flow distribution is altered again at flood stage when the blockage caused by the roadway embankment forces the left floodplain flow back into the main channel just upstream of the bridge crossing. By comparing HEC-RAS modeling results with field measurements of flow velocity, it was clear that HEC-RAS is unable to predict the velocity distribution at

the bridge site correctly. A 2D model was created in FESWMS and calibrated using flow velocity data collected at the bridge crossing during two floods in 1993. A sensitivity analysis was conducted to quantify the effects of uncertainty in the input parameters on the outputs. The calibrated model was used to examine the hydraulic and geomorphic factors that affect the main channel and floodplain flows and the flow interactions between the two portions. Results from the 2D model were also compared to the results from a 1D model created from the same survey data. The rating curves derived from the 2D model and the results of Erosion Function Apparatus (EFA) tests were used with the SRICOS method to predict local scour at the northern- and southern-most piers. The computed scour depths were compared to the observed scour, and recommendations are given to improve the accuracy of pier scour predictions in cohesive soils. The SRICOS method and EFA test are explained in Section 4.3.

Several areas for further research were identified in the Big Sioux River study. The width of the floodplain is about 2,500 ft. upstream and downstream of the SD 13 Bridge. It is desirable to also investigate the hydraulic conditions of a severely contracted bridge opening. Second, flow measurements were available only at the bridge crossing. To evaluate the performance of a 2D river model for predicting the flow interactions between the different portions of a compound channel, it is desirable to have detailed flow data through the bridge opening and over a large area upstream and downstream of the bridge. Third, the topographic and bathymetric data used for creating the 2D model at the Big Sioux River site required a three-day field survey. A considerable amount of time was spent surveying the floodplain. LiDAR data are available for the eastern part of South Dakota, and NED data are available for the entire state. The vertical resolutions of LiDAR and NED data are approximately 1 ft. and 10 ft., respectively. Hence, LiDAR and NED data can be a cost-effective source of topographic data for 2D river models.

In the second case study, the 2D depth-averaged model FESWMS was employed to simulate the hydraulic conditions at the SD 37 bridges over the James River near Mitchell, South Dakota. The parallel bridges are located in a crossing between the two bends of a meander (see Figure 5.1). The floodplain upstream and downstream of bridge crossings is about one-mile wide and bounded by high bluffs. As the channel meanders between the walls of the river valley, the main body of flow is shifted constantly between the left and right floodplains. The blockage caused by the roadway embankment then forces the majority of the left floodplain flow back into the main channel between the upstream bend and bridge crossing. Because all of the floodplain flow contracts through the bridges, the site has a large potential for scour. The site is listed in the National Bridge Scour Database (http://water.usgs.gov/osw/techniques/bs/BSDMS). The USGS National Bridge Scour Team conducted detailed measurements of flow velocities and channel bathymetry during the flood of April 2001 (approximately a 25-year event) by using an Acoustic Doppler Current Profiler (ADCP). Additional flow data included stream flow gauging data from a 50-year event in 1997 and a 100-year event in 2011. LiDAR and NED data are also available. This comprehensive data set allowed us to create and validate a 2D flow model for the bridge site. Two 2D models were created using LiDAR and NED data as well as a 1D model created in HEC-RAS. The validated LiDAR 2D model was used to examine the effects of meander, floodplain topography, and land cover on the velocity distributions and flow exchanges between the main channel and floodplain. Results from the 2D model and soil erosion tests were used to evaluate contraction scour using the scour equations in HEC-18 and a method that takes into account the slower rate of scour in cohesive soils.

2.5 Concluding Remarks

NCHRP Project 24-24 has developed a decision matrix for selecting hydraulic models. The decision process requires the engineer to evaluate site conditions, design considerations, and project-related considerations. The site characteristics that determine the hydraulic conditions at bridge sites with compound channel flows are not well understood. The emphasis of this present study is to develop the knowledge base to improve hydraulic analysis of bridge waterways. Two bridge sites in South Dakota with compound channel flows were selected to conduct the case studies.

Gosselin et al. (2006) commented that 2D flow modeling may take less time to perform than 1D modeling. They stated that this is a reflection on the experience of the modeler and the tools available for creating 2D models. Hence, the final decision to use 1D or 2D models may come down to data availability and the experience of the modeler. It is anticipated that the results of the case studies in this report would serve as a useful guide, and thus encourage more engineers to use 2D flow models in hydraulic analysis of bridge waterways.

Table 2.1 Decision Tool for Selecting Hydraulic Models (After Gosselin et al. 2006)

Design Criteria	Weight	One Dimensional Model		Two Dimensional Model	
		Score 1=low 3=medium 5=high	Weight x Score	Score 1=low 3=medium 5=high	Weight x Score
Site Conditions	(1-10)				
Multiple Openings					
Bridges Located on River Bends					
Bridges near Confluences					
Bridges with Significant Constrictions					
Overtopping Flow					
Embankment Skew					
Bridges over Meandering Rivers					
Bridges with Asymmetric Floodplains					
Bridges with Large Piers/High Blockage					
Tidal Hydraulics					
Design Requirements	(1-10)				
Riprap					
Armor Units					
Concrete Block					
Abutment Scour Calculation					
Pier Scour Calculation					
FEMA "No-Rise"					
Bendway Weirs					
Other Considerations	(1-10)				
Modeler Experience					
Scheduling					
Data Availability					
Totals (Sum of Weight x Score)					

3. TELEPHONE SURVEY

3.1 Research Questionnaire

As part of the literature search, a number of state DOT offices across the country were contacted to find out what computer models and engineering tools they have used or are regularly using to conduct bridge hydraulic analysis. A list of questions was developed by the principal investigator. The questions were generated from topics that were deemed relevant to the scope of research. The questionnaire was forwarded to the technical panel for review and comment in July 2010. The revised questionnaire was sent to 15 state DOTs around the country together with a request for a telephone interview.

During August and September 2010, those state DOTs that had responded were contacted via telephone and asked a list of standard questions. The list of questions that form the questionnaire is presented in Table 3.1. Specifically, the following state DOT personnel were interviewed using the survey questionnaire:

- California, Kevin Flora, hydraulic specialist and senior bridge engineer;
- Florida, Rick Renna, state hydraulic engineer;
- Illinois, Matthew O'Connor, hydraulic engineer;
- Iowa, David Claman, bridge engineer;
- Maryland, Andrzej Kosicki, bridge hydraulics manager;
- Minnesota, Petra DeWall, assistant state hydraulic engineer;
- Nebraska, Donald Jisa, assistant bridge engineer;
- Texas, John Delphia, geotechnical engineer;
- Texas, Amy Ronnfeldt, chief hydraulic engineer.

Table 3.2 provides a summary of the survey responses. The principal investigator also contacted Dr. Kornel Kerenyi, hydraulics R&D program manager at the Federal Highway Administration to obtain an update on current research efforts on bridge hydraulics and scour at FHWA.

3.2 Survey Summary

Most states interviewed have either used 2D flow models in bridge hydraulic analysis or have received training on using 2D flow models. Several of the state personnel interviewed have significant experience with 2D flow modeling. Those state DOTs found that it often takes no more time to create a 2D model than a 1D model, and in some cases it is even faster to use a 2D model. This is because 2D models are more structured so there is less guessing with the input parameters (e.g., how to define ineffective flow areas). Florida DOT uses 2D flow models routinely because flows at coastal bridges are typically two-dimensional. In some states, one or more engineers in the DOT offices serve as champions for using 2D models. These persons either have prior training and experience with 2D flow modeling, or have an interest in numerical modeling so they taught themselves on 2D flow modeling and use it as often as possible in their work. Individual motivations together with support from management appear to be the two main factors in determining whether 2D flow models are used in a state DOT office. None of the states interviewed has a formal decision process for deciding whether to use 1D or 2D flow models. The decision to use 2D models is made on a case-by-case basis, and is driven typically by needs and time frame rather than costs. All the state personnel interviewed have a good understanding of the situations in which 2D flow effects may be important. The 2D models reported being used include FESWMS, RMA2, ADCIRC, TUFLOW, and SRH-2D. All the models have been interfaced with SMS. One of the main difficulties cited with using 2D models is to obtain adequate flow data for model calibration. Flow measurements are typically collected during low or medium flows. Only high water marks are usually available for large floods. Technical support is another important issue. Although all state DOTs have

access to SMS and its supported models under software licensing agreements arranged by the FHWA, the vendors do not provide technical support and would refer all questions from the states to FHWA. Another issue is the large amount of topographic and bathymetric data needed to create a 2D model. Iowa is completing a joint project with DENR and USGS to collect LiDAR data for the entire state, and would be used to produce contour maps with ± 8 inches accuracy. They recommended using LiDAR data to reduce the effort invested in field surveying on the ground.

Although not part of the formal questionnaire, all the state DOT staff interviewed were asked how many bridge hydraulic engineers they have in their offices and the percentage of work done in house and by consultants. It is apparent that those states using 2D flow models generally have more staff members on a regular basis.

Table 3.1 Questionnaire

1. How long have you been involved with hydraulic analysis of bridges over waterways in your state and what was your involvement?
2. Please describe some of the applications and design issues related to bridge hydraulic analysis in your state?
3. What computer model(s) do your engineers use for bridge hydraulic analysis?
4. Have you encountered situations when 1D flow model does not work well and can you provide some specifics of these situations?
5. Have you used 2D model in bridge hydraulic analysis? If "yes", which model(s) have you used and what are some of the features that you like and don't like about the model(s)?
6. Describe some of problems that you have used 2D model for and what are the principal results that you have obtained/learned from 2D model.
7. Have your state used field measurements to verify the results of 1D and/or 2D models. If "yes", what field measurements are typically collected?
8. Does your state have a decision process for deciding whether to use 1D or 2D model in bridge hydraulic analysis? What do you think are the principal barriers for using 2D model?
9. Does your State DOT have any published procedures or guidelines on bridge hydraulic analysis?
10. What do you think State DOTs can do to improve hydraulic analysis of bridge waterways?
11. Is your State DOT currently conducting or supporting research projects on bridge hydraulics or use of numerical modeling in bridge hydraulic analysis?

Table 3.2 Summary of Responses from Telephone Survey

Question	Summary of Responses
1. How long have you been involved with hydraulic analysis of bridges over waterways in your state and what was your involvement?	Year of experience of survey participants varied from 15 to 40 years, most of which was spent on bridge hydraulic analysis and/or bridge scour.
2. Please describe some of the applications and design issues related to bridge hydraulic analysis in your state?	Most common applications involve backwater and scour analysis for structure replacement. Hydraulic analyses are also conducted to meet FEMA and DENR requirements, and to examine channel degradation and bank stability.
3. What computer model(s) do your engineers use for bridge hydraulic analysis?	Most of State DOTs surveyed use HEC-RAS for bridge hydraulic and HY-8 for culvert hydraulic analysis. California also uses a normal depth program called BrEase which was developed in-house.
4. Have you encountered situations when 1D flow model does not work well and can you provide some specifics of these situations?	Situations in which 1D flow model does not work well cited by survey participants include: skewed bridges during high flows, bridge crossings on river bends, severely contracted bridge openings, significant lateral flows involving a main bridge and one or more relief bridges, bay causeways, change in thalweg in the vicinity of bridge, split flows created by bridge overtopping, and situations in which it is difficult to define the ineffective flow areas.
5. Have you used 2D model in bridge hydraulic analysis? If "yes", which model(s) have you used and what are some of the features that you like and don't like about the model(s)?	Almost all of State DOTs interviewed have either used 2D flow models in bridge hydraulic analysis or have received training on 2D flow modeling. The 2D models that were reported being used are FESWMS, RMA2, ADCIRC, TUFLOW, and SRH-2D. Four of the State DOTs interviewed commented that they have experienced problems with FESWMS in handling wetting and drying, bridge deck overtopping, and weir flows. Two of these DOT offices have also worked with TUFLOW which they found to be more stable (have better solution convergence).

Question	Summary of Responses
6. Describe some of problems that you have used 2D model for and what are the principal results that you have obtained/learned from 2D model.	Recently completed or on-going projects using 2D flow models include a study to investigate fish passage design at road culverts, flows involving a railway bridge upstream of a roadway crossing over a meandering channel, flow going over a heavily skewed bridge, and the use of LiDAR data to construct 2D flow model on a historic bridge with two 90˚ bends and complicated split flows. In addition, Florida has done a large amount of 2D flow modeling on coastal bridges since overland flooding in coastal areas is primarily a two-dimensional problem, requiring accurate information on both velocity magnitude and flow angle. Results from 2D flow models have been used to assess bank shear stresses to determine the potential of stream bank migration, to compute backwater effects, and to calculate flow velocity and angle of attack for scour predictions.
7. Have your state used field measurements to verify the results of 1D and/or 2D models. If "yes", what field measurements are typically collected?	Lack of field data for model calibration was cited as one of the main barriers for using 2D flow models. Often the only flow data available are high water marks and estimates of flow velocities. Sometimes, experience is used to judge if the computed results are reasonable. Some states have collected water level and scour measurements after major floods. Some of the State DOTs surveyed do not have the infrastructure to collect flow measurements themselves and have to contract agencies such as the USGS to do the field measurements.
8. Does your state have a decision process for deciding whether to use a 1D or 2D model in bridge hydraulic analysis? What do you think are the principal barriers for using 2D model?	Most State DOTs surveyed use 2D flow models only in high-profile cases and cases with no alternative methods. The decision to use 2D models is made primarily based on needs, the information available and time frame rather than costs. One state reported that they have used the selection criteria developed in NCHRP Project 24-24. One interviewee commented that 2D flow models should be used anytime when velocity and flow direction cannot be reliably estimated, and the environmental conditions are severe and the structure so expensive that reliable results are critical. States that have significant experience with 2D flow modeling found that it is almost as easy to create a 2D model as a 1D model. Modeler experience, data availability and scheduling were cited as principal barriers for using 2D models.

Question	Summary of Responses
9. Does your State DOT have any published procedures or guidelines on bridge hydraulic analysis?	The HEC-RAS manuals are used extensively by State DOTs in bridge hydraulic analysis. Most State DOTs have also developed their own design guidelines for bridges and culverts which are published on their websites.
10. What do you think State DOTs can do to improve the hydraulic analysis of bridge waterways?	Several states commented that they need better technical support on 2D flow modeling. FHWA has software licenses for a number of 2D river models. Although all State DOTs can use these models for free, there is very limited technical support from FHWA. It was also commented that training courses organized by vendors use case studies that always work, but individual cases are not so straightforward. Some State DOTs commented that NHI courses are too basic, and it is becoming difficult to get NHI to offer custom-built courses. Good access of information through interagency cooperation, good communication with surveying people, support from management, and training were cited as important elements for maintaining a strong and progressive hydraulic division. Iowa recommended using LiDAR data to produce contour maps of the floodplain for use in 2D flow modeling.
11. Is your state currently conducting or supporting research projects on bridge hydraulics or use of numerical modeling in bridge hydraulic analysis?	Most of the State DOTs surveyed have strong research programs in place, although the number of active research projects has decreased in recent years due to state budget constraints. Recently completed and on-going research projects in river or coastal hydraulics include: the relationship between ultimate scour depth and soil parameters; long-term channel degradation; comparison of bridge scour depth with computation from HEC-RAS; remote scour monitoring equipment; fish passage performance; regional trends and bounds in flow velocities at bridge crossings; down cutting and river hydraulics involving main stem and tributary streams; 3D flow modeling of bridge hydraulics; horizontal and uplifting forces on bridge decks; and statistical wind hind-casting.

4. HYDRAULIC AND SCOUR ANALYSIS, SD 13 BRIDGE OVER BIG SIOUX RIVER NEAR FLANDREAU, SOUTH DAKOTA

4.1 Site Description

The SD 13 Bridge (structure number 51-150-099) over the Big Sioux River near Flandreau is located on South Dakota (SD) Highway No. 13, 0.3 miles north of Flandreau in east-central South Dakota. The bridge was built in 1964 and has four spans, with an overall length of 436 ft. It has three octagonal pier sets with webs (Bents 2, 3, and 4) located on pilings. Each pier set is 3-ft. wide and 30-ft. long. The low-flow channel runs through the center part of the bridge opening where Bent 3 is located. The bridge opening is classified as a spill-through abutment with three horizontal to one vertical slope embankment protected by riprap. The USGS measured river bottom profiles at the bridge site on December 5, 1991 (low flow), June 20, 1992 (discharge 1,624 $ft.^3/s$), June 22, 1992 (4,346 $ft.^3/s$), March 30, 1993 (9,090 $ft.^3/s$), and July 7, 1993 (7,774 $ft.^3/s$). The measured profiles on July 7, 1993, showed 8.5 ft. of local scour around the northern-most pier (Bent 2) and up to 1 ft. of contraction scour. The peak flow between December 5, 1991, and July 7, 1993, occurred on July 4, 1993, with a recorded hourly mean flow of 13,300 $ft.^3/s$ (daily mean flow 9,870 $ft.^3/s$) at the gauging station near Brookings (site number 06480000) located 22 miles upstream. The USGS collected flow velocity data at the bridge on March 30 and July 7, 1993. These measurements showed concentrated channel flow around Bent 2. The estimated drainage areas at the Brookings gauging station and bridge site are 3,898 mi^2 and 4,096 mi^2, respectively. The estimated 2-, 100-, and 500-year flow discharges at the bridge site are 2,320, 31,300, and 53,100 $ft.^3/s$ (Niehus 1996). The bank full capacity of the river is approximately equal to 4,000 $ft.^3/s$.

The Flandreau site has complex channel and floodplain geometry as shown in Figure 4.1. The river crossing is located at the 90º bend of a compound channel with asymmetric floodplains. Concentrated channel flow develops at the right bank as the river flows parallel to the highway and then abruptly crosses underneath it. The flow distribution is altered again at flood stage when the blockage caused by the roadway embankment forces the left floodplain flow back into the main channel just upstream of the bridge crossing. Figs. 4.2 through 4.6 show pictures of the bridge site taken by Francis Ting on April 6, 2007, when the recorded daily mean flow was 1,968 $ft.^3/s$. A low-head dam is located ¼-mile downstream from the bridge (Figure 4.6). The dam has a crest length of 175 ft., and its primary influence on the hydraulics is to raise the water level at the bridge.

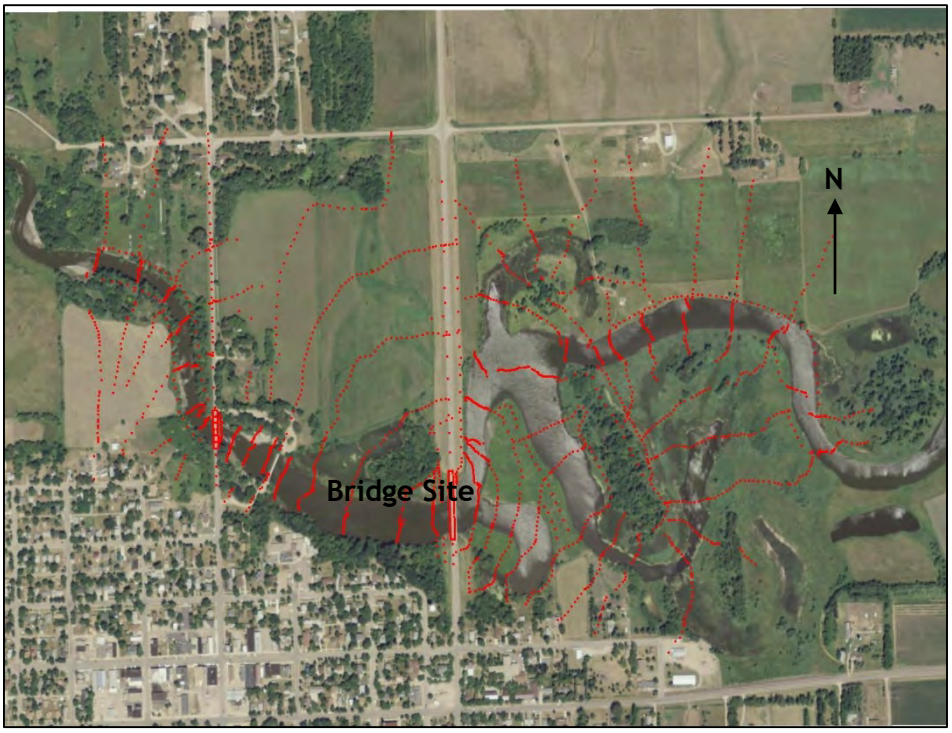

Figure 4.1 Aerial photograph of the SD 13 Bridge site near Flandreau, South Dakota, showing the bridge crossing over the Big Sioux River and field survey points for the 2D river model (background image courtesy of United States Geological Survey)

A bathymetric and topographic survey of the bridge site was conducted most recently by the USGS August 3-6, 2009, using a GPS topographic survey system. Figure 4.1 shows the locations of the survey points overlaid on a geo-referenced image of the study area. There were 3,705 survey points in the main channel and floodplain. Coordinates of survey points were collected in units of feet by using the North American Datum of 1983 (NAD 83) and National Geodetic Vertical Datum of 1929 (NGVD 29). The study area falls within Universal Transverse Mercator (UTM) Zone 14 (US National Geodetic Survey 1986).

Figure 4.2 SD 13 Bridge from left bank facing along upstream face toward right bank. The pier sets in the photograph are, from left to right, Bents 4, 3, and 2

Figure 4.3 From SD 13 Bridge facing upstream toward the right bank. Note the 90º bend in the channel in front of the bridge

Figure 4.4 From SD 13 Bridge facing upstream toward left floodplain

Figure 4.5 From SD 13 Bridge facing downstream

Figure 4.6 From ¼-mile downstream facing upstream toward the SD 13 Bridge. Note the low-head dam across the channel

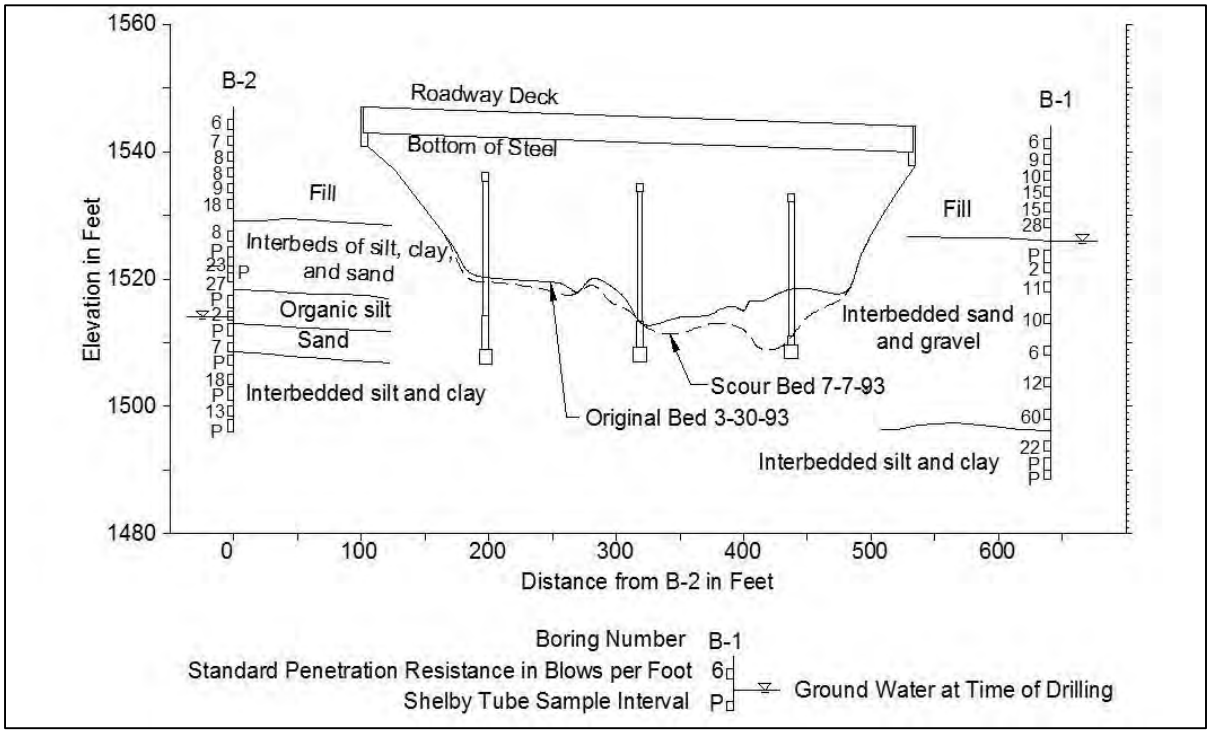

Figure 4.7 Generalized subsurface profile at the SD 13 Bridge site

Figure 4.7 shows the generalized subsurface conditions at the bridge site. Two borings were completed on the north and south abutments on June 12, 2007. Sampling with standard penetration testing (SPT) was performed from the ground elevation to the foundation elevation to delineate the soil stratigraphy. Thin wall tube samples were collected at selected depths from each drill hole for soil erosion rate testing. The general site soil materials that were observed during drilling included about 15 ft. of loose to medium dense fill soils overlying alluvial soils consisting of inter-bedded layers of silts, clays, and sands. At a depth of about 20 ft., black organic silt was encountered at the south abutment. Coarser grained materials were observed at the north abutment.

Figure 4.7 also shows the measured river bottom profiles and foundation depths at the bridge crossing. After the flood on July 4, 1993, a scour hole about 8.5-ft. deep and 50-ft. wide was observed around the northern-most pier (Bent 2). This scour hole can also be seen in the downstream bridge section (see Niehus 1996), but its location has shifted to the south side of the pier. The amount of observed scour at the southern-most pier (Bent 4) was less than 0.5 ft. and was mostly contraction scour.

4.2 Flow Models

A 2D model of the bridge site was created in SMS using the 2D depth-averaged model FESWMS. The process of constructing a 2D model in SMS consists of the following major steps. First, an aerial photograph of the study area is imported into SMS (Figure 4.1). Then, feature arcs are drawn on the background image to create an outline of the main channel and floodplain. Different material regions are then delineated and material properties are assigned to the individual domains (Figure 4.8). Next, a computational mesh is generated from the conceptual model and ground elevations are interpolated to the mesh. The final step before running the model is to assign values to specific model parameters and to define the inflow and outflow boundary conditions.

Two computational meshes were created to model the flow at the bridge site. The larger of the two meshes encompasses all of the floodplain surveyed up the boundary of the 100-year flood and can be seen in Figure 4.8. The material types in Figure 4.8 are prairie grass (A), trees (B), pasture (C), cattail (D), road ditch (E), road (F), and river channel (G). The corresponding Manning's n values are 0.06, 0.05, 0.04, 0.07, 0.04, 0.015, and 0.03, respectively. This mesh was used for medium to high flows (7,500 to 40,000 $ft.^3/s$), when the river has overtopped its banks and inundated the floodplain. In order for the model to run properly, the inflow and outflow boundaries must remain "wet." This was accomplished by adding two "hydraulic bridges" at the upstream and downstream ends. The hydraulic bridges have a constant ground elevation of 1,517 ft., which is low enough for the inflow and outflow boundaries to be submerged at all discharges. The 2D model would become unstable (the solution diverges) if too many elements become "dry." Therefore, a second and smaller mesh (see Larsen 2010) was created for the discharges below 7,500 $ft.^3/s$. The smaller mesh stops at the low-head dam and includes a smaller portion of the floodplain. Its extent was determined by using the large mesh to compute the inundated area for a discharge of 7,500 $ft.^3/s$. Numerical solutions obtained using several levels of mesh resolutions were used to select an acceptable mesh density.

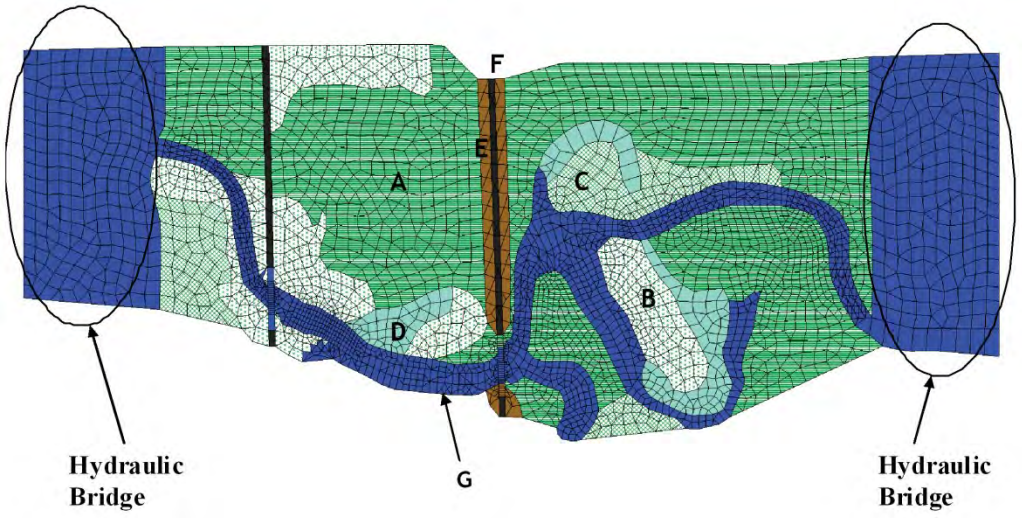

Figure 4.8 Finite-element mesh and material properties of the study area

The 2D model was calibrated using the flow measurements collected by the USGS on March 30, 1993, (9,090 ft.^{3}/s) and July 7, 1993 (7,774 ft.^{3}/s). On these days, water surface elevation and lateral distributions of flow velocity and flow angle of attack were measured on the upstream face of the bridge. A sensitivity analysis was conducted to assess the effects of varying the model's input parameters on the modeling results. The parameters examined included the Manning coefficient and eddy viscosity values, downstream water surface elevation, density of channel and overbank topographic data, and mesh density.

A 1D flow model was created in HEC-RAS for comparison. Twenty (20) cross sections were extracted from the larger computational mesh of the 2D model and input into HEC-RAS to capture all the bends in the main channel. In both the 1D and 2D models, flow discharge was specified at the inflow boundary and normal depth was assumed at the outflow boundary. The average channel slope (0.00049) was estimated from the channel cross sections downstream of the dam and entered into HEC-RAS to calculate the normal depth. For the smaller mesh, the water surface elevation upstream of the dam computed by HEC-RAS (with normal depth as the downstream boundary condition) was applied as the downstream boundary condition in FESWMS. Details of 1D and 2D flow model construction can be found in Larsen (2010).

4.3 Scour Model

The SRICOS method was used to predict the pier scour depths at Bent 2 and Bent 4 produced by the floods of June and July 1993. In the SRICOS method, the hydrograph is represented by a sequence of constant flow discharges such as the hourly or daily mean flow. The discharge is first converted into flow velocity using a hydraulic model. Each constant discharge or velocity is treated as an individual flood. The method assumes that the scour history for each flood follows a hyperbolic function. A hyperbolic function is uniquely defined by two parameters: the initial rate of scour and equilibrium scour depth. The equilibrium scour depth is a function of the bridge and flow parameters, and is calculated using an empirical equation. The initial rate of scour is determined by the soil erodibility and bed shear stress. A hyperbolic function is generated for each time step in the hydrograph. The series of hyperbolic functions created are fitted together to form a continuous scour history. The scour depth at the end of the hydrograph is the predicted final scour depth (Briaud et al. 1999, 2001a).

Briaud et al. (1999) proposed an empirical equation for calculating the equilibrium scour depth in clays (see also Ting et al. 2001). The original equation was developed for a circular pier. Correction factors were subsequently introduced to account for shallow water, pier spacing, pier shape, and flow angle of attack effects. The general equation for calculating the equilibrium scour depth at a complex pier is given by (Briaud et al. 2004):

$$z_{\max}(mm) = 0.18 \cdot K_w \cdot K_{sp} \cdot K_{sh} \cdot K_a \left(\frac{BV_1}{\nu} \right)^{0.635} \tag{4.1}$$

where B is pier width, V_1 is approach flow velocity, ν is kinematic viscosity, and K_w, K_{sp}, K_{sh}, and K_a are correction factors for shallow water effect, pier spacing, pier shape, and flow angle of attack.

Eq. (4.1) relates equilibrium scour depth to the pier Reynolds number BV_1 / ν. This parameterization disagrees with current practice since the pier Reynolds number is not considered important under prototype flow conditions. Ting et al. (2010) showed that the pier scour equation proposed by Briaud et al. (1999) would produce results similar to the HEC-18 equation for the range of laboratory flow conditions under which their equation was developed. Because the HEC-18 equation is widely used by engineers for predicting pier scour, both equations have been used in this study to estimate the equilibrium scour depth.

To determine the initial rate of scour, the maximum initial bed shear stress around the pier is calculated at each time step using Eq. (2.1). The corresponding scour rate is then obtained from a measured curve of erosion rate versus shear stress. Figure 4.9 shows the measured curves showing erosion rate versus shear stress for the very silty fine sand collected from the north abutment. In this context, very silty soil composes 30% to 50% of the total soil.

Soil erosion rates were determined by testing a thin wall tube sample of the soil in an erosion function apparatus (EFA). This device uses a stepping motor and a piston to push 1 mm of soil out of the thin wall tube into a water tunnel. The amount of time it takes to erode the 1-mm protrusion is recorded to calculate the soil erosion rates (Briaud et al. 1999, 2001b). The operator also assesses the surface texture of the soil sample and estimates the bed roughness as the soil erodes. The measured flow velocity in the EFA and the estimated bed roughness are entered into the Colebrook formula (e.g., Munson et al. 2009) to calculate the applied bed shear stress. As shown in Figure 4.9, two different values (ε = 0 and 1 mm) of bed roughness have been used to calculate the bed shear stress. These two curves were used to examine the sensitivity of the predicted scour depth to the critical shear stress and erosion rate constant.

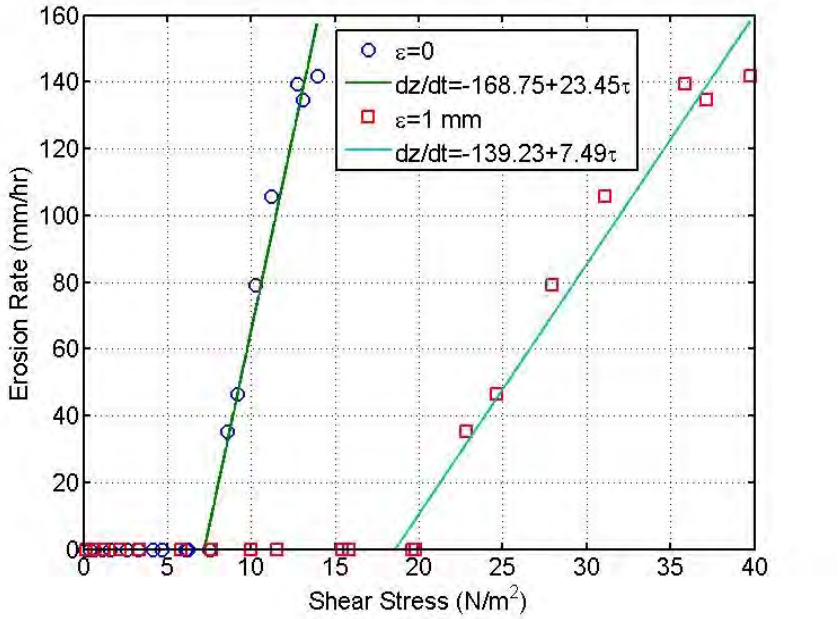

Figure 4.9 Curve of measured erosion rate versus shear stress for very silty fine sand from a depth of 19.5 to 21.5 ft. on the north abutment

4.4 Flow Measurements and Scour Predictions

Figure 4.10 shows the recorded hourly mean flow at the Brookings streamflow gauging station from March 28 to July 7, 1993. The total number of data points is 2,640. The measured discharges shown were multiplied by 1.025 in the SRICOS simulation to account for the increase in drainage area between the Brookings station and bridge site. During this period, three major floods (maximum hourly mean flow of 7,490, 9,530, and 13,300 $ft.^3/s$) were recorded on March 30, June 21, and July 4, respectively. The USGS conducted flow and scour measurements at the bridge site on March 30 near peak flow (measured discharge 9,090 $ft.^3/s$) and on July 7 when the flood was receding (measured discharge 7,774 $ft.^3/s$). Comparison with the channel cross section measured in June 1992 (see Niehus 1996) showed that little scour was produced by the March 30 flood, but the measurements taken on July 7 showed an 8- to 9-ft. deep scour hole around Bent 2. After the July flood, the scour hole at Bent 2 was filled in with riprap. The change in channel elevation from March 30, 1993, to July 7, 1993, and to August 4, 2009, can be seen in Figure 4.11. The abscissa is the distance from the left (south) abutment, and the ordinate is the bed elevation above mean sea level. Note that the 2D model was constructed using topographic and bathymetric data collected in 2009.

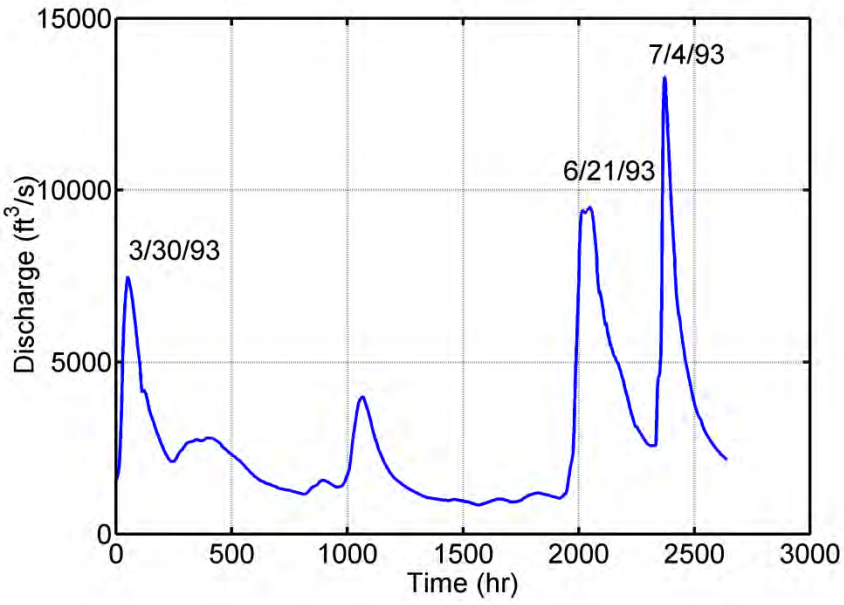

Figure 4.10 Recorded hourly mean flow from Big Sioux River near Brookings streamflow gauging station (site number 06480000) from March 28 to July 7, 1993

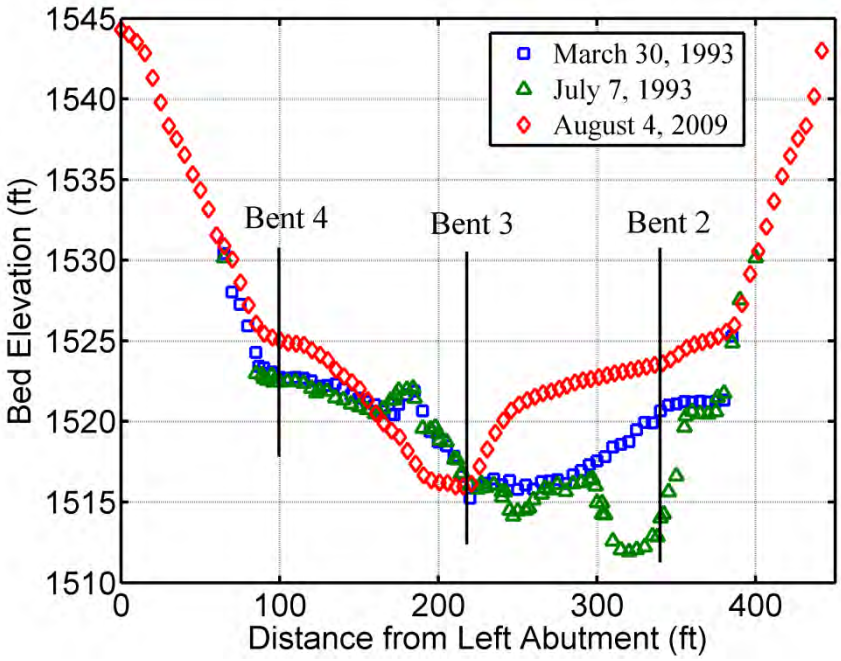

Figure 4.11 Measured channel profiles on upstream face of SD 13 Bridge in 1993 and 2009; the bridge piers are located at 98 ft. (Bent 4), 219 ft. (Bent 3), and 338 ft. (Bent 2) from the left abutment

Figure 4.12 shows a comparison of the computed and measured distributions of flow velocity magnitude and flow angle of attack on the upstream side of the bridge for a discharge of 9,090 ft.^{3}/s. The flow angle of attack is defined as the angle between the direction of the bridge pier and the direction of the flow. The field measurements show a flow concentration at Bent 2. The 2D model also predicts a flow

concentration, but it is located between Bent 2 and Bent 3 and is not as pronounced as the field measurements show. Similar results were found for the discharge of 7,774 ft.^{3}/s (see Larsen 2010). Figure 4.12 indicates that the approach flow followed the sharp bend at the bridge crossing better than the model predicted. This is also evident from the smaller flow angle of attack shown by the field measurements. The measured flow angle of attack at Bent 2 was about 35° compared with 40° predicted by the 2D model. Changes in channel cross sections at the bridge site after 1993 might have contributed to the observed differences between the computed and measured flow velocities, since the bathymetric data used to construct the 2D model and the flow measurements were collected many years apart.

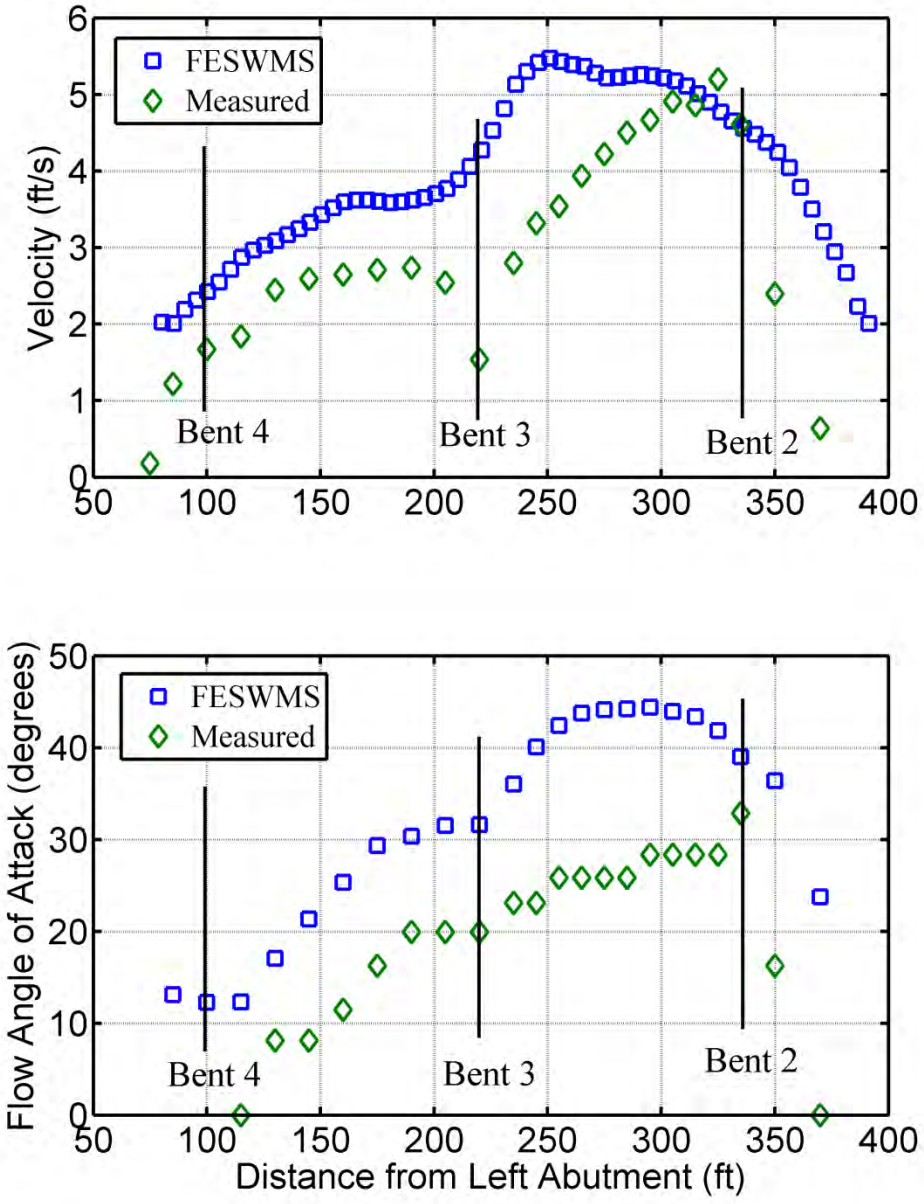

Figure 4.12 Measured and computed distributions of flow velocity magnitude (top plot) and flow angle of attack (bottom plot) on upstream face of SD 13 Bridge for discharge of 9,090 ft.^{3}/s; the computed and measured water surface elevations at the left bank are 1,530.49 and 1,530.42 ft., respectively

Figure 4.13 shows the computed velocity distribution at the bridge for a discharge of 15,000 ft.^{3}/s. The flow concentration on the north side of the channel is still visible at this discharge. In Figure 4.13, the downstream water surface elevation (WSEL) has been varied by two, 1-ft. increments (± 1 ft) about the normal depth to observe the model's sensitivity to the downstream WSEL. A 1-ft. increment in WSEL is equivalent to about a 10% change in water depth downstream. At Bent 2, the flow velocity varies by 0.22 ft./s and the WSEL by 0.29 ft. over the ± 1 ft increments. Hence, the flow velocity and water depth at the bridge are moderately affected by the downstream WSEL. The results of the sensitivity analyses for other discharges can be found in Larsen (2010).

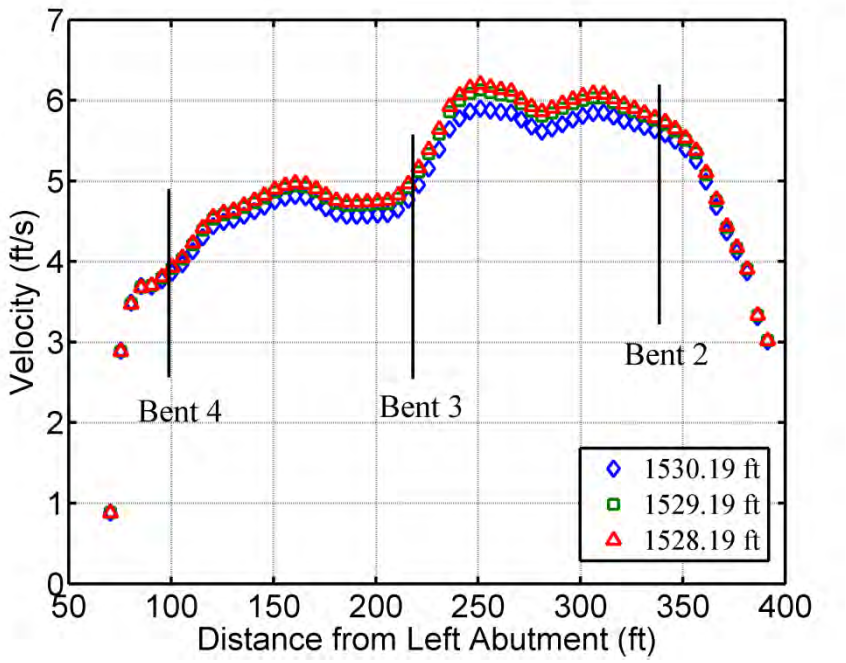

Figure 4.13 Effect of downstream water surface elevation on computed flow velocity distribution on upstream face of SD 13 Bridge for discharge of 15,000 ft.^{3}/s; the downstream water surface elevation at normal depth is 1,529.19 ft.

Figure 4.14 shows a comparison of the 1D and 2D models' results for two different discharges: 10,000 ft.^{3}/s and 31,300 ft.^{3}/s (100-year event). The 2D model predicts that a flow concentration begins to develop at Bent 2 around 3,500 ft.^{3}/s and is most prominent between 7,500 and 10,000 ft.^{3}/s. The flow concentration becomes less noticeable as the discharge is further increased and is almost non-existent at 30,000 ft.^{3}/s. The 1D model predicts, for all discharges, a flow concentration in the deepest portion of the channel where Bent 3 is located. Because HEC-RAS apportions flow based on conveyance, the highest velocity is always calculated to be in the deepest portion of the channel.

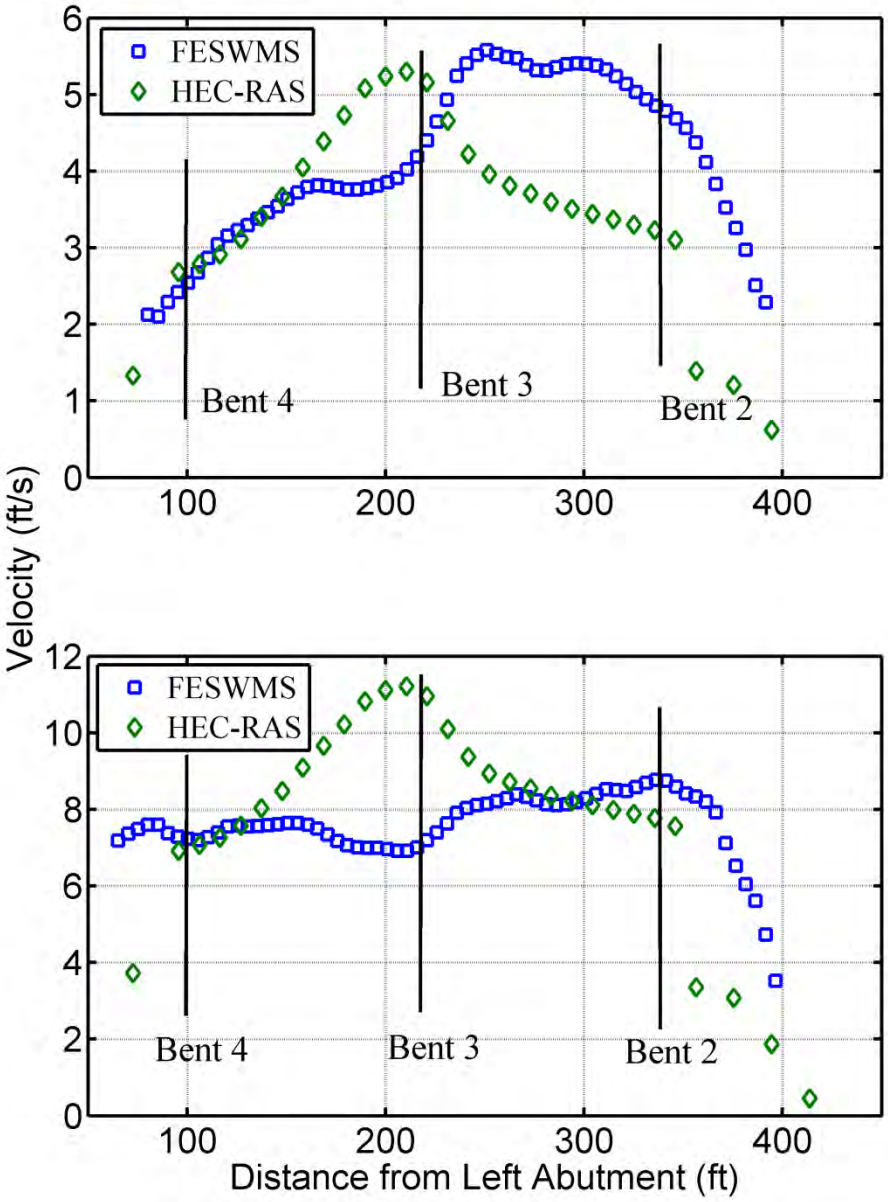

Figure 4.14 Comparison of computed velocity distributions on upstream face of SD 13 Bridge from FESWMS and HEC-RAS for discharge of 10,000 ft.^{3}/s (top plot) and 31,300 ft.^{3}/s (bottom plot)

The topographic and bathymetric data used for creating the 2D model required a three-day field survey. A considerable amount of time was spent surveying the floodplain. Therefore, a sensitivity analysis was conducted to determine if the modeling results are sensitive to the density of floodplain topographic data. For two different discharges (9,090 ft.^{3}/s and 31,300 ft.^{3}/s), the number of survey points in the floodplains upstream of the bridge and downstream of the dam used in creating the 2D model were reduced by about 40%. This reduction has virtually no effect on the computed WSEL and only minor effects (about 6%) on the computed flow velocities at the bridge (see Larsen 2010). Based on these results, it was concluded that the density of topographic data in the floodplain can be reduced considerably to save time spent in surveying.

4.5 Geomorphic Factors

To better understand how the flow concentration at Bent 2 develops and the effect of the floodplain flow on the flow distribution at the bridge crossing, seven observation arcs and one flow distribution arc were drawn upstream of the bridge (Figure 4.15). Arc 1 is located at the bridge. The distance measured along the channel centerline from arc 1 to arc 2 is 220 ft., from arc 2 to arc 3 is 120 ft., from arc 3 to arc 4 is 130 ft., from arc 4 to arc 5 is 170 ft., from arc 5 to arc 6 is 170 ft., and from arc 6 to arc 7 is 145 ft. The contour variable is water depth. The contour color changes from blue to green to brown as the water depth increases. Note that the thalweg (brown contour) is adjacent to the right bank where the river flows parallel to Highway 13, but shifts to the middle pier (Bent 3) at the bridge crossing.

The observation arcs were used to observe the lateral distribution of flow velocity at various locations along the main channel. The flow distribution arc was used to calculate the discharge in the main channel and floodplain. Table 4.1 gives the computed flow angle of attack at Bent 2 and the channel flow to total flow ratio at the flow distribution arc for nine different discharges ranging from 1,000 ft^3/s to 30,000 ft^3/s. From these results, it can be inferred that the floodplain flow has a significant effect on the flow through the bridge. When the channel flow to total flow ratio is 1.0, the computed flow angle of attack is between 42° and 47°. As the channel flow to total flow ratio decreases, the flow angle of attack decreases and the flow concentration at the right bank becomes less noticeable (compare Figures 4.12, 4.13, and 4.14).

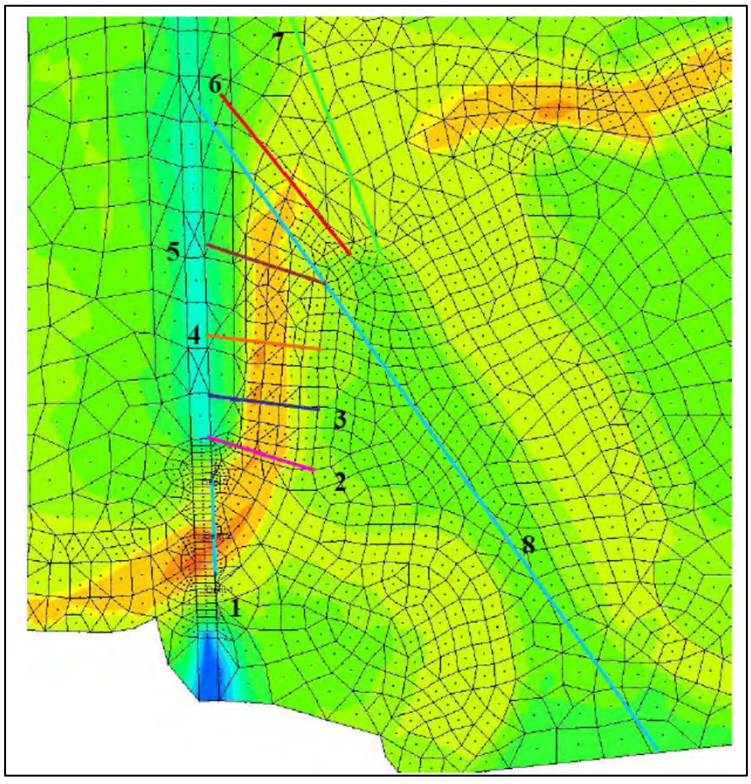

Figure 4.15 Observation arcs in FESWMS; brown color indicates larger flow depth

Table 4.1 Flow Angle of Attack at Bent 2 and Channel Flow to Total Flow Ratio at Arc 8 for Various Discharges; the Flow Angle of Attack Shown Is the Average of Seven Points Spaced at 5-ft. Intervals Centered on Bent 2

Discharge (ft^3/s)	Flow Angle of Attack (degrees)	Channel Flow/Total Flow
1000	47.2	1.00
3500	42.7	1.00
7500	41.1	0.67
10000	34.1	0.48
12500	30.6	0.37
15000	27.8	0.32
17500	26.0	0.29
20000	25.6	0.26
30000	17.0	0.22

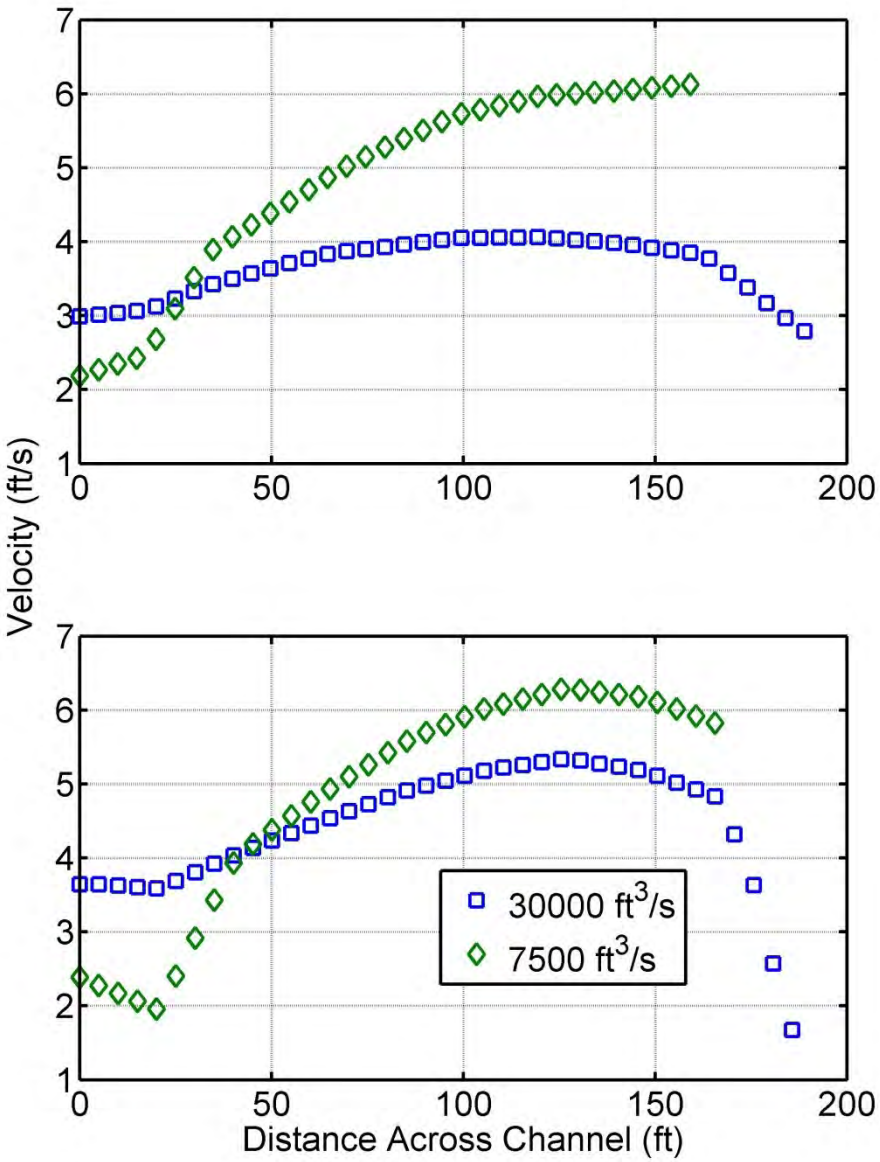

Figure 4.16 Computed flow velocity distributions across the main channel at arc 4 (top plot) and arc 3 (bottom plot) for discharge of 7,500 and 30,000 ft.^{3}/s

The lateral distribution of flow velocity at arc 3 and arc 4 is presented for a medium flow (7,500 ft.^{3}/s) and a high flow (30,000 ft.^{3}/s) in Figure 4.16. At arc 4, the river has completed a 90˚ turn and is flowing parallel to Highway 13. The deepest portion of the channel (the thalweg) is adjacent to the right bank (see Figure 4.15) where high flow velocity can be seen at the medium discharge. At arc 3, 340 ft. upstream of the bridge opening, the flow concentration adjacent to the right bank is well established at both medium and high flows. However, the flow velocity is more uniformly distributed at the high flow. This is due to the floodplain flow re-entering the channel across the left bank (see Figure 4.18). The flow velocity is also high at the left bank. Consequently, the flow concentration on the right side of the channel is less pronounced.

Computed 2D flow distribution at the SD 13 Bridge is shown in Figures 4.17 and 4.18 for the discharge of 7,774 ft.^{3}/s and 31,300 ft.^{3}/s, respectively. At 7,774 ft.^{3}/s, the left floodplain upstream of the bridge is inundated but most of the discharge is still carried by the main channel (see Table 4.1). Figure 4.17 indicates that the flow distribution at the bridge is determined primarily by the approach flow in the channel upstream. At 31,300 ft.^{3}/s, most of the upstream flow is carried in the left floodplain. Figure 4.18 shows that the flow distribution at the bridge is significantly altered when the roadway embankment forces the left floodplain flow back into the main channel just upstream of the bridge crossing.

Other factors affecting the velocity distribution at the bridge include bed roughness in the main channel and floodplains. For a discharge of 9,090 ft.^{3}/s, the Manning coefficient for different material types (see Figure 4.8) was varied one at a time from the base values to examine their effects on the modeling results. It was found that the main channel roughness has a significant effect on the velocity distribution at the bridge. When the Manning's *n* value in the channel is increased from 0.02 to 0.04, the flow velocity at Bent 2 decreases from 6.61 ft./s to 4.48 ft./s and the flow angle attack decreases from 38.7˚ to 33.8˚, while the water surface elevation increases from 1530.03 ft. to 1531.05 ft. For the floodplain materials, the trees and prairie grass were found to affect the velocity distribution at the bridge the most, but in opposite ways. When the Manning's *n* value for the trees is increased from 0.04 to 0.15, the flow velocity at Bent 2 decreases from 5.32 ft./s to 5.11 ft./s, while the water surface elevation increases from 1530.53 ft. to 1530.83 ft. It appears that the trees downstream of the bridge create a backwater effect, which causes the water surface elevation at the bridge to increase and the flow velocity to decrease. When the Manning's *n* value for the prairie grass is increased from 0.04 to 0.15, the flow velocity at Bent 2 increases from 5.12 ft./s to 5.47 ft./s, while the water surface elevation stays about the same. Increasing the floodplain flow resistance would cause more flow to be carried in the main channel, which would in turn increase the flow velocity at the right bank. Detailed results of the sensitivity analysis can be found in Larsen (2010).

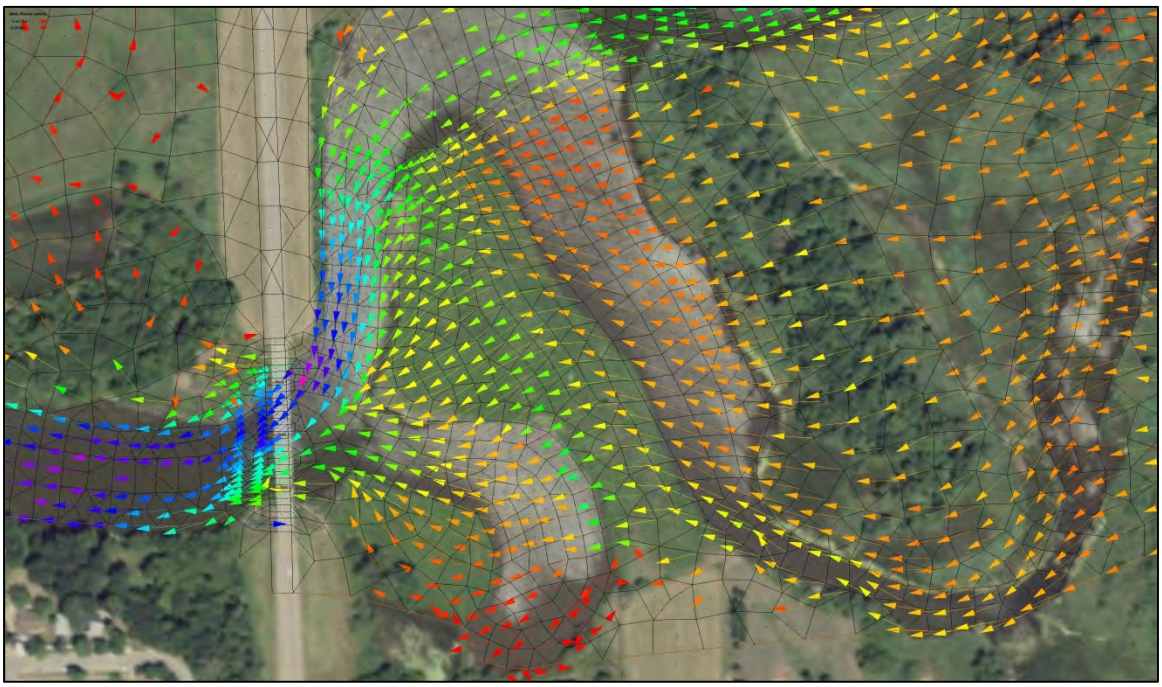

Figure 4.17 Computed 2D flow distribution for discharge of 9,090 ft.^{3}/s; dark red vectors indicate 0 ft./s and dark blue vectors indicate 4.5 ft./s

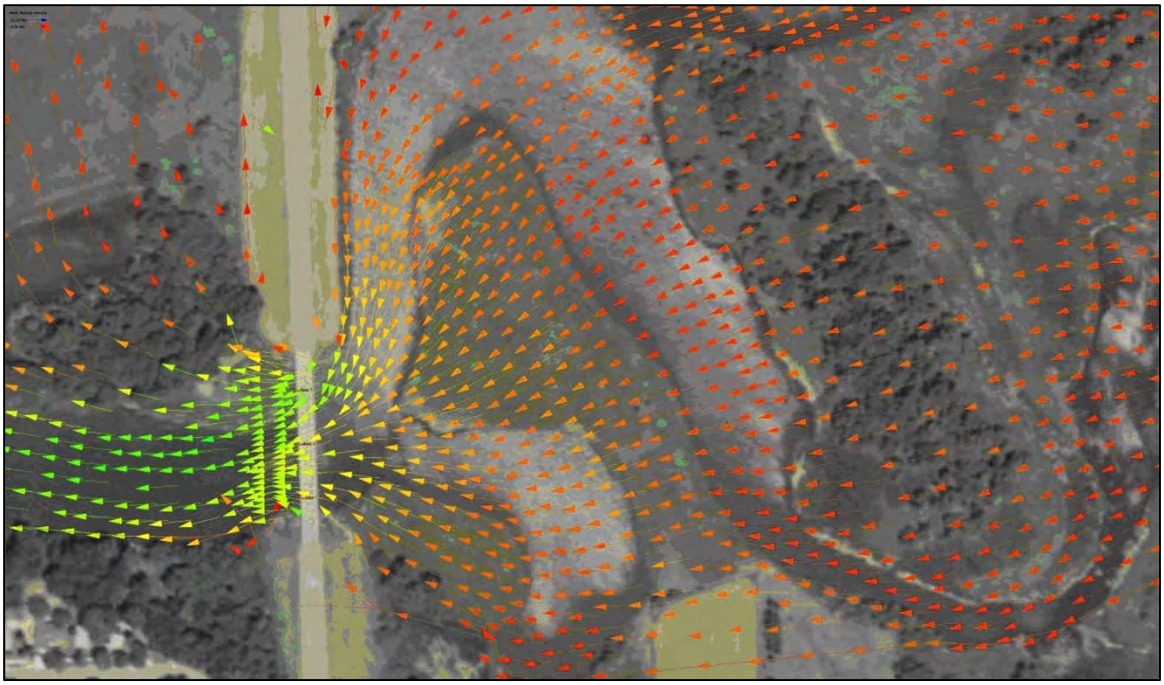

Figure 4.18 Computed 2D flow distribution for discharge of 31,300 ft.^{3}/s; dark red vectors indicate 0 ft./s and green vectors indicates 8.0 ft./s

4.6 Scour Analysis

The SRICOS method was used to predict local scour at Bent 2. Table 4.2 summarizes the input parameters used in the scour calculations. Figs. 4.19-4.21 show the approach flow velocity, flow angle of attack, and water surface elevation rating curves for Bent 2 derived from the 2D model. In the SRICOS simulations, a drainage area ratio adjustment of $\sqrt{4096 / 3898} = 1.025$ has been applied to transfer the recorded hydrograph at the Brookings station (Figure 4.10) to the bridge site. Figure 4.22 shows the results of the SRICOS simulation for Bent 2 from March 28 through July 7, 1993; the discharge is hourly mean flow. From top to bottom, the plots represent the time history of flow discharge Q, approach flow velocity V_1, approach flow depth y_1, initial bed shear stress τ, initial rate of scour dz/dt, maximum (equilibrium) scour depth z_{max}, and predicted scour depth z. The critical shear stress τ_c for the very silty fine sand is shown as a dashed line in the initial bed shear stress plot; the curve of measured erosion rate versus shear stress for $\varepsilon = 0$ mm (see Figure 4.9) has been used for scour calculations. Figure 4.22 shows that the critical shear stress is exceeded most of the time during the three large floods on March 30, June 21, and July 4. The predicted final scour depth on July 7, 1993, is 14.5 ft., which is much larger than the observed scour depth of 8 to 9 ft. The latter was measured after the flood subsided and does not account for partial refill of the scour hole. Hence, the maximum scour depth that occurred during the flood might have been higher. However, SRICOS predicts that 10.6 ft. of scour is produced by the March 30 flood, which is not confirmed by the measured channel cross section (see Figure 4.11). The difference between the predicted and measured scour depths was examined by conducting a sensitivity analysis of final scour depth to the input parameters.

Table 4.2 Summary of Input Parameters for Scour Predictions at Bent 2

Pier geometry	Pier width B = 3 ft., pier length L = 30 ft., pier shape rectangular pier with round nose
Channel geometry	Channel width W_1 = 436 ft., number of piers N = 3, pier spacing S = 120 ft., initial bed elevation Y_0 = 1520.72 ft. (June 22, 1992)
Flow parameters	See rating curves (Figures 4.19, 4.20 and 4.21)
Fluid parameters (20˚ C)	Density ρ = 998.2 kg/m^3, kinematic viscosity v = 1.004 × 10^{-6} m^2/s
Soil parameters	See EFA curves (Figure 4.9)
Hydrograph	See recorded hydrograph (Figure 4.10)

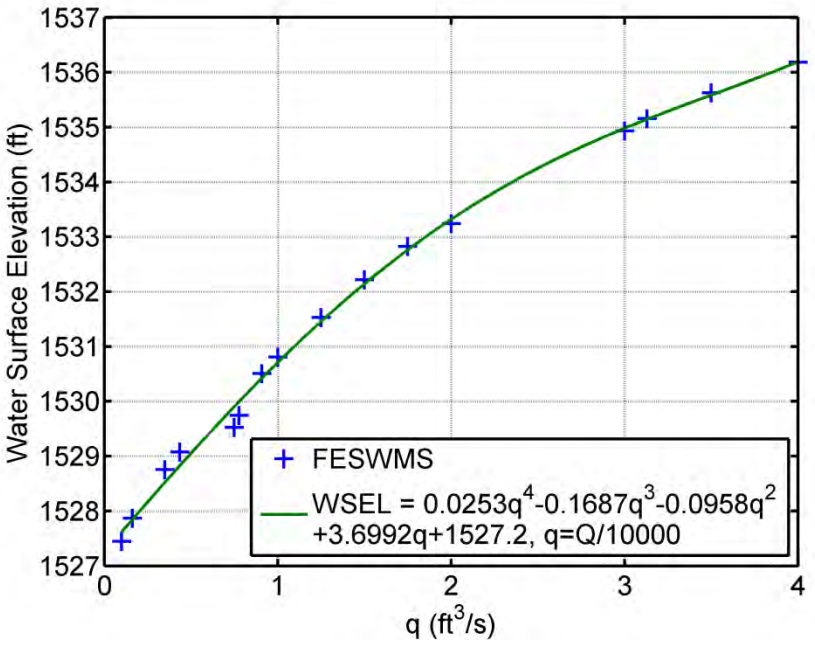

Figure 4.19 Water surface elevation rating curve for Bent 2 derived from a 2D model

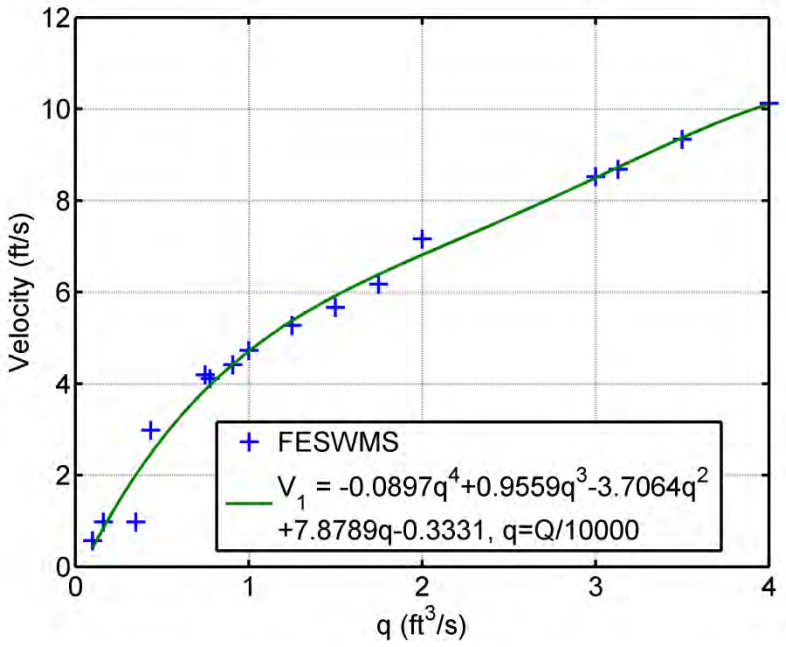

Figure 4.20 Approach flow velocity rating curve for Bent 2 derived from a 2D model

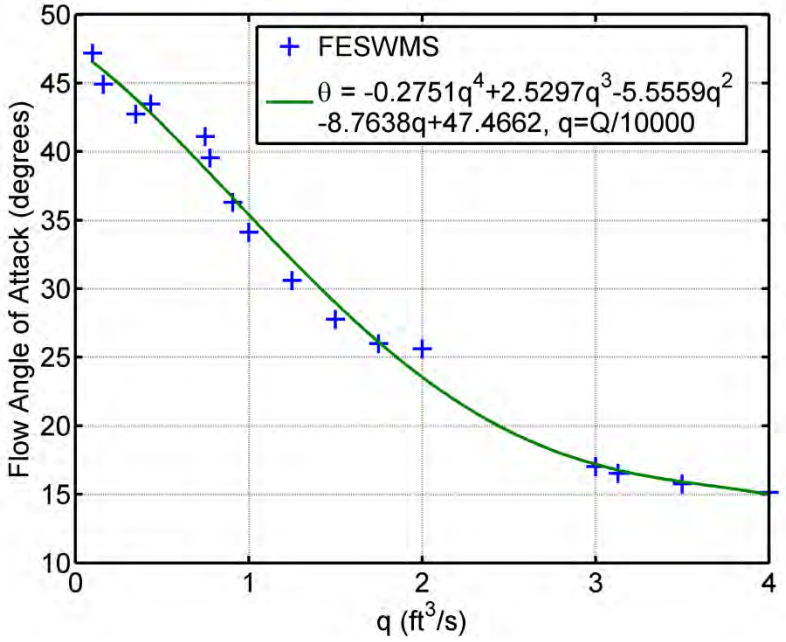

Figure 4.21 Flow angle of attack rating curve for Bent 2 derived from a 2D model

A sensitivity analysis was conducted to examine the sensitivity of the predicted final scour depth to the following input parameters: approach flow velocity, flow angle of attack, critical shear stress, and slope of the curve of erosion rate versus shear stress. The sensitivity analysis was conducted by varying the aforementioned parameters one at a time. Except for the critical shear stress, the other three parameters have only minor effects on the predicted scour depth for reasonable ranges of the parameters (see Table 4.3). For example, decreasing the approach flow velocity by 20% or the flow angle of attack by 33% or the slope of the curve of erosion rate versus shear stress by 80% only reduces the predicted final scour depth from 14.5 ft. to 12.1 ft. The predicted final scour depth is particularly insensitive to the slope of the curve of erosion rate versus shear stress. This is because the critical shear stress was exceeded most of the time during the three floods, and the soil erosion rate is so high (see Figure 4.9) that the scouring process has sufficient time to approach equilibrium condition. Note that the predicted final scour depth from SRICOS is close to the maximum equilibrium scour depth of 16.1 ft. predicted for the July 4 flood.

Table 4.3 Variations of Computed Final Scour Depth with Approach Flow Velocity, Flow Angle of Attack, and Slope of Curve of Erosion Rate versus Shear Stress

Percent Change from Base Value shown in Figure 4.22	Variation of Final Scour Depth (ft) with Approach Flow Velocity	Variation of Final Scour Depth (ft) with Flow Angle of Attack	Variation of Final Scour Depth (ft) with Slope of EFA Curve
0 (Base Value)	**14.5**	**14.5**	**14.5**
-10	13.4	13.8	14.4
-20	12.1	13.1	14.3
-30	10.7	12.3	14.1
-40	8.4	11.5	14.0
-60	–	–	13.4
-80	–	–	12.1

The parameter that has a significant effect on the predicted final scour depth is the critical shear stress. Increasing the critical shear stress from 7.2 N/m^2 to 18.6 N/m^2 and simultaneously decreasing the slope of the curve of erosion rate versus shear stress from 23.5 to 7.5 $mm/hr/(N/m^2)$ will reduce the predicted final scour depth from 14.5 ft. to 9.7 ft. The new soil parameters correspond to the curve of erosion rate versus shear stress for $\varepsilon = 1$ mm shown in Figure 4.9.

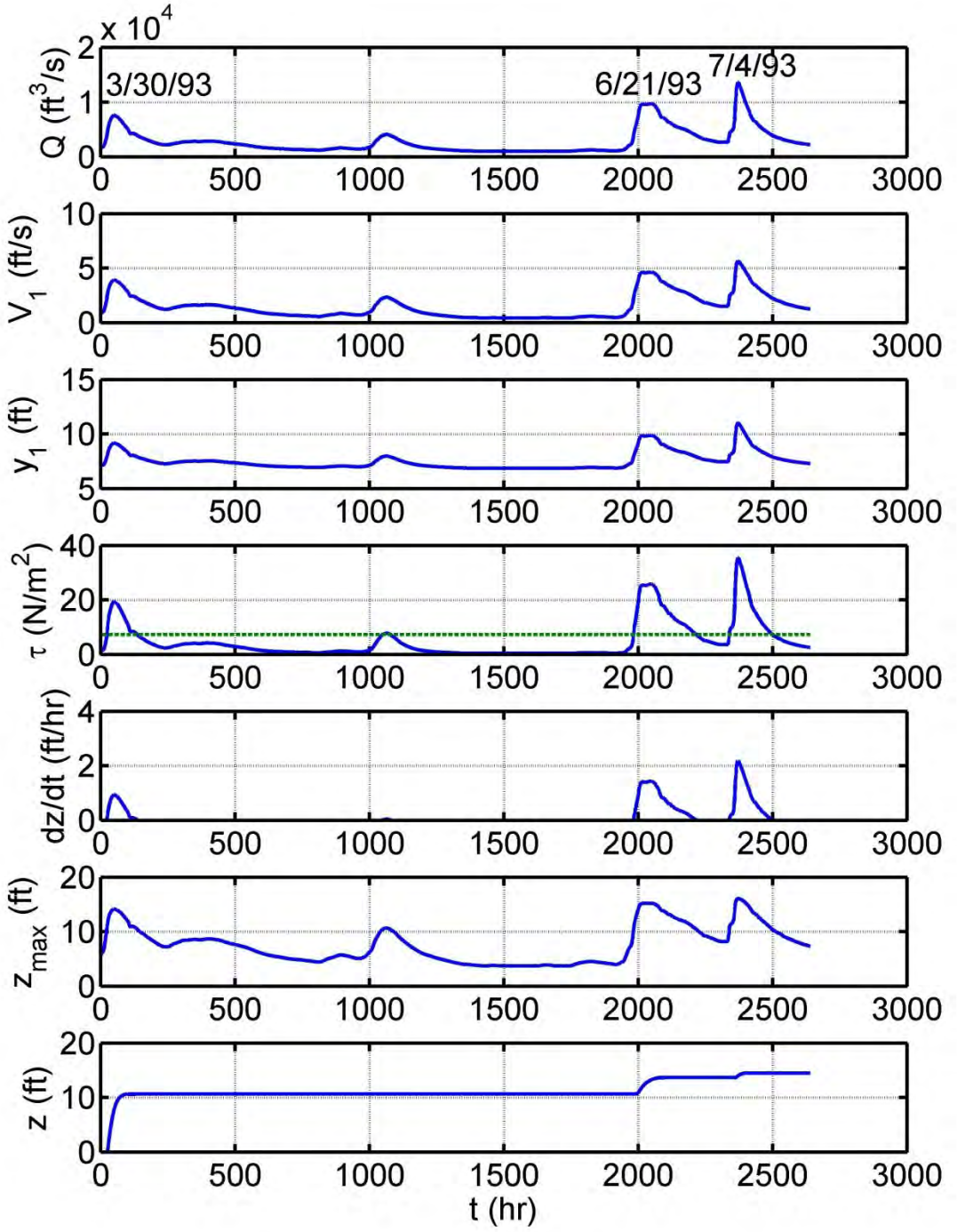

Figure 4.22 SRICOS simulation for Bent 2, March 28 to July 7, 1993 (ε = 0 mm)

Many researchers have commented on the accuracy of the EFA tests (e.g.,Trammell 2004, Annandale 2006). The main advantage of the EFA is that soil samples collected from a specified depth can be tested in this device at prototype flow velocities relatively "undisturbed." The current design, however, is not particularly accurate because the operator monitors the erosion and decides when to advance the soil sample. In addition, the applied shear stress is calculated using equations developed for pipe flows. When the soil surface erodes non-uniformly, vortices and eddies are formed on the irregular surface. The erosive action of the flowing water on the surface of an extremely rough sample can be quite different from that on a smooth surface. Also, it will be difficult to determine when the sample should be advanced. Consequently, there are large uncertainties in both the estimated shear stresses and measured erosion rates. These problems, however, did not occur with the very silty fine sand. This soil had a threshold velocity for erosion of about 1.9 m/s. Above the threshold velocity, the soil eroded particle by particle more or less uniformly so that it was relatively easy to decide when to advance the soil sample. Two sets of tests were completed on the same sample on two separate days. When plotted together, those results collapse on the same curve (see Figure 4.9), which gives confidence to the repeatability of the tests. Second, the soil surface eroded uniformly, which would have minimized the production of turbulence eddies. Since the soil eroding surface composed only about 2% of the surface area of the water tunnel, it is reasonable to assume that the effective roughness of the EFA was close to that of a smooth wall ($\varepsilon = 0$ mm); there was no justification for assuming a larger roughness height. As the curve for erosion rate versus shear stress for $\varepsilon = 1$ mm has produced results that better match the observed scour (see Figure 4.23), we can only conclude that the soil strata on the channel bed were more erosion resistant than the thin wall tube sample collected at a similar depth on the right abutment.

At the higher critical shear stress of 18.6 N/m^2, the predicted final scour depth becomes very sensitive to the approach flow velocity and somewhat sensitive to the flow angle of attack, but still relatively insensitive to the slope of the curve of erosion rate versus shear stress. For example, decreasing the approach flow velocity or flow angle of attack or slope of the curve of erosion rate versus shear stress curve by 10% will reduce the predicted final scour depth from 9.7 ft. to 6.3 ft., 9.1 ft. and 9.4 ft., respectively. The results for the second case are shown in Figure 4.23. At the discharge of 9,090 $ft.^3/s$, the observed flow angle of attack at Bent 2 is about 39° compared with 34° predicted by the 2D model (see Figure 4.12). Hence, we estimated that the 2D model over-predicts the flow angle of attack at Bent 2 by about 10%.

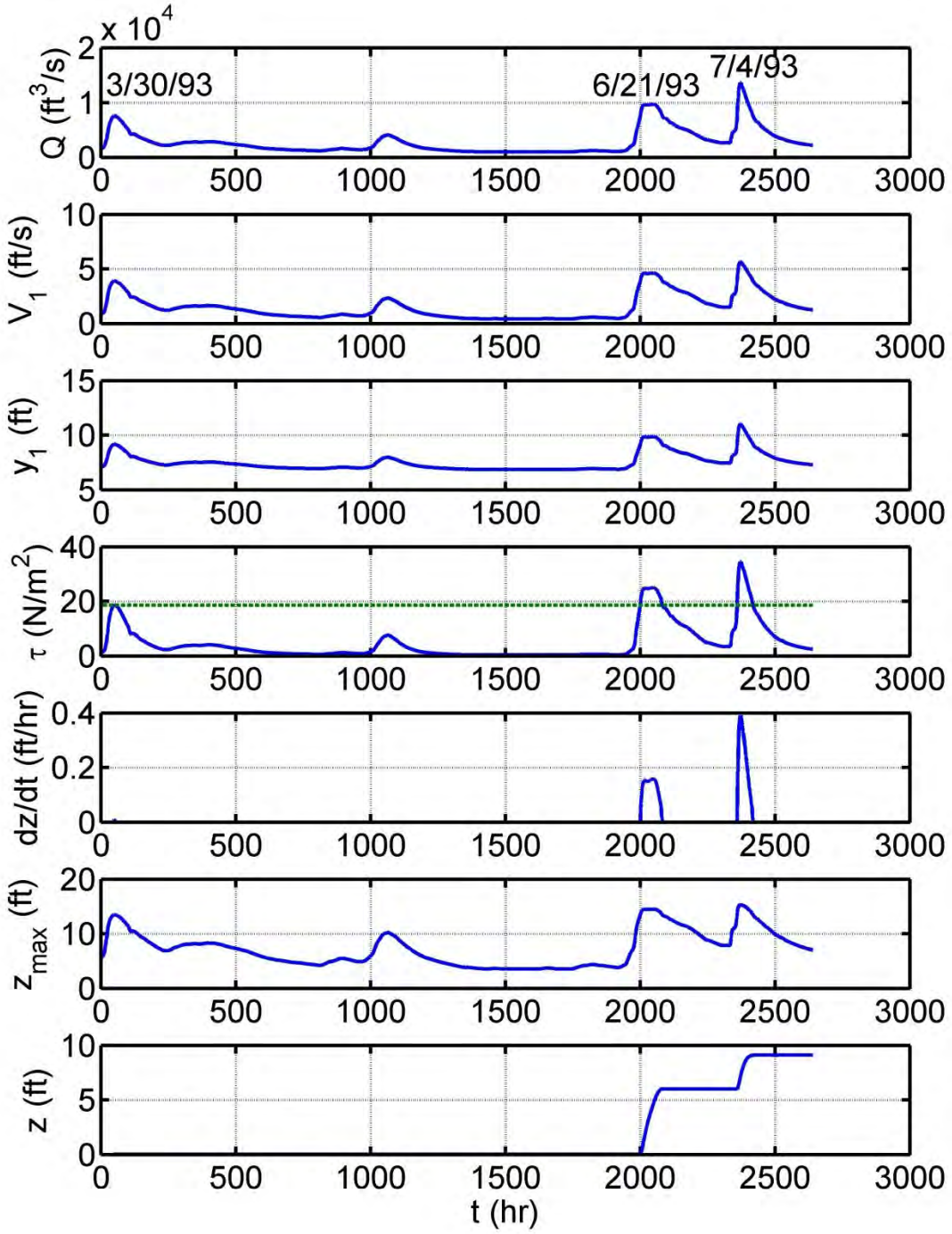

Figure 4.23 SRICOS simulation for Bent 2, March 28 to July 7, 1993 (ε = 1 mm)

The predicted scour history shown in Figure 4.23 is consistent with the observed scour. The scour at Bent 2 is produced entirely by the two larger floods on June 21 and July 4, 1993. The predicted final scour depth is very sensitive to the approach flow velocity because the initial bed shear stress is roughly proportional to the velocity squared [see Eq. (2.2)]. Decreasing the approach flow velocity will reduce both the equilibrium scour depth [see Eq. (4.1)] and the initial bed shear stress. The latter will reduce the rate of scour as well as the amount of time when the critical shear stress is exceeded. All of these factors

will act together to reduce the final scour depth. Decreasing the slope of the curve of erosion rate versus shear stress, however, will only reduce the time rate of scour. Hence, the critical shear stress and approach flow velocity are the two dominant parameters that influence the final scour depth for these flow and soil conditions.

We have also used the HEC-18 equation [Eq. (2.1)] instead of Eq. (4.1) to calculate the equilibrium scour depth. Eq. (2.1) was applied with $K_1 = K_3 = K_4 = 1$. When the equilibrium scour depths from Eq. (2.1) were used with SRICOS to predict scour, the predicted final scour depth was 9.8 ft., which is about 8% larger than the final scour depth of 9.1 ft. if Eq. (4.1) is used to calculate the equilibrium scour depths. We found that the HEC-18 equation generally predicts larger equilibrium scour depth compared with Eq. (4.1). For example, Eq. (2.1) predicts a maximum equilibrium scour depth of 18.1 ft. for the July 4, 1993, flood, compared with 15.3 ft. by Eq. (4.1). This is not surprising because the HEC-18 equation was developed as an "envelope" curve for use in design, whereas Eq. (4.1) is a "best-fit'' line to experimental data.

We have used the curve of measured erosion rate versus shear stress for organic silt collected from the left abutment and the rating curves for Bent 4 derived from the 2D model to predict local scour at the southern-most pier for the same floods. SRICOS predicts less than 1 ft. of pier scour for $\varepsilon = 0$ mm and no scour for $\varepsilon = 1$ mm, respectively (see Larsen 2010). These results are consistent with the measured channel cross sections shown in Figure 4.11.

4.7 Concluding Remarks

The two-dimensional depth-averaged river model FESWMS was used to predict velocity distribution at the SD 13 Bridge over the Big Sioux River at Flandreau, South Dakota. The Flandreau site has complex channel and floodplain geometry that produces unique flow conditions at the bridge crossing. The 2D model was calibrated using flow measurements obtained during two floods in 1993. The calibrated model was used to examine the hydraulic and geomorphic factors that affect the main channel and floodplain flows and the flow interactions between the two portions. A 1D flow model of the bridge site was also created in HEC-RAS for comparison. Soil samples were collected from the bridge site and tested in an EFA to determine the critical shear stress and erosion rate constant. The results of EFA testing and 2D flow modeling were used as inputs to the SRICOS method to predict local scour at the northern- and southern-most piers.

At the Flandreau site, concentrated flow develops upstream of the bridge crossing where the thalweg runs adjacent to the right bank. The thalweg is located around the center pier at the bridge crossing. Because the bridge crossing is located at a sharp bend, the concentrated channel flow is directed to the northern-most pier, which would not normally experience the observed high velocity if the channel were straight. The bridge is also located in a compound channel with asymmetric floodplains. At high flow, blockage caused by the roadway embankment forces the left floodplain flow back into the main channel just upstream of the bridge crossing. The exchange of flow between the main channel and left floodplain increases the flow velocity on the left side of the channel. Consequently, the flow concentration at the right bank appears diminished although concentrated flow still exists in the main channel upstream of the bridge. Because the relative amount of flow in the main channel and floodplain varies with discharge, it would be difficult to adjust the results of a 1D model to account for the 2D flow effects observed. A simple correction that may work for low to moderate flows would not yield the correct results at high flow. A 2D model satisfactorily predicts the flow concentration at the bridge crossing and provides insights into the effects of the channel bend and asymmetric floodplain on flow distribution. The study has also demonstrated that, because flow magnitude and flow angle of attack can change with the stage, it is important to evaluate the potential pier scour over the possible range of flood stages to determine the

worst-case scenario. In addition, because of the potential for thalweg migration, it would be prudent to apply the worst-case pier scour estimate to all the piers within the main channel.

Reliable flow data are crucial for accurate prediction of bridge scour depths. Hydraulic analysis of bridge waterways is commonly conducted using 1D river models such as HEC-RAS. One-dimensional models apportion flow based on conveyance and may not predict the velocity distribution accurately when 2D flow effects are important. This can have a significant effect on pier scour predictions. For example, Figure 4.14 shows that at a discharge of 10,000 ft.^{3}/s, the approach flow velocity at Bent 2 computed by HEC-RAS is about 65% of the prediction by FESWMS. When the water surface elevation and approach flow velocity computed by HEC-RAS and an estimated flow angle of attack of 30˚ were used to predict scour for the 1993 floods, SRICOS predicted no pier scour at Bent 2. It is clear that approach flow velocity is a critical input parameter in pier scour prediction using the SRICOS method. On the other hand, it is well known that the HEC-18 equation generally over-predicts scour, sometimes significantly, because it does not account for the slower rate of scour in cohesive soils. If Eq. (2.1) is used with the hydraulic parameters derived from the 2D model to predict scour, the maximum calculated equilibrium scour depth at Bent 2 for the July 4, 1993, flood will be 18.1 ft. (peak discharge = 13,633 ft.^{3}/s, y_1 = 11.0 ft., V_1 = 5.6 ft./s, θ = 30.7˚). Hence, using more accurate hydraulic input by itself does not necessarily improve scour predictions. Indeed, the predicted final scour depth may actually be more conservative (higher) if the larger flow velocity is computed by the 2D model rather than by the 1D model, even though the results from the 2D model may be more accurate. The benefits of using more advanced flow models for evaluating scour at bridges become apparent only when they are used in conjunction with more accurate methodologies for scour prediction.

Numerical testing was conducted to assess the variation in predicted scour depth due to variation in input parameters. It was found that the approach flow velocity and critical shear stress were the two most sensitive parameters. Uncertainty in critical shear stress was related to uncertainty about the soil types at the piers and uncertainty in the results of soil erosion rate testing. Thus, drilling and soil sampling should be conducted as close as practically possible to the bridge pier where the scour depth is to be predicted. This is not always feasible, and how to infer the soil stratigraphy at the pier from borehole data collected on the bridge abutments remains a challenge for geotechnical engineers. Still, the SRICOS method has produced scour estimates that are much closer to the measured scour than the HEC-18 method, since the latter does not account for the slower rates of scour in cohesive soils.

Eq. (4.1) predicts equilibrium scour depth that is about the same as that by the HEC-18 equation [Eq. (2.1)]. Although recent research has indicated that the equilibrium scour depth in cohesive soils may be less than that in non-cohesive soils, any empirical equations that relate the equilibrium scour depth to soil properties can be confidently applied only to the soils that were used to develop the equations. Hence, these equations may not be applicable to the soils at other bridge sites. The EFA only measures soil erosion rates. Without a reliable method to test soils from the bridge site to determine the equilibrium scour depth, it would be prudent to assume that the equilibrium scour depth is the same in cohesive and non-cohesive soils. This implies that the HEC-18 equation or other similar equations may also be used to calculate the equilibrium scour depth in SRICOS. Note that for cohesive soils, the SRICOS method would still produce more realistic scour depth than the HEC-18 method because the latter does not account for the rate of soil erosion.

5. HYDRAULIC AND SCOUR ANALYSIS, SD 37 BRIDGES OVER JAMES RIVER NEAR MITCHELL, SOUTH DAKOTA

5.1 Site Description

The SD 37 bridges (structure number 56-150-176 and 56-149-176) over the James River are located on South Dakota (SD) Highway No. 37 northbound and southbound, respectively, about 20 miles north of the city of Mitchell in southeast South Dakota. The bridges are both three-span, pre-stressed girder bridges, 353 ft. in length. The northbound bridge was built in 1992 and the southbound bridge in 2002. The bridges both have two pier sets with three 3.75-ft.-diameter cylindrical piers per set located on pilings. The bridge openings are classified as a spill-through abutment with two horizontal to one vertical slope embankment protected by riprap. The pier sets and abutments are skewed at an angle of 35° parallel to the general direction of the flow. The low-flow channel is confined between the pier sets.

The James River near Forestburg streamflow gaging station (site number 06477000) is located about 4.5 miles upstream of the bridge site and has a contributing drainage area of 15,549 miles^2. This station has been operated since 1950. The largest recorded peak discharge was 28,000 ft.^{3}/s on March 25, 2011. The predicted 2-, 100-, and 500-year peak discharges are 1,840, 27,100, and 46,500 ft.^{3}/s, respectively (Sando et al. 2008). The bank full capacity of the river is approximately equal to a 2.5-year event.

The United States Geological Survey (USGS) National Bridge Scour Team conducted real-time scour measurements at the bridge site during the flood of April 2001 (Wagner et al. 2006). Flow velocities and bed elevations were measured by using an acoustic Doppler current profiler (ADCP). The discharge measured by the USGS was 15,200 ft.^{3}/s, which is approximately a 25-year event (14,800 ft.^{3}/s). This data set was accessed through the National Bridge Scour Database (http://water.usgs.gov/osw/techniques/bs/BSDMS/) and used to validate the 2D flow model.

Figure 5.1 shows an aerial photograph of the bridge site. The James River flows west to east. The bridge crossing is located on a straight reach of stream between two meander loops. The river valley is approximately one-mile wide and bounded by high bluffs. The floodplains are composed primarily of farmland and pasture, but the left overbank in the meander upstream and downstream of the parallel bridges is heavily vegetated by trees. The channel slope in this reach averages about 0.5 feet per mile. As the channel meanders across the floodplain, exchange of flow takes place repeatedly between the left and right floodplains. Because all of the floodplain flow contracts through the bridge openings, the site has a large potential for scour. Figures 5.2 through 5.6 show pictures of the bridge site taken by Francis Ting on March 24, 2011, near the peak of a 100-year event.

Figure 5.1 Aerial photograph of the SD 37 bridges over the James River north of Mitchell, South Dakota (image courtesy of United States Geological Survey)

The bathymetric and topographic data used for constructing the 1D and 2D flow models were obtained from the USACE Omaha District. The data were collected by Horizons, Inc. of Rapid City, South Dakota, in the fall of 2002 in support of a flood damage reduction study being performed on the James River in South Dakota.The land-surface elevation data were acquired from an aircraft using a LiDAR system. The mapping procedures were such as to provide a map scale of 1:2400 with a 2-ft. contour interval. LiDAR is unable to provide a profile of the channel because it cannot penetrate the water. The bathymetric data were collected from a boat using a single beam sounder and then merged with the LiDAR data into a combined data set. The elevation data were developed using the South Dakota State Plane Coordinate System. The horizontal and vertical projections were the North American Datum of 1983 (NAD 83) and North American Vertical Datum of 1988 (NAVD 88), respectively.

Figure 5.2 Bridge crossing from right bank facing along upstream face of southbound bridge toward left bank

Figure 5.3 Bridge crossing from right bank facing Bent 2 of southbound bridge

Figure 5.4 Bridge crossing from right bank facing along downstream face of northbound bridge toward left bank

Figure 5.5 From right bank facing the downstream 90º bend and the floodplain beyond

Figure 5.6 From the high bluff in the north overlooking the river and inundated floodplain

In addition to the surveys in 2001 and 2002, the USGS and SDDOT conduct stream flow gaging and scour monitoring at the bridge site regularly. Figures 5.7 and 5.8 show the measured channel cross sections at the southbound and northbound bridges between 2001 and 2011. At the upstream face of the southbound bridge, measured pier scour depths are 4 to 5 ft. at Bent 3 and 2 to 3 ft. at Bent 2. The local scour was most likely developed during the flood of May 2007, which was the first major flood event to occur after the bridge was built. At the downstream face of the southbound bridge, the depth of scour at both piers is about 2 ft. Additionally, there are 4 to 5 ft. of channel bed aggradation at the upstream face of the bridge between 2002 and 2006 and 2 to 3 ft. of bed degradation at the downstream face between 2002 and 2004. Up to 2 ft. of increase and decrease in channel bed elevation has been measured at the northbound bridge since 2002.

The bathymetric data that were merged with the LiDAR data have a more pronounced V-shaped channel than the other data due to fewer data points in the channel. Depending on the width and depth of the river, the bathymetry survey was conducted either in multiple profiles along the river or in a zigzag pattern in narrow areas. The data collection errors were about 0.5 ft. in elevation. The uncertainty in channel bed elevation amounts to only a few percent of the local water depth. Hence, the V-shaped curve does not affect the results of the 2D flow analysis. It was found that the alignment of the floodplain relative to the channel and bridge crossings has more effects on the hydraulic conditions than the uncertainty in the floodplain and channel elevations..

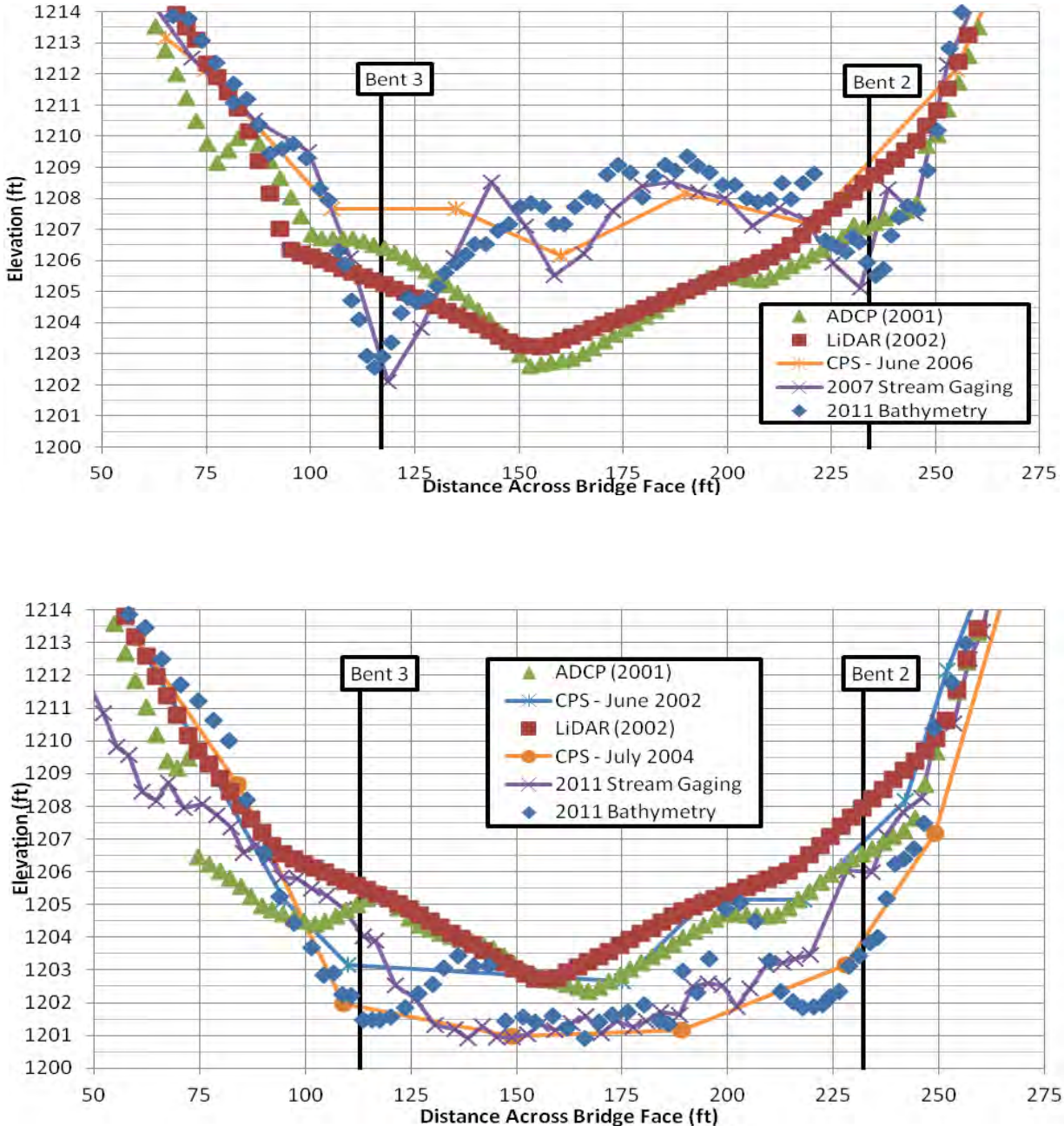

Figure 5.7 Measured channel cross sections at upstream (upper plot) and downstream (lower plot) faces of southbound bridge between 2001 and 2011

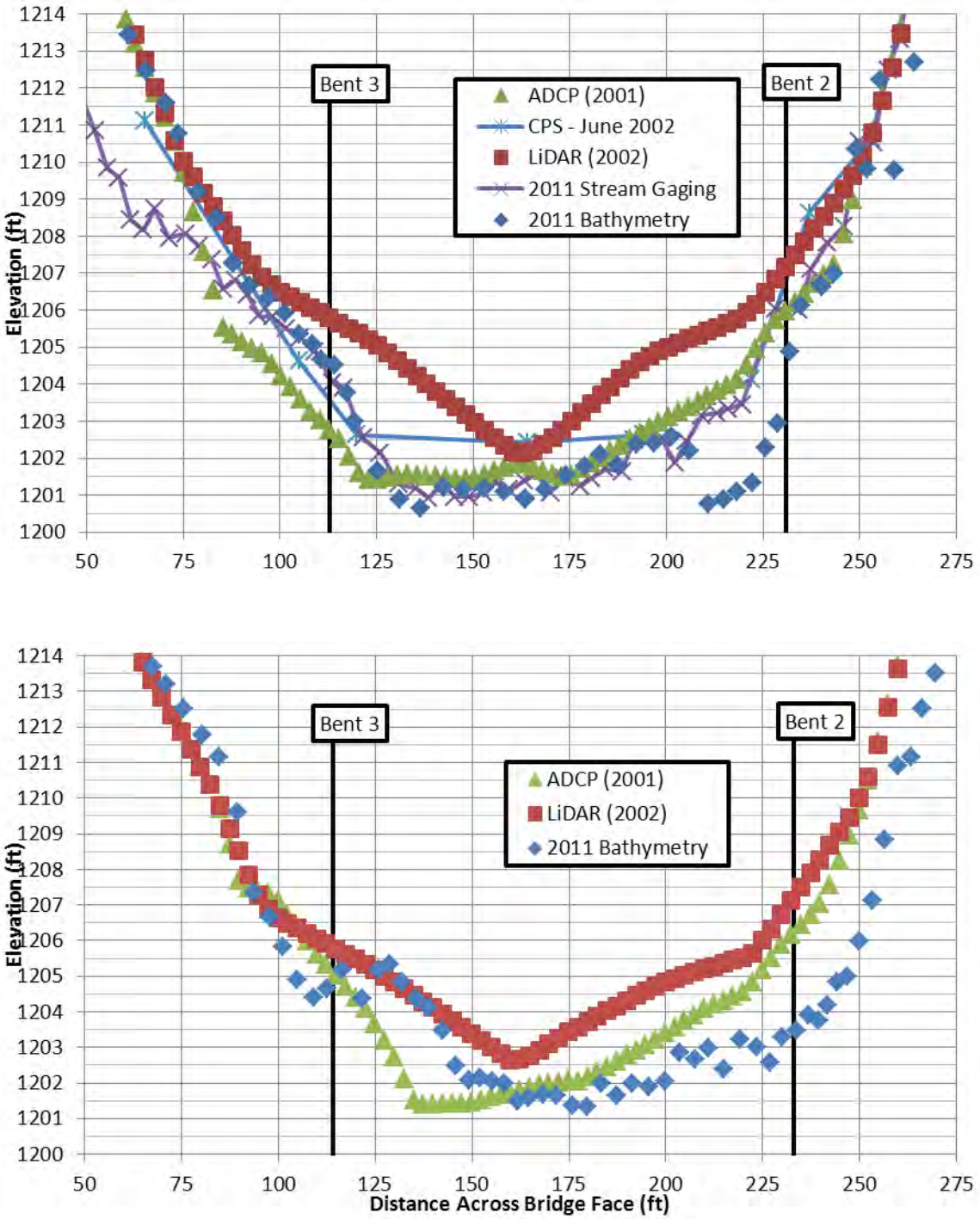

Figure 5.8 Measured channel cross sections at upstream (upper plot) and downstream (lower plot) faces of northbound bridge between 2001 and 2011

One boring was completed on the north abutment between the northbound and southbound bridges on March 8, 2012, by SDDOT. The soil materials that were observed during drilling included approximately 25 ft. of clay and silt overlying 10 ft. of silt and sand. Coarse sand and gravel were encountered at a depth of 35 ft. Two thin wall tube samples were collected from the drill hole at depths of 24 to 26.5 ft. and 29 to 31.5 ft. A third sample was collected by Francis Ting and Ryan Rossell near the left edge of the water just upstream of the southbound bridge on November 17, 2011, when the measured daily mean flow was 2,810 $ft.^3/s$. This sample consisted primarily of a mildly cohesive clayey-silt.

5.2 Flow Model

A 2D flow model of the bridge site was created in SMS using the numerical model FESWMS. Figure 5.9 shows the area modeled and the material types. The upstream and downstream boundaries were located where the channel is relatively straight; the distance from the bridge crossings is approximately 5,000 ft. and 6,000 ft., respectively. The left and right boundaries were located at the elevation of the 100-year flow. The bridge crossings were modeled as parallel bridges. In the active flow areas, high elevation gradients exist along the bridge abutments, roadway embankment, and where the floodplain boundaries are close to the main channel. In these areas, mesh elements were constructed to run parallel to the elevation contours so that boundary elements would become dry in a uniform fashion. Note that the roadway is not overtopped in any of the floods, but the high Manning's *n* value helped to keep flow velocities low as elements became dry during computation. To add model stability, drying elements that could destabilize the surrounding elements were turned off manually as the model was spun down to the final flow boundary conditions. Details of 2D model construction and steering are described in Rossell (2012).

LiDAR data have a vertical resolution of approximately 1 ft. The existing National Elevation Dataset (NED) has a vertical resolution of about 10 ft. A second 2D flow model of the bridge site was created using 1/3 arc-second NED data. When the two datasets were compared, the NED data has a deeper main channel (2 to 7 ft.) and higher elevations (about 2 ft.) in the floodplains compared with the LiDAR data, but closer to the bridges the differences are not as large. The biggest difference between the two data sets is the channel migration downstream of the bridge crossings. Figure 5.10 shows elevation contours derived from the NED data collected between 1920 and 1959 overlaid on a 2008 photograph of the bridge site. Notice that the downstream meander loop has migrated laterally down the river valley over time.

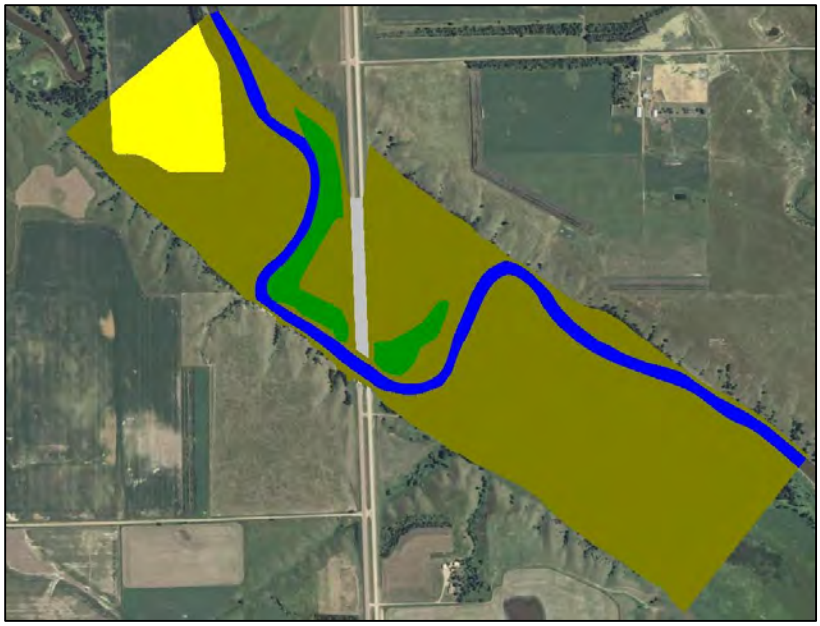

Figure 5.9 Study area modeled in FESWMS and the material types: main channel (blue), floodplain (brown), trees (green), cultivated areas (yellow), and roadway (grey); the corresponding Manning's *n* values are 0.035, 0.04, 0.12, 0.03, and 0.5, respectively

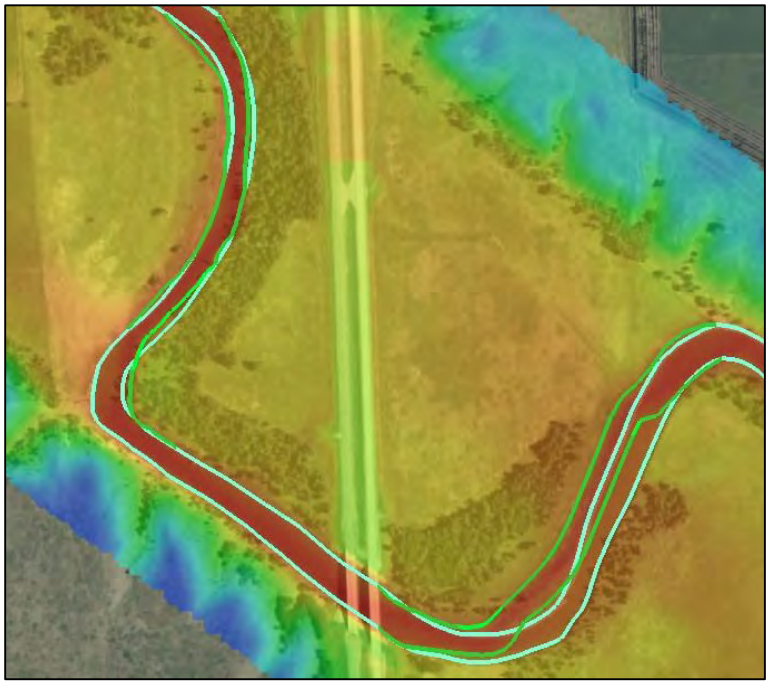

Figure 5.10 Outline of main channel depicted in recent photograph (blue lines) and older NED data (green lines) showing migration of meander loop downstream of the bridge crossings

To create a 1D model for comparison, 26 channel cross sections were extracted from the 2D model and inserted into HEC-RAS. The locations of the HEC-RAS cross sections are shown in Figure 5.11. Ineffective flow areas were placed at the cross sections adjacent to the bridges to mimic the flow contraction and expansion predicted by the 2D model. The Skew Cross Section option in HEC-RAS was

selected to compute the equivalent cross sections perpendicular to the flow. In both the 1D and 2D models, flow discharge was specified at the inflow boundary and normal depth at the outflow boundary unless stated otherwise. The average channel slope (0.000104) was entered into HEC-RAS to calculate the normal depth.

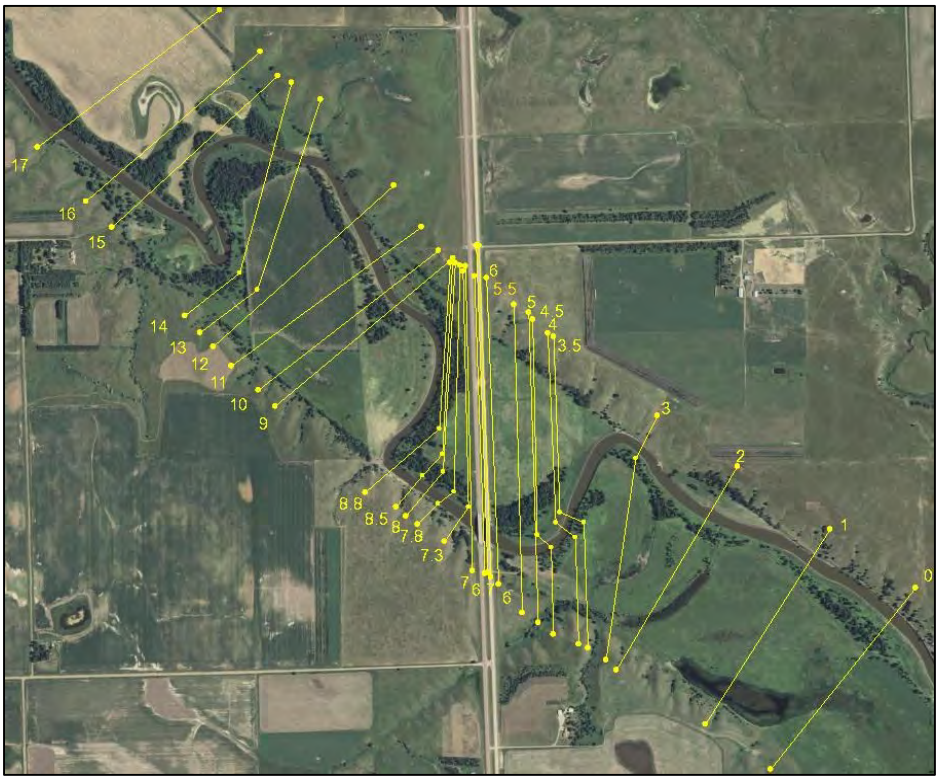

Figure 5.11 Location of HEC-RAS cross sections

The 2D model was validated using flow measurements collected on April 15, 2001, (15,200 ft.^{3}/s), May 8, 2007, (20,800 ft.^{3}/s), and March 24, 2011, (27,100 ft.^{3}/s), which correspond approximately to the 25-, 50-, and 100-year flows, respectively. In order to compare flow velocities, the computed water surface elevation (WSEL) at the bridge (northbound or southbound) was matched to the measured elevation for each discharge by adjusting the unknown WSEL at the outflow boundary. A sensitivity analysis was conducted to examine the effects of varying the Manning's *n* values and downstream WSEL on the modeling results.

5.3 Scour Model

Contraction scour was evaluated at the bridge site using the live-bed and clear-water scour equations in HEC-18 (Arneson et al. 2012) and a method modified from Güven et al. (2002). In clear-water scour, scour depth will increase until the bed shear stress is equal to the critical shear stress of the bed material. The HEC-18 method only calculates the equilibrium scour depth, whereas the method by Güven et al. (2002) computes scour depth as a function of time. Their method is based on energy balance between the contracted section (2) at the bridge crossing and the downstream section (3) where the flow is fully expanded. The model assumes uniform velocity distributions, constant discharge, and constant head loss between sections 2 and 3. In addition, the total head at Section 3 is assumed to remain constant during the development of scour in the contraction. We modified their model by allowing both head loss and

discharge to vary with time. For a constant discharge, the time rate of change of flow depth in the contraction can be expressed as (Rossell 2012):

$$\frac{dy_2}{dt} = \frac{R(\tau)}{\left[1-(1-C)\frac{q^2}{gy_2^3}\right]} \tag{5.1}$$

where q = unit discharge, g = acceleration of gravity, C = expansion loss coefficient (≈ 0.5), and $R(\tau)$ = time rate of scour as a function of bed shear stress τ. The latter is calculated as:

$$\tau = \frac{\rho g n^2 q^2}{y_2^{7/3}} \tag{5.2}$$

where ρ = fluid density and n = Manning's coefficient. The scour depth in the contraction, y_s, is given by (cf., Güven et. al. 2002):

$$y_s = y_2 + (1-C)\frac{q^2}{2gy_2^2} - \left(y_0 + (1-C)\frac{q^2}{2gy_0^2}\right) \tag{5.3}$$

where y_0 = initial flow depth in the contraction before scour.

Starting with $y_2 = y_0$ and $y_s = 0$, the bed shear stress is calculated using Eq. (5.2) and the corresponding soil erosion rate $R(\tau)$ is computed using a curve of measured erosion rate versus shear stress. The time rate of change of flow depth in the contraction dy_2/dt is found using Eq. (5.1). The new flow depth is then calculated as $y_2 + dy_2/dt \cdot \Delta t$ and the new scour depth as $y_s + R(\tau)\cdot\Delta t$, where Δt is length of time step. This procedure is repeated to give the variations of bed shear stress, flow depth and scour depth as a function of time.

To calculate contraction scour for unsteady flows, the above algorithm is applied to each time step of the hydrograph. The flow depth at the beginning of a time step is found for the corresponding discharge by using a rating curve derived from the 2D model. This flow depth is revised to account for the increase in flow depth in the contraction due to pre-existing scour. Assume the total head downstream at Section 3 is not affected by scouring in the contraction, the flow depth with pre-existing scour, y_A, can be related to the flow depth from the rating curve, y_B, by (Rossell 2012):

$$y_A = y_B + y_s + (1-C)\frac{q^2}{2g}\left(\frac{1}{y_B^2} - \frac{1}{y_A^2}\right) \tag{5.4}$$

where y_s = pre-existing scour depth at the beginning of the new time step, and q = unit discharge at the new time step. Note that $y_A \approx y_B + y_s$ if the change in velocity head in the contraction due to scouring is small.

To obtain the soil erosion function $R(\tau)$, a tilting flume with a fixed gravel bed was used to create a fully developed, uniform turbulent flow. A 3-in. diameter, 0.75-in. long sample extruded from the thin wall tube was placed in a circular recess in the flume floor. A uniform flow was created, and the depth of soil eroded after a length of time ranging from 15 minutes to one hour was measured using a point gage to estimate the soil erosion rate. The bed shear stress was calculated from the measured water depth and channel slope. The test results for the clayey silt from the main channel are shown in the top plot of Figure 5.12. This soil has very high erosion rates and might have been deposited recently. The critical shear stress for initiation of sediment motion is between 5 and 6 N/m^2. The test results for the high plasticity clay from the north abutment are shown in the bottom plot. The maximum shear stress applied was about 24 N/m^2. Except for small pockets of sand, which eroded rapidly, the clay hardly eroded. In the scour analysis, the critical shear stress and slope of the curve of erosion rate versus shear stress were varied to examine the effects of these soil parameters on the predicted scour depth.

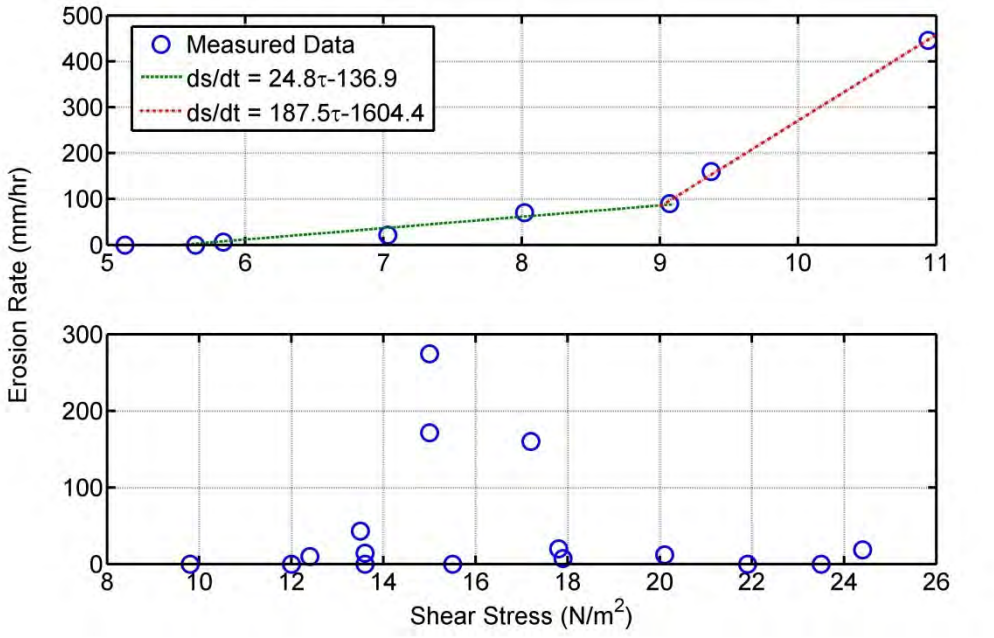

Figure 5.12 Variations of measured soil erosion rate with bed shear stress for mildly cohesive clayey silt (top plot) and clay/silt (bottom plot)

5.4 Model Validation

The 2D model was first validated using the ADCP measurements collected by the USGS on April 15, 2001. Computed and measured flow velocities were compared along 15 transects, shown in Figure 5.13, throughout the reach extending upstream and downstream of the bridge crossing. The measured discharge at the time of ADCP measurements was 15,200 ft.^{3}/s, which is approximately a 25-year event. The computed WSEL at the northbound bridge was matched to the measured elevation of 1225.1 ft. by adjusting the unknown WSEL at the outflow boundary in the 1D and 2D models.

Figure 5.13 Location of ADCP measurements in April 2001 used for validation of 2D flow model

Figures 5.14 through 5.18 show the results for transects 19, 14, 11, 23, and 22. The results for the remaining cross sections can be found in Rossell (2012). Transect 19 is located 645 ft. upstream of the northbound bridge. The LiDAR 2D model correctly predicts a flow concentration on the right side of the channel with a maximum velocity equal to about 6 ft./s (Figure 5.14). The observed flow concentration is not predicted by the 1D model. In addition, the 1D model apportions more flow to the floodplain, and thus significantly under-estimates the flow velocities in the main channel. The NED 2D model correctly predicts the location of the concentrated flow, but under-predicts the maximum velocity by about 1 ft./s. Similar results can be seen at transect 14 (Figure 5.15) located 342 ft. upstream of the bridge. The agreement between 1D model and ADCP measurements is better at transect 11, 48 ft. upstream of the northbound bridge (Figure 5.16). At this location, almost all of the flow is in the main channel.

The good agreement between the LiDAR 2D model and ADCP measurements suggests that the LiDAR model having the channel in more of a V shape does not affect the modeling results. The uncertainty in channel bed elevation is small compared with the water depth.

The NED 2D model was developed using older topographic data collected before the downstream meander loop had migrated (see Figure 5.10). Because of this, the computed velocity distribution from the model does not match the ADCP measurements downstream of the bridge crossing (see Figures 5.17 and 5.18). Transect 23 is located 403 ft. downstream of the bridge just before the 90° bend. At this location, the measured velocity distribution is more uniform and predicted well by both the LiDAR 1D and 2D models (Figure 5.17). However, the boundaries of ineffective flow areas in the 1D model were determined by examining the flow pattern predicted by the 2D model. Without the 2D model, the 1D model would not be able to predict the flow velocities correctly. Figure 5.17 shows that the 1D model predicts much lower flow velocities in the main channel compared with the ADCP measurements when ineffective flow areas are not included in the model.

As the main channel turns to the north, a flow concentration reappears on the right side of the channel. This can be seen in transect 22, which is located just after the 90° bend. The LiDAR 2D model predicts a steady increase in flow velocity toward the right bank in agreement with the ADCP measurements, whereas the 1D model predicts nearly uniform velocity in the main channel (Figure 5.18).

The LiDAR 2D model was also validated for higher discharges (20,800 and 27,100 $ft.^3/s$) using velocity measurements collected at the southbound bridge. The complete results can be found in Rossell (2012).

Figure 5.19 shows the comparison between modeling results and ADCP measurements for the discharge of 27,100 ft.^{3}/s, which is a 100-year event. As with the 25-year event, the LiDAR 2D and NED 2D models both predict a flow concentration on the right side of the channel, but the maximum velocity predicted by the NED 2D model is about 1 ft./s lower compared with the LiDAR 2D model.

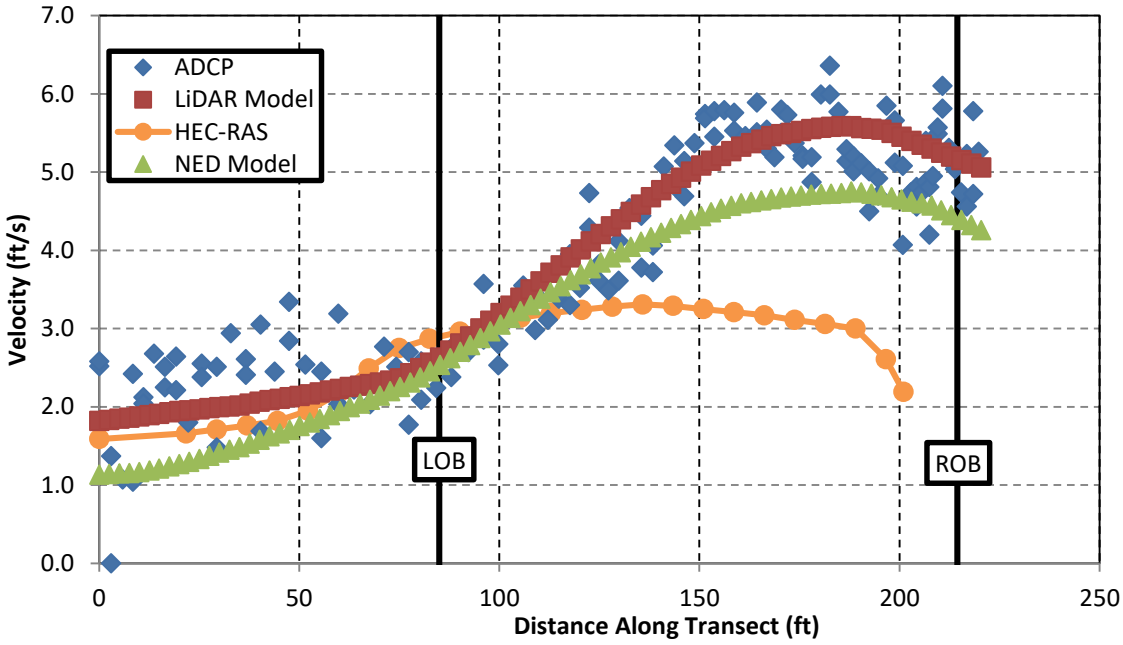

Figure 5.14 Measured and computed distributions of flow velocity magnitude along transect 19

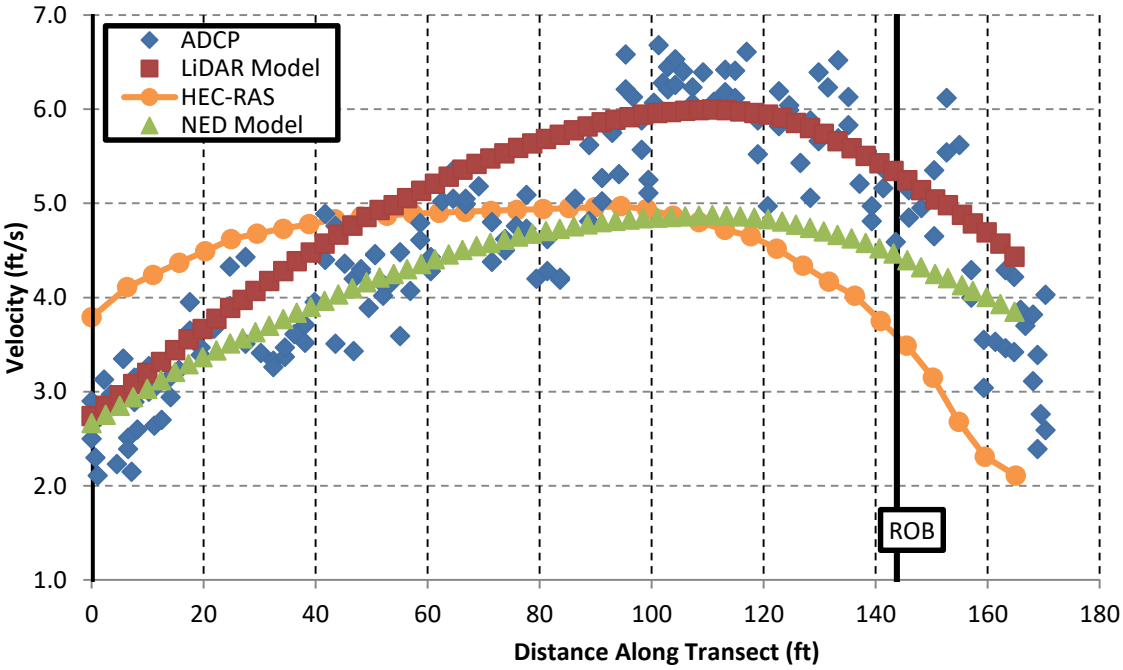

Figure 5.15 Measured and computed distributions of flow velocity magnitude along transect 14

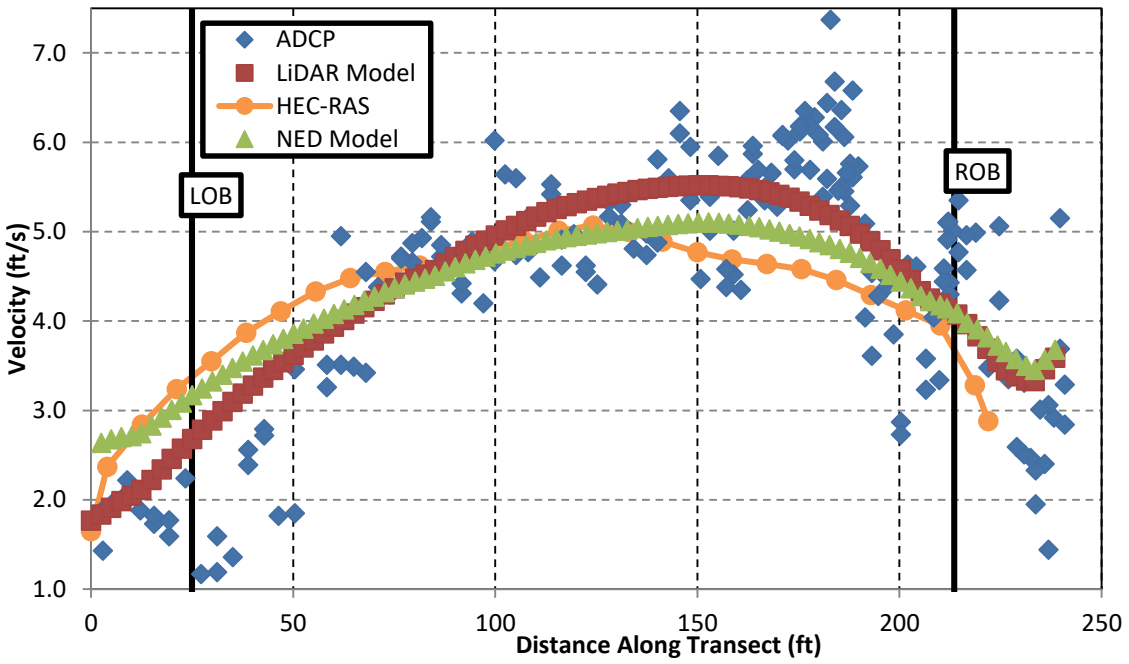

Figure 5.16 Measured and computed distributions of flow velocity magnitude along transect 11

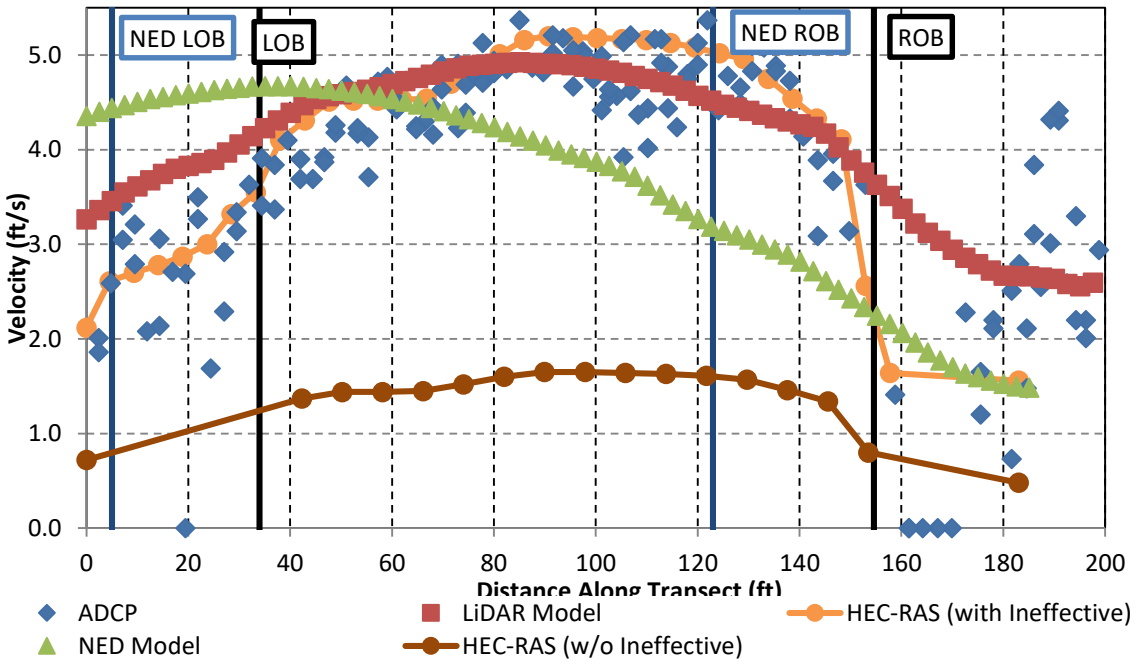

Figure 5.17 Measured and computed distributions of flow velocity magnitude along transect 23

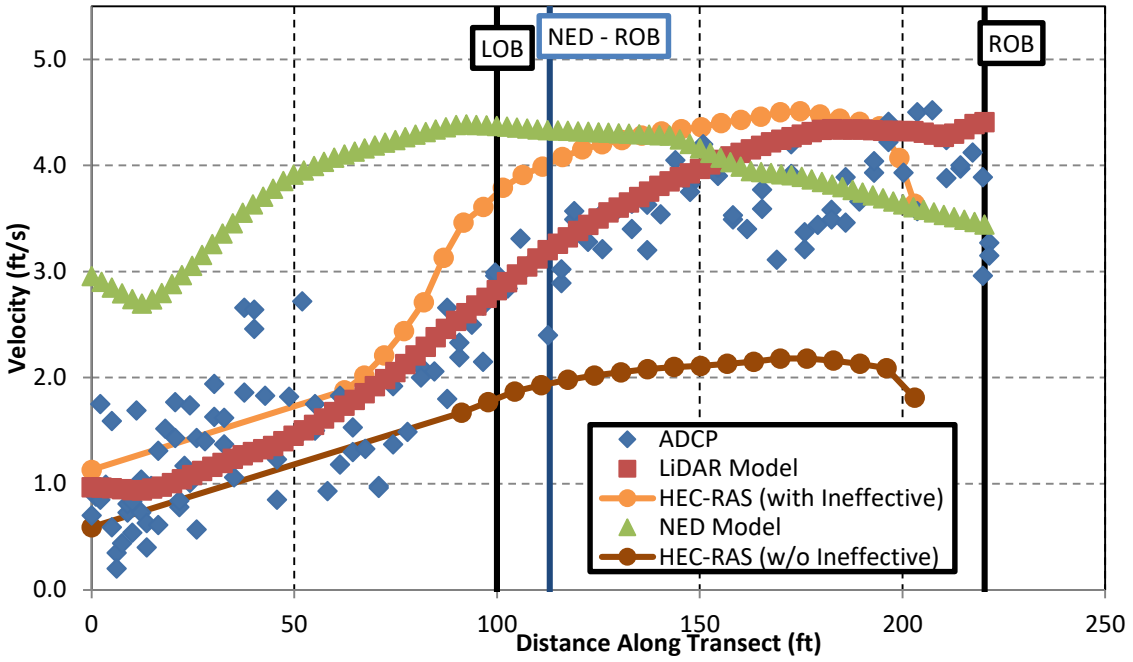

Figure 5.18 Measured and computed distributions of flow velocity magnitude along transect 22

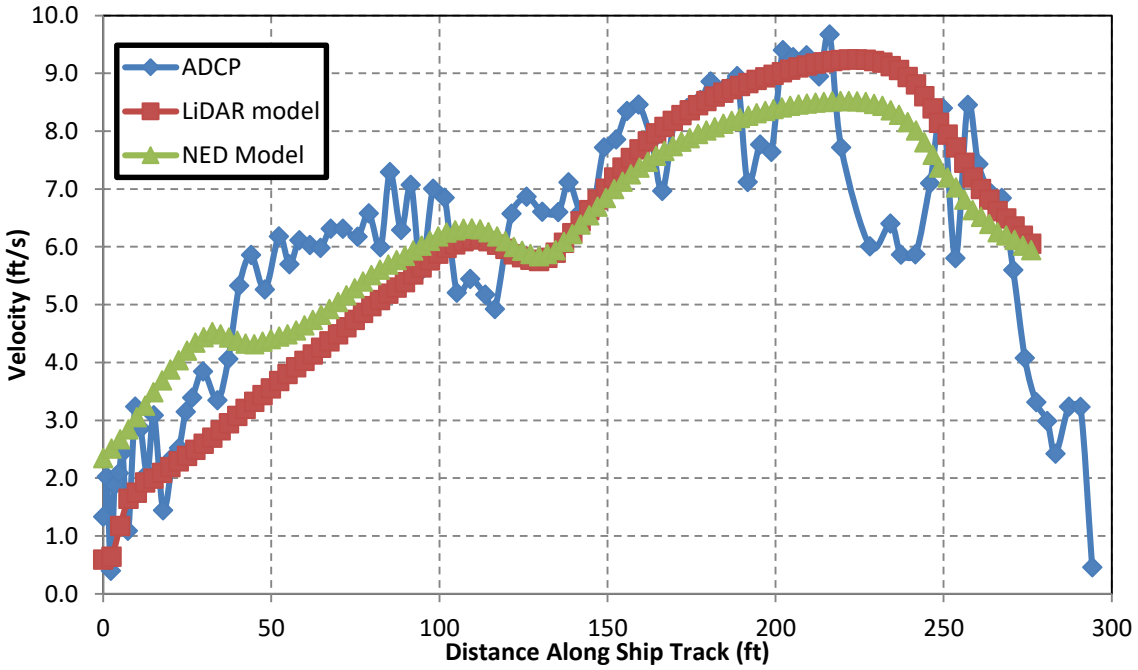

Figure 5.19 Measured and computed distributions of flow velocity magnitude at southbound bridge for discharge of 27,100 ft.^{3}/s

A sensitivity analysis of the LiDAR 2D model was conducted for the discharges of 15,200 and 27,100 $ft.^3/s$. The Manning's *n* values for the main channel, floodplain, and dense tree material types were varied. Additionally, for the 100-year event, the specified downstream WSEL was varied. The results, when examined in different channel cross sections between the upstream bend and northbound bridge, were similar for both discharges. It was found that varying the main channel or floodplain, Manning's value by $\pm 20\%$ changed the peak velocity by only about $\pm 5\%$ and the water surface elevation by less than $\pm 2\%$. Varying the Manning's value of the dense trees by $\pm 20\%$ produced negligible effects on the flow conditions at the bridge, but changed the maximum velocity in the approach flow by up to $\pm 10\%$. The downstream WSEL affects the modeling results most. Increasing the downstream WSEL will decrease both the discharge and velocities in the main channel and vice versa. For the 100-year event, when the downstream WSEL was varied from -1.5 to +1.5 ft. (approximately $\pm 8\%$ of normal depth) relative to the normal depth, the flow depth at the northbound bridge increased from 22.8 to 25.0 ft. and the maximum velocity decreased from 9.5 to 8.2 ft./s. However, to match the computed and measured WSELs at the bridge for the 50- and 100-year events, the downstream WSEL only has to be varied by 0.3 ft. or less from the normal depth. Hence, the WSEL in the vicinity of the bridge crossings are predicted accurately for the high-flow events by specifying the normal depth at the downstream boundary. Detailed results from the sensitivity analysis can be found in Rossell (2012).

5.5 Geomorphic Factors

Computed results from the 2D model suggest that flow returning from the left floodplain and the high bluffs along the right bank produce the concentrated channel flow upstream of the SD 37 bridges. Figure 5.20 shows the computed flow pattern for the 25-year peak flow. At this discharge, the floodplain carries about 80% of the total flow. The upstream meander loop causes the main body of flow to shift from the right to the left floodplain and also brings the main channel close to the right floodplain boundary. The roadway embankment then forces the left overbank flow back into the main channel between the upstream bend and bridge crossings. The contracted flow enters the channel at an angle of around 60°, and the high bluffs re-direct this flow along the right bank. The velocity distribution becomes more uniform after the bridge crossings, but concentrated flow again develops around the downstream bend due to the natural momentum of the flow to leave the channel and enter the right floodplain instead of turning through the bend. Areas of high flow velocities are susceptible to erosion. As shown in Figure 5.10, the downstream meander loop has migrated laterally down the river valley over time.

Figure 5.20 Computed flow pattern for 25-year peak flow; the range of flow velocities is from ≈ 0 (red) to 6.5 ft./s (dark blue)

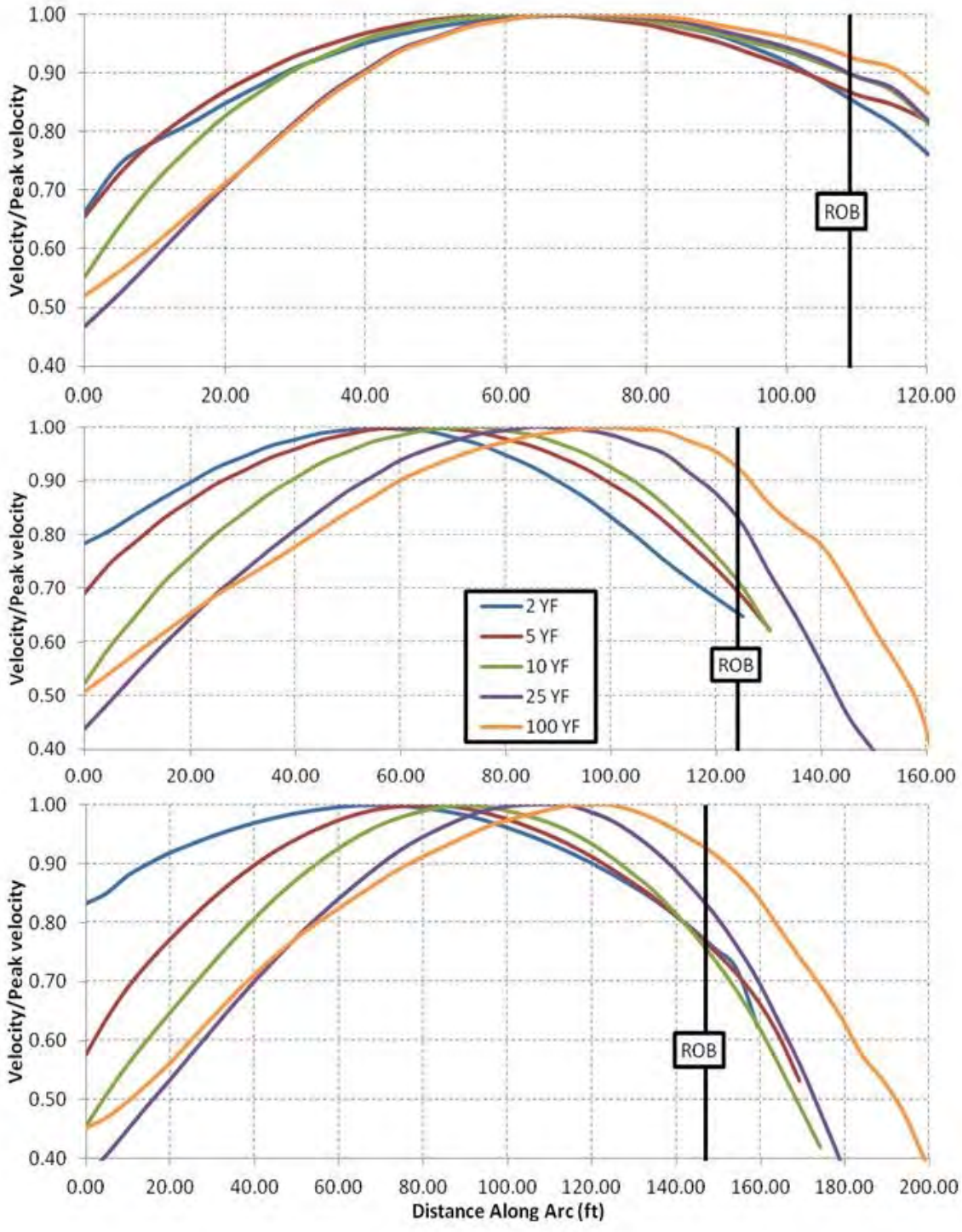

Figure 5.21 Normalized velocity distributions for 2-, 5-, 10-, 25-, and 100-year peak flows from LiDAR 2D model at 987 ft. (top plot), 615 ft. (middle plot), and 210 ft. (bottom plot) upstream of the southbound bridge

The 2D model predicts that the concentrated channel flow upstream of the parallel bridges is influenced by discharge and the presence of dense trees in the left overbank. Figure 5.21 shows the computed velocity distributions in the main channel at three locations (210, 615, and 987 ft.) upstream of the southbound bridge for various discharges up to the 100-year flood. The computed velocities have been normalized by the maximum velocity at each discharge. As the discharge increases, the flow concentration is shifted more toward the right bank. In the top plot, the maximum velocity is found approximately 40 ft. from the right bank for all of the discharges. In the middle and bottom plots, the maximum velocity is found approximately 70 ft. and 25 ft. from the right bank for the 2- and 100-year peak flows, respectively.

Figure 5.22 shows the computed velocity distributions 210 ft. upstream of the southbound bridge for the 100-year peak flow with and without the dense trees in the left overbank. When the dense trees are removed, flow velocities decrease in the main channel and increase in the left floodplain. Consequently, the flow concentration in the main channel becomes less pronounced, although the location of maximum velocity remains at about the same location.

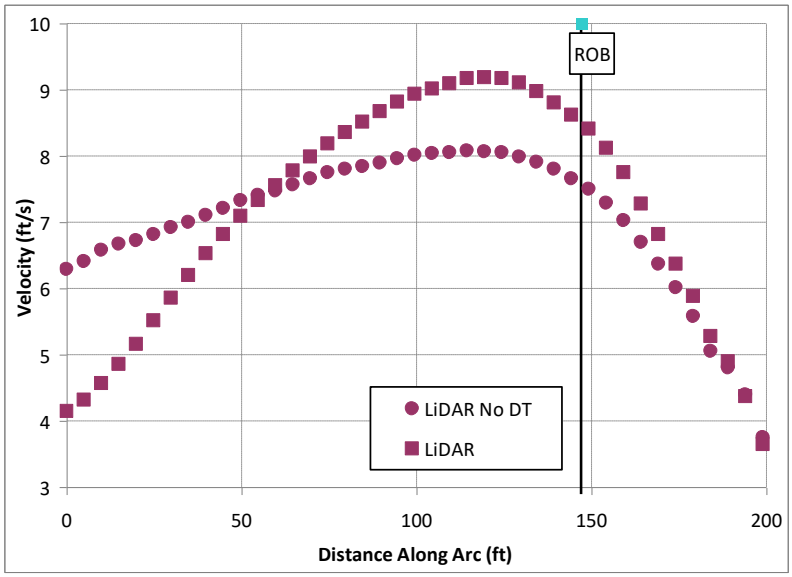

Figure 5.22 Effect of dense trees (DT) on computed velocity distribution at 210 ft. upstream of southbound bridge for the discharge of 27,100 ft.^{3}/s

Figure 5.23 shows the partition of flow between the main channel and left and right floodplains for the 2-, 5-, and 10-year peak flows. The results for the 25-, 50-, and 100-year peak flows are shown in Figure 5.24. The discharge in each portion Q has been normalized by the total discharge Q_T. In both figures, Beg Do and End Do mark the beginning and end of the upstream meander loop, Beg Up and End Up mark the same for the downstream meander loop, and BR denotes the northbound bridge. The abscissa is the main channel distance in feet from the downstream boundary of the model. Referring to Figure 5.23, the flow is primarily confined to the main channel ($Q/Q_T > 0.9$) for the 2-year flow. For the 5- and 10-year flows, the main channel flow decreases and the flow in the right floodplain increases as the discharge increases. The flow in the left floodplain is relatively small, typically less than 20%. For both the 5- and 10-year flows, there is some flow exchange between the main channel and floodplains around the upstream and downstream bends (End Do and Beg Up). Along the upstream meander loop (Beg Do to End Do), flow leaves the right floodplain and primarily enters the main channel, although some flow (< 20%) also enters the left floodplain in the case of the 10-year flow. Downstream of the bridge crossing,

the flow is primarily in the main channel for both the 2- and 5-year flows. For the 10-year flow, about 40% of the flow is re-established across the right floodplain.

For the 25-, 50-, and 100-year peak flows (Figure 5.24), about 80% of the total flow is in the right floodplain at the beginning of the upstream meander loop (Beg Do). Along the upstream meander loop, flow is exchanged between the left and right floodplains while the discharge in the main channel remains nearly constant. At the end of the upstream meander loop (End Do), the left floodplain flow begins to contract into the main channel, and the main channel flow ratio Q/Q_T increases rapidly as one approaches the parallel bridges. Downstream of the parallel bridges, some overbank flow is re-established in the left floodplain, but most of the flow exchange takes place between the main channel and right floodplain along the downstream meander loop (Beg Up to End Up). The flow ratio in the right floodplain increases as the discharge increases. Downstream of the meander, the discharge in the main channel is nearly constant; the percentage of flow carried by the main channel is about 30% for the 25-year flow and 20% for the 100-year flow.

Figure 5.25 shows the computed hydraulic grade lines (HGL) and energy grade lines (EGL) along the main channel for the 100-year peak flow. The LiDAR 2D model predicts that most of the changes occur in the straight reach between the upstream and downstream meander loops (End Do to Beg Up); the changes in both WSEL and total head are about 2 ft. Large head loss in the reach is associated with high flow velocities in the main channel. The 1D model predicts bridge backwater about 0.7 ft. higher than the 2D model. However, the results of the 1D model are very sensitive to the placement of ineffective flow areas. Difficulties with defining ineffective flow areas can produce large uncertainties in bridge backwater calculations as well as approach flow velocities, both of which are important parameters for scour prediction. The NED 2D model predicts backwater elevation that is about 0.5 ft. lower than the LiDAR 2D model.

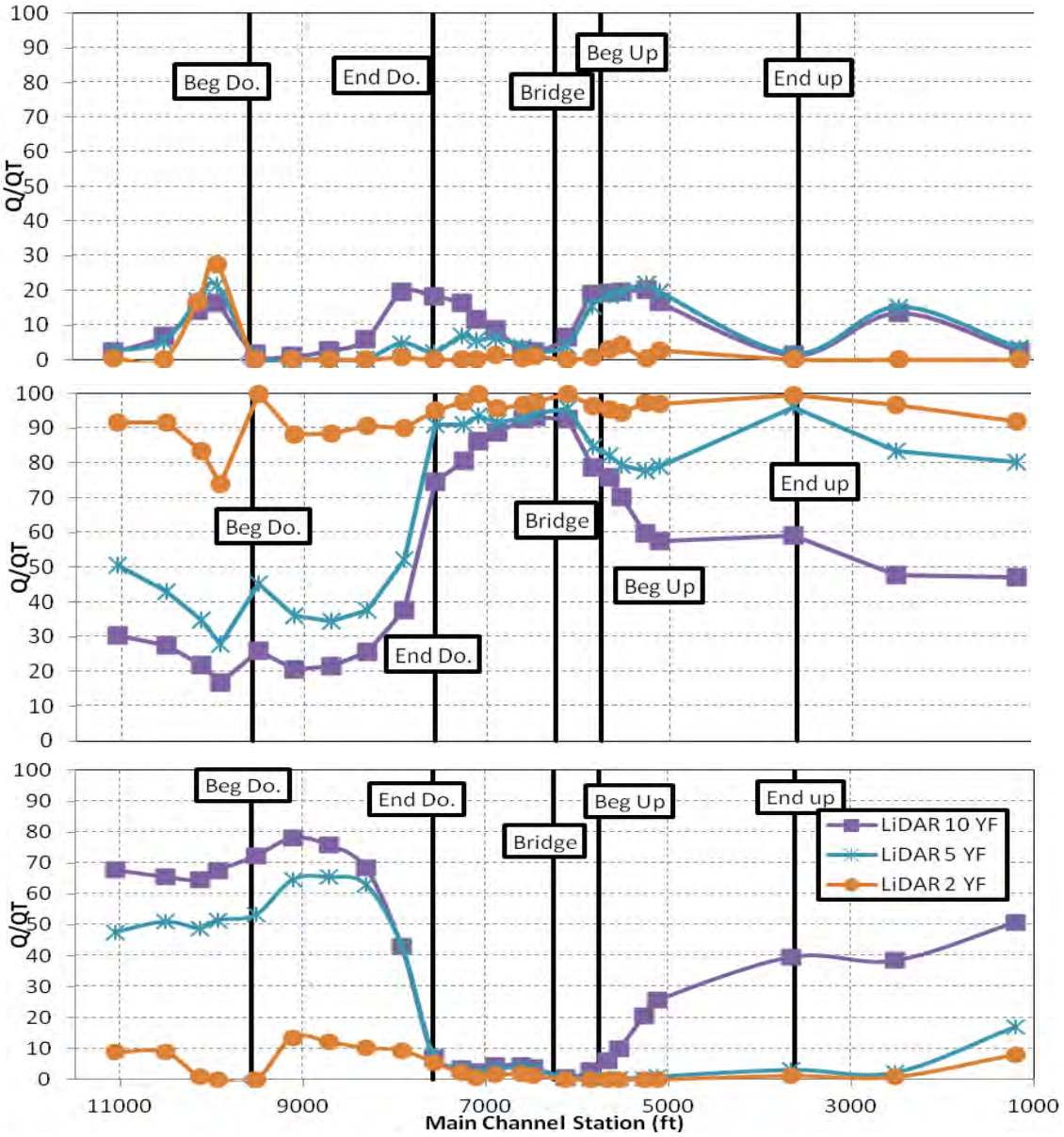

Figure 5.23 Partition of flow between the left floodplain (top plot), main channel (middle plot), and right floodplain (bottom plot) for 2-, 5- and 10-year peak flows

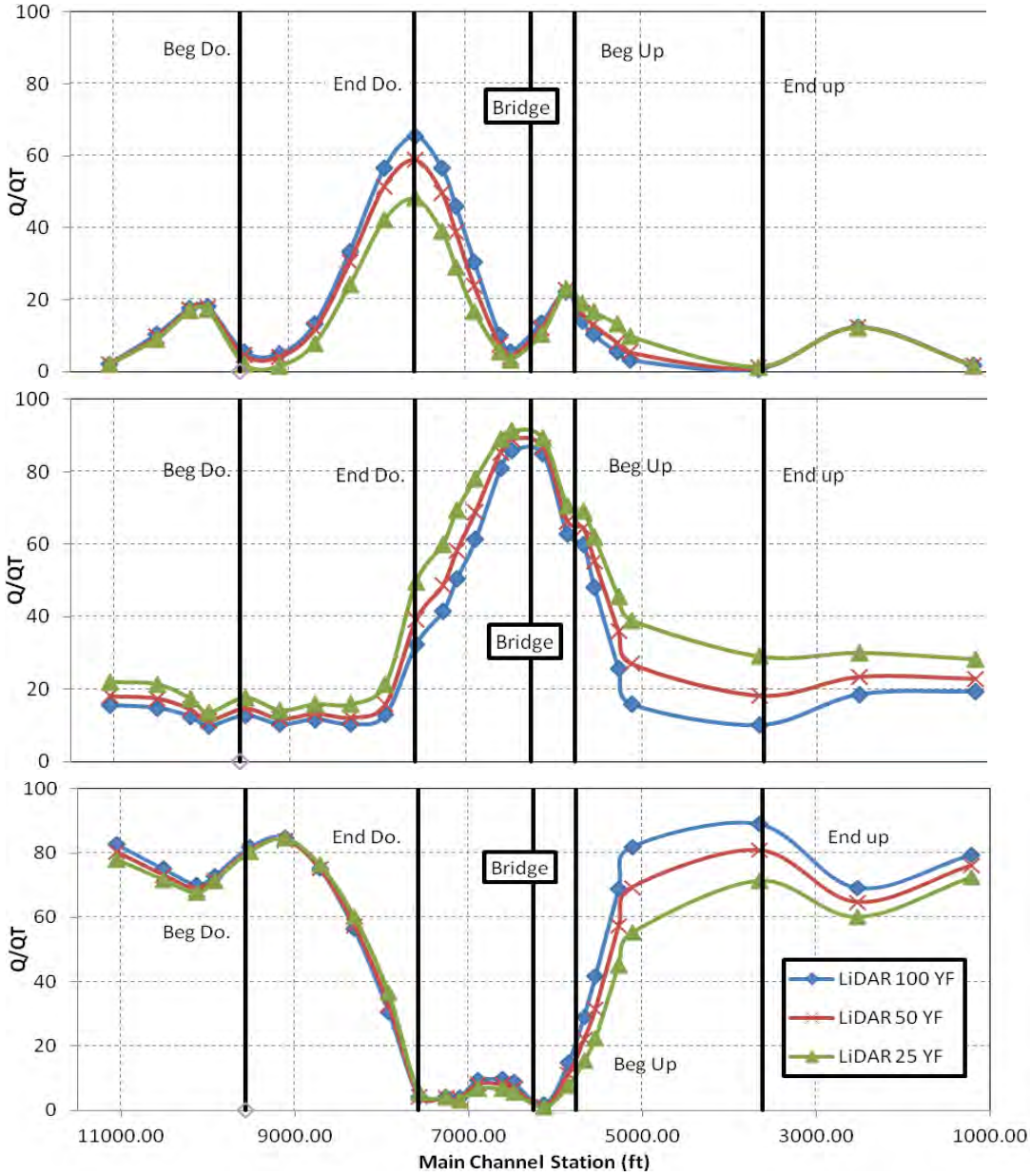

Figure 5.24 Partition of flow between the left floodplain (top plot), main channel (middle plot), and right floodplain (bottom plot) for 25-, 50- and 100-year peak flows

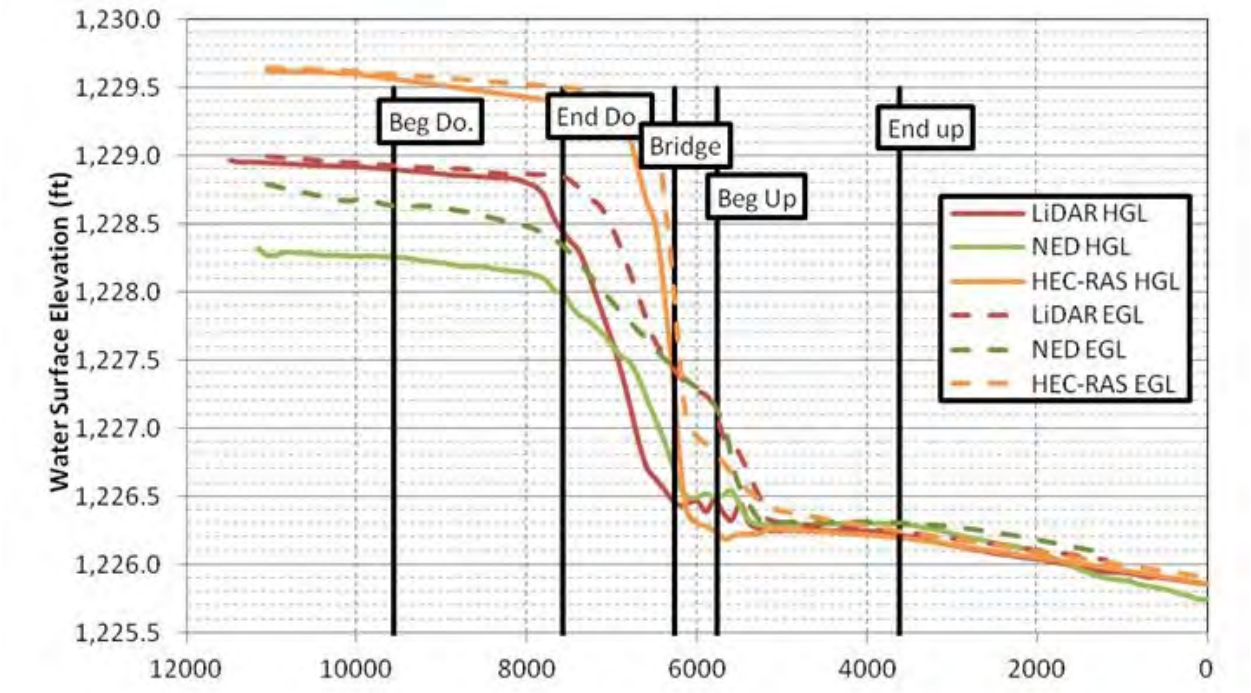

Figure 5.25 Computed hydraulic grade lines (HGL) and energy grade lines (EGL) for 100-year peak flow

5.6 Scour Analysis

Figure 5.26 shows the computed rating curves for unit discharge and average flow depth in the contracted section between the southbound and northbound bridge. The contracted section is taken to be the low-flow channel between the pier sets where flow velocities are highest. The rating curves are applied to a constant discharge of 27,100 ft.^{3}/s and the flood of March 2011 to predict contraction scour at the bridge crossing. Figure 5.27 shows the hydrograph recorded at 15-minute intervals at the Forestburg gaging station 4.5 miles upstream of the bridge site from March 19 to 31, 2011. The peak discharge (28,000 ft.^{3}/s) was measured on March 25, 2011. The measured discharge exceeded the 100-year peak flow for 42.5 hours and remained relatively steady during this time period. Table 5.1 summarizes the input parameters used in the scour calculations. Briaud et al. (2008) have produced curves of erosion rate versus shear stress for different soil classifications. The erodibility of soils varies significantly among soil types. Fine sand may have a critical shear stress of 0.1 to 0.2 N/m^2 and erosion rates greater than 100 mm/hr/(N/m^2); low plasticity clay may have a critical shear stress between 1 and 10 N/m^2 and erosion rates of 1 to 10 mm/hr/(N/m^2); while high plasticity clay may have a critical shear stress greater than 10 N/m^2 and erosion rates less than 1 mm/hr/(N/m^2). Based on our own results shown in Figure 5.12 and the charts published by Briaud et al. (2008), scour calculations were performed for three different τ_c values (2, 10, and 24 N/m^2) and three different C_1 values (0.1, 1, and 10 mm/hr/(N/m^2)) to examine the susceptibility of the bridge site to clear-water contraction scour. The results are plotted in Figures 5.28 to 5.30.

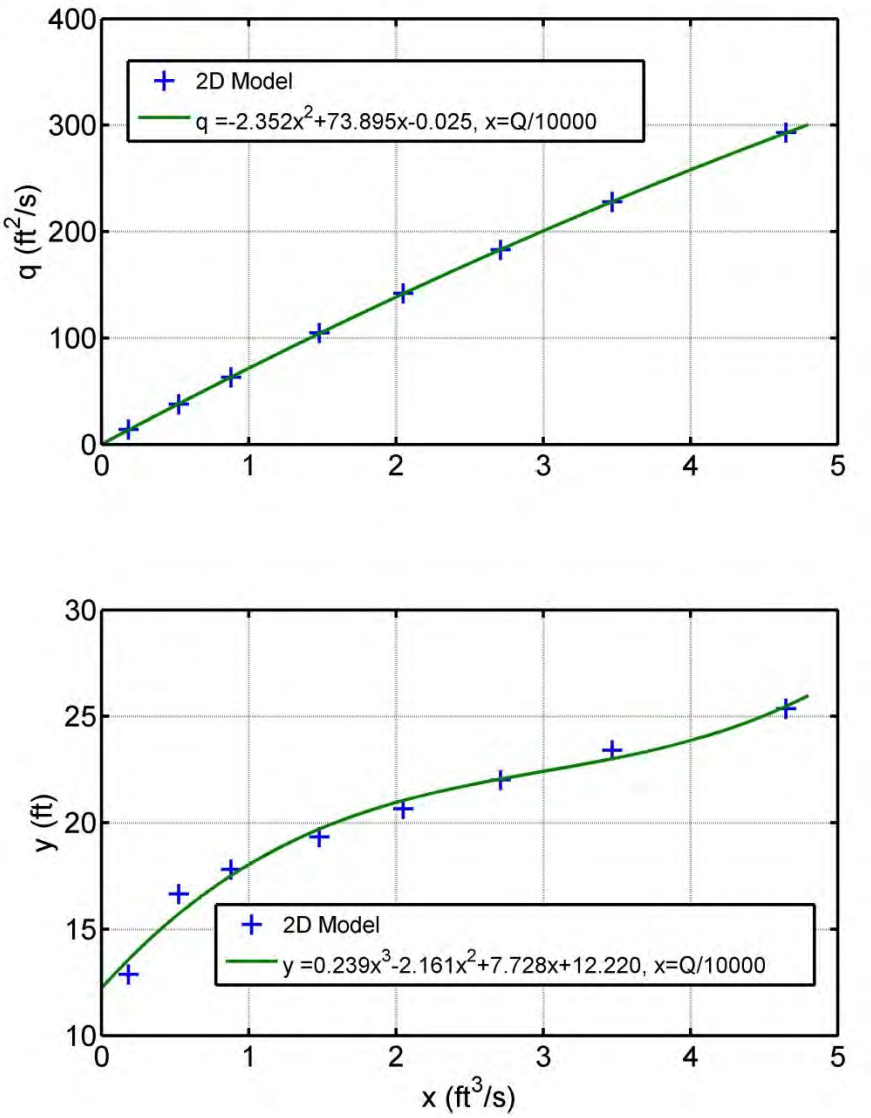

Figure 5.26 Rating curves for unit discharge (top plot) and water depth (bottom plot) in contracted section

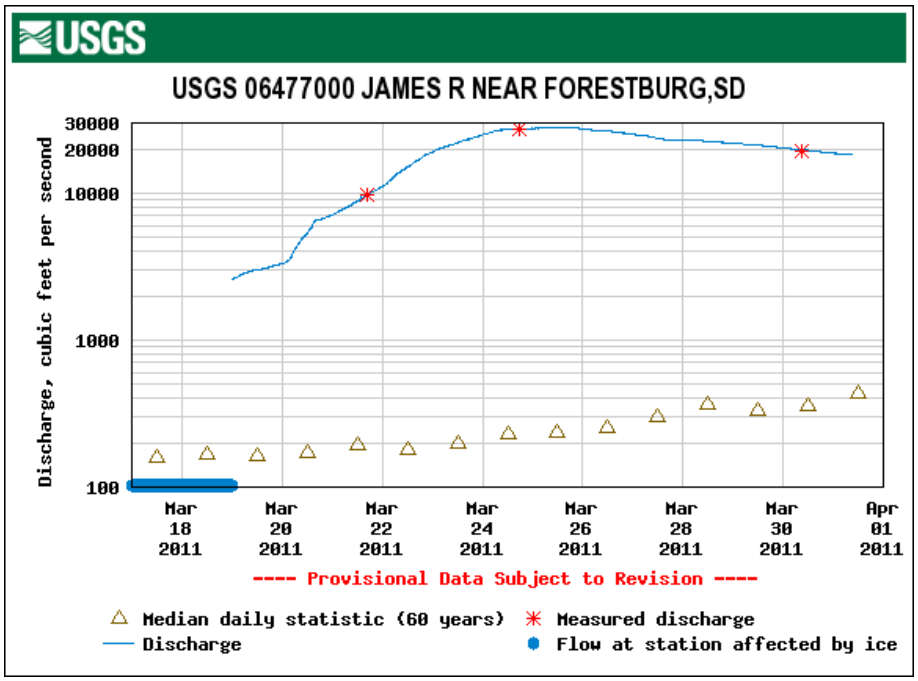

Figure 5.27 Recorded hydrograph for the flood of March 2011

Figure 5.28 shows the development of flow depth, bed shear stress, and scour depth with time over a period of two weeks for a constant discharge of 17,100 ft.^{3}/s. The results are summarized in Table 5.2. The equilibrium scour depths for τ_c = 2, 10, and 24 N/m^2 are 57.8, 18.0, and 5.5 ft., respectively. Note that the slope of the curve of erosion rate versus shear stress does not affect the equilibrium scour depth, only the time rate of scour. The computed final scour depth varies significantly with critical shear stress and soil erosion rate. For τ_c = 2 N/m^2, the final scour depths are 3.5, 17.3, and 44.2 ft. for C_1 = 0.1, 1, and 10 mm/hr/(N/m^2), respectively. For τ_c = 24 N/m^2, the final scour depths are 1.5, 5.1, and 5.5 ft., respectively. In particular, the computed final scour depth for C_1 = 0.1 mm/hr/(N/m^2) is much smaller than the equilibrium scour depth for all of the τ_c values. However, the equilibrium scour depth (5.5 ft.) is also small for τ_c = 24 N/m^2. The clear-water contraction scour equations in HEC-18 predict the equilibrium scour depth based on a single design flood. Figure 5.28 suggests that accounting for the time rate of scour would reduce the design scour depth significantly only if the critical shear stress and soil erosion rates are both small. Soils that fall into this category may include coarse sand, fine gravel, and low plasticity clay (Briaud et al. 2008).

Table 5.1 Input Parameters for Clear-Water Contraction Scour Calculations

Model input	Parameter value
Unit discharge q (ft^2/s)	183
Initial flow depth y_i (ft)	22
Manning's n	0.035
Fluid density ρ (kg/m^3)	998.2
Expansion loss coefficient C	0.5
Critical shear stress τ_c (N/m^2)	2, 10, 24
Erosion function slope C_1 (mm/hr/(N/m^2))	0.1, 1, 10
Time step Δt (hr)	0.25

Table 5.2 Computed Clear-Water Contraction Scour Depths at 3 and 14 days for Constant Discharge of 27,100 ft.^{3}/s

C_1 (mm/hr)/ (N/m^2)	τ_c = 2 N/m^2		τ_c = 10 N/m^2		τ_c = 24 N/m^2	
	3 days	14 days	3 days	14 days	3 days	14 days
0.1	0.9	3.5	0.7	2.8	0.4	1.5
1.0	6.4	17.3	5.0	12.1	2.6	5.1
10.0	25.2	44.2	15.6	18.0	5.5	5.5

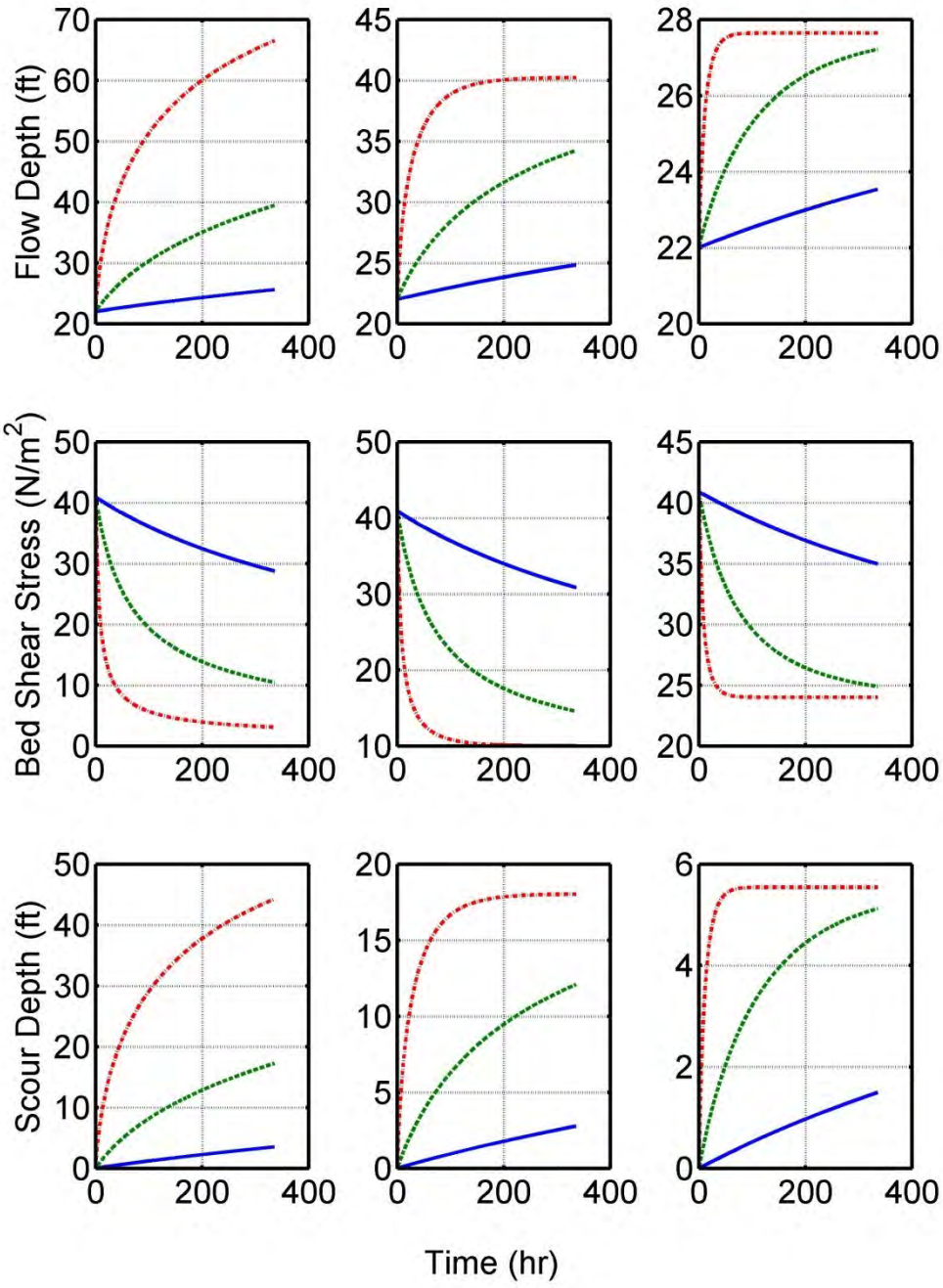

Figure 5.28 Simulation of clear-water contraction scour for a discharge of 27,100 ft.^{3}/s; critical shear stress (2 N/m^2 – left plot, 10 N/m^2 – middle plot, 24 N/m^2 – right plot); erosion rate (0.1 mm/hr/(N/m^2) – solid line, 1 mm/hr/(N/m^2) – dashed line and 10 mm/hr/(N/m^2) – dash dotted line)

The steady flow solution predicts that, for a constant discharge, flow depth will increase and bed shear stress will decrease as scour depth increases with time. In addition, bed shear stress will increase if the discharge is increased. The reality can be quite different, depending on the soil erodibility. The recorded hydrograph from a 100-year event (March 19 to April 1, 2011) at the Forestburg station 4.5 miles upstream of the bridge site was used to predict clear-water contraction scour. The results are presented in Figs. 5.29 (τ_c = 24 N/m^2) and 5.30 (τ_c = 2 N/m^2) for three different soil erosion rates [C_1 = 0.1, 1, and 10 mm/hr/(N/m^2)]. Comparing Figure 5.29 with the right plots in Figure 5.28 for C_1=10 mm/hr/(N/m^2), the maximum bed shear stress is much smaller for the unsteady flow. This is because the discharge increases gradually in the hydrograph and the flow does not reach the 100-year discharge until significant scour has already developed. Further increase in bed shear stress due to an increase in discharge is reduced by the large flow depth in the contraction due to scouring. In this case, the scour depth in the contraction increases so rapidly that bed shear stress starts to decrease before the peak flow arrives, although it is still greater than the critical shear stress for the scour depth to continue to increase. For C_1= 10 mm/hr/(N/m^2), the soil erosion rate is so high that the maximum scour depth is reached at about the same time as the peak discharge. The maximum scour depth produced by the flood is 5.6 ft., which is about the same as the equilibrium scour depth (5.5 ft.) for the 100-year peak flow. Both flow depth and scour depth increase more slowly as soil erosion rate decreases. For C_1 = 1 mm/hr/(N/m^2), a higher maximum bed shear stress of 37.2 N/m^2 is developed in the contraction. The scour depth continues to increase for about another 48 hours after the peak discharge before reaching a final scour depth of 2.8 ft. For C_1 = 0.1 mm/hr/(N/m^2), the scour depth increases so slowly that the changes in flow depth and bed shear stress are determined primarily by the discharge. Scouring continues for a long time after the peak discharge. The final scour depth is 0.54 ft., which is much less than the equilibrium scour depth of 5.5 ft. for the 100-year peak flow.

Figure 5.30 shows the computed results for τ_c = 2 N/m^2. Critical shear stress has a significant effect on equilibrium scour depth. Reducing the critical shear stress from 24 to 2 N/m^2 increases the equilibrium scour depth from 5.5 to 57.8 ft. for the 100-year peak flow. However, the time to reach equilibrium scour depth also increases. The computed final scour depth for C_1 = 0.1, 1 and 10 mm/hr/(N/m^2) are 2.2, 12.3, and 34.1 ft., respectively. In the first two cases, several large floods would be required to generate the equilibrium condition, and using the equilibrium scour depth as the design scour depth may be overly conservative.

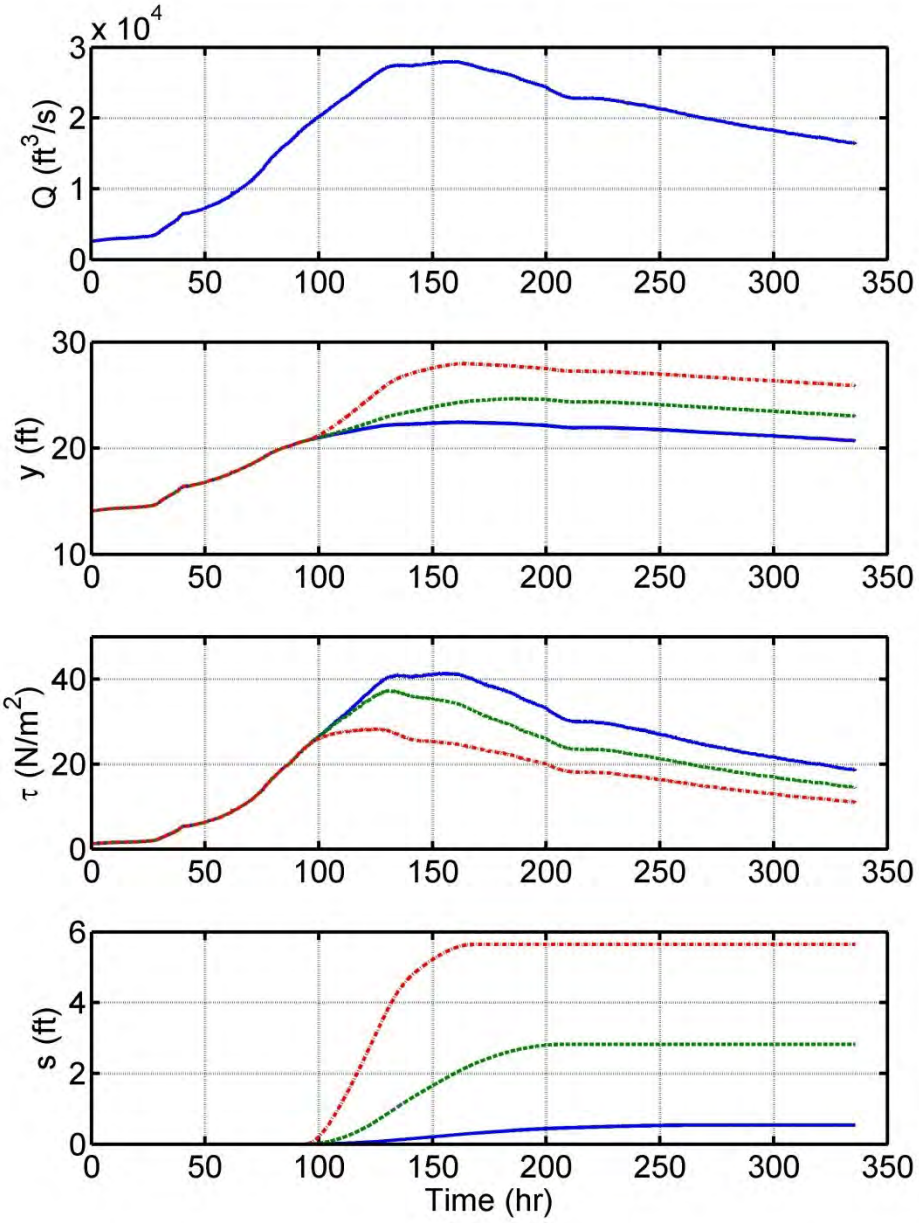

Figure 5.29 Simulation of clear-water contraction scour, March 19 to April 1, 2011; critical shear stress, 24 N/m^2; erosion rate, 0.1 mm/hr/(N/m^2) – solid line, 1 mm/hr/(N/m^2) – dashed line and 10 mm/hr/(N/m^2) – dash dotted line

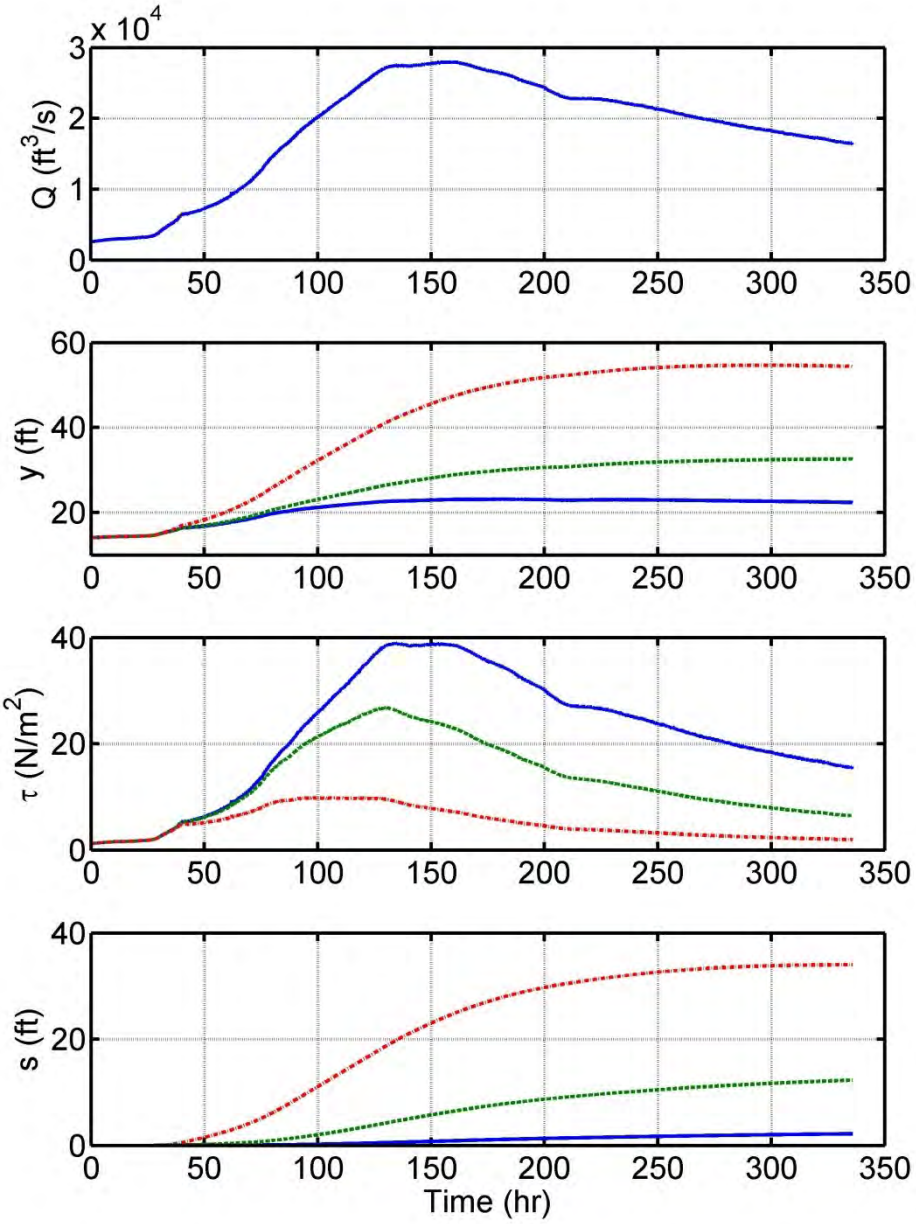

Figure 5.30 Simulation of clear-water contraction scour, March 19 to April 1, 2011; critical shear stress, 2 N/m^2; erosion rate, 0.1 mm/hr/(N/m^2) – solid line, 1 mm/hr/(N/m^2) – dashed line and 10 mm/hr/(N/m^2) – dash dotted line

The bridge site was also evaluated for live-bed contraction scour using Eqs. (2.3) and (2.4). The input parameters are given in Table 5.3. Because the width of the contracted section and upstream section are about the same, the live-bed contraction scour estimates depend primarily on the flow ratio Q_2 / Q_1. As before, the contracted section (Section 2) is taken to be the low-flow channel between the two pier sets. As for the approach section (Section 1), Figure 5.24 shows that the flow normally carried by the main channel is about 20%. The roadway embankment forces left the floodplain flow back into the main channel between the upstream bend and bridge crossing. Taking the un-contracted section in the meandering loop upstream (Case 1), Eqs. (2.3) and (2.4) yield a live-bed contraction scour depth of 35.5 ft. However, the average velocity in the main channel in the meander loop is only 2.6 ft./s and the

corresponding bed shear stress from Eq. (5.2) is 4.3 N/m^2. If the mildly cohesive clayey silt found in the main channel at the bridge crossing is representative of the bed material upstream, Figire 5.12 indicates that the bed shear stress in the meander loop would be below the critical shear stress and, consequently, live-bed scour would not occur. If Section 1 is located at transect 18 (see Figure 5.13) after the upstream bend (Case 2), the predicted live-bed contraction scour depth will be 8.5 ft. This location is more representative of the portion of the channel in which live-bed transport would be expected.

Table 5.3 Input Parameters for Live-Bed Contraction Scour Calculations

Parameters	Case 1	Case 2
Q_1 (ft^3/s)	5420	11,503
W_1 (ft)	114	111
y_1 (ft)	18.3	19
Q_2 (ft^3/s)	18,259	18,259
W_2 (ft)	98	98
y_0 (ft)	22	22
k_1	0.69	0.69

5.7 Concluding Remarks

A 2D flow model of the SD 37 bridges over the James River near Mitchell, South Dakota, was created using the numerical model FESWMS. Computed velocity distributions were compared with field measurements collected at the bridge site by the USGS during three high-flow events with return period ranging from 25 to 100 years. A 1D flow model was also created in HEC-RAS for comparison. The 2D model produced results that matched the measured data much better than the 1D model. The 1D model failed to predict the concentrated flows on the right side of the main channel both upstream of the bridge crossings and around the downstream bend, while the 2D model estimated the velocity distributions correctly. In addition, assignment of ineffective flow areas was ambiguous for the 1D model due to the skewed bridges and meandering channel. Ineffective flow areas in the 1D model were defined based on the flow patterns predicted by the 2D model.

The topographic data used for creating the 1D and 2D models were acquired using a LiDAR system and have a vertical resolution of 1 ft. The Existing National Elevation Dataset (NED) has a vertical resolution of approximately 10 ft. A 2D flow model of the bridge site was also created using 1/3 arc-second NED data. When the two datasets were compared, the NED data showed a deeper main channel (2 to 7 ft.) and higher floodplain elevations (about 2 ft.) compared with the LiDAR data, but closer to the bridges the differences are not as large. Nevertheless, the NED 2D model was able to predict the location of maximum velocity in the approach flow correctly, although it under-estimated the velocity magnitude by 0.5 to 1 ft./s for all the flood events. The agreements with flow measurements were also better for the NED 2D model than the HEC-RAS model. These results suggest that at this bridge site, alignment of the floodplain relative to the main channel and skewed bridges have more effects on the hydraulic conditions than the uncertainties in floodplain and channel elevations.

Numerical simulations were conducted for a wide range of discharges and Manning's *n* values to examine the site characteristics influencing the concentrated channel flow upstream of the bridges. It was found that flow discharge and the presence of dense trees along the left bank have a significant effect on the velocity distribution in the main channel. The location of maximum velocity shifts progressively toward the right bank as the discharge is increased, which suggests that the momentum of the flow entering from the left floodplain is an important factor. When the dense trees are removed, more flow remains in the left floodplain until close to the bridge crossings. The flow velocity decreases on the right side of the main channel but increases on the left side; consequently, the velocity distribution becomes more uniform.

For the SD 37 bridges, a 2D flow model provides substantial improvements in hydraulic analysis. The results can be used with the equations in HEC-18 or employed with more advanced methodologies to predict scour. In the case of live-bed scour, the 2D model provided more reliable estimates of discharge in the upstream main channel and in the contracted channel. The clear-water scour equations in HEC-18 only predict the equilibrium scour depth. For cohesive soils, the final scour depth can be much smaller than the equilibrium depth. Briaud et al. (2005) developed the Scour Rate in Cohesive Soils (SRICOS) method for contraction scour. The equations in SRICOS were developed based on flume tests in a rectangular channel, which are difficult to apply to a complex site like the SD 37 bridges. Instead, the more general energy method developed by Güven et al. (2002) was modified to predict clear-water scour for a 100-year event using rating curves of average unit discharge and flow depth derived from the 2D flow model. The predicted final scour depth was very sensitive to the critical shear stress and slope of the curve of erosion rate versus shear stress. When τ_c and C_1 values comparable to those of a high plasticity clay were used for scour prediction, the results were consistent with the contraction scour depth (1 to 2 ft.) observed at the bridge site. The analysis highlights the importance of accurately determining the critical shear stress and erosion rate constant of the foundation soils.

In a recent study, Harris (2005) used modeling results from FESWMS to calculate the 2D distribution of scour at the Choctawhatchee River Bridge near Newton, Alabama. The scour calculations were conducted for different lengths of time for a constant discharge. At each time step, the bed shear stress was calculated at each node of a 2D mesh and used with the results of EFA tests to determine the local rate of scour. The three-dimensional (3D) channel bathymetry was then updated to incorporate the changes due to scouring, and the 2D flow model was run again to produce a new bed elevation. In our analysis, the hydraulic results were derived from a 2D flow model with a fixed bed and then applied to a 1D scour model. The effect of pre-existing scour on flow depth was estimated by assuming the total head downstream of the contracted section to remain constant (for sub-critical flow) during the development of scour in the contracted section. This method is simple to apply, and further study to verify the method is warranted.

6. FINDINGS AND CONCLUSIONS

6.1 Literature Review/Telephone Survey

The final report for NCHRP Project 24-24 (*Criteria for Selecting Hydraulic Models*; Gosselin et al. 2006) provides a list of the most commonly used 1D and 2D numerical models for hydraulic analysis of bridge waterways. The report identifies the site characteristics that would create 2D flow conditions at a bridge site. Results of numerical simulations from 1D and 2D models are presented for a wide range of idealized site conditions. This information can be used in conjunction with the decision matrix they developed (see Table 2.1) to guide the engineer in selecting hydraulic models.

The final report for NCHRP project 24-14 (*Scour at Contracted Bridges*; Wagner et al. 2006) identifies the hydraulic and geomorphic factors affecting scour magnitude at contracted bridges. The report documented field data collected at 15 bridge sites that can be used for additional flow and scour analysis using physical and/or numerical models. The report discusses the difficulties of applying experimental results that were obtained under simplified conditions in the laboratory to the field situations. The report also emphasizes the importance of using case studies to understand the effects of site characteristics on bridge hydraulics.

A questionnaire on the state of the practice for hydraulic analysis of bridge waterways was sent to bridge engineers at 15 state DOT offices. Nine responded and were interviewed by the principal investigator over the phone. None of the state engineers interviewed had a formal decision-making process for whether to use 1D or 2D flow models. The decision to use 2D models is made on a case-by-case basis, and is driven typically by needs and time frame rather than costs. One interviewee commented that 2D flow models should be used anytime when flow velocity and direction cannot be reliably estimated, and the environmental conditions are severe and the structure so expensive that reliable results are critical. The 2D models reported being used include FESWMS, RMA2, ADCIRC, TUFLOW, and SRH-2D. Modeling results have been used to compute backwater effects, flow velocity magnitude, and flow angle of attack for prediction of scour, to assess bank shear stresses to determine the potential of stream bank migration, model overland flooding, and others. Human resources, training and technical support, lack of field data for model calibration, and needs for detailed bathymetric and topographic data were cited as the major barriers for using 2D models. Iowa DOT recommended using LiDAR data to produce high resolution contour maps for the floodplain to reduce the effort invested in field surveying on the ground.

Some interviewees commented that for an experienced modeler, 2D flow model does not take significantly more time to create than 1D model. There were consensuses from those who have used 2D models that training and motivation of the modeler and support from management are key factors in determining whether 2D flow models are used regularly in a design office. All the state DOTs interviewed have a good understanding of the situations in which 2D flow effects may be important. Some common 2D flow situations that are also encountered at the two bridge sites in our case studies are:

- Embankment skew (SD 37 bridges)
- Bridge crossing on river bend (SD 13 Bridge)
- Severely contracted bridge openings (SD 37 bridges)
- Change in position of thalweg in vicinity of bridge (SD 13 Bridge)
- Highly meandering channels (SD 13 and SD 37 bridges)
- Asymmetric floodplains/encroachments (SD 13 and SD 37 bridges)
- Situations in which it is difficult to define the ineffective flow areas (SD 13 and SD 37 bridges)

6.2 Hydraulic and Scour Analysis, SD 13 Bridge Over Big Sioux River Near Flandreau, South Dakota

This site was selected to conduct a 2D flow analysis because of the 8.5-ft.-deep pier scour hole observed at the northern-most pier during the floods of 1993 and the failure of HEC-RAS to predict the concentrated channel flow adjacent to the right abutment. Detailed conclusions from the case study are given in Section 4.7. In this summary, we focus on those findings related to the selection of hydraulic models and prediction of scour. The hydraulic analysis showed that change in the thalweg position near the bridge and the bridge crossing being located at a river bend are the two main factors that produced the observed flow concentration at the northern-most pier. Modeling results also showed that the flow magnitude increases while the approach flow angle of attack decreases as the discharge increases due to more floodplain flow returning to the main channel just upstream of the bridge crossing. Thus, channel bathymetry and floodplain alignment relative to the bridge and channel combine to produce the unique hydraulic conditions at the SD 13 Bridge. The resulting flow pattern is inherently 2D and cannot be accurately predicted using a 1D model. An experienced hydraulic engineer should be able to recognize these characteristics after studying an aerial photograph of the bridge site along with the results of bathymetric and topographic survey. However, predicting the velocity distribution at the bridge is far more difficult. Because the flow magnitude and flow angle of attack change with stage, a 1D model that is calibrated to work for one flow condition would not work for other flow conditions. It will be necessary to evaluate the potential pier scour over the possible range of stages to determine the worst-case scenario, and because of the potential for thalweg migration it would be prudent to apply the worst-case pier scour estimate to all the piers within the main channel.

The pier scour equations in HEC-18 generally over-predict scour, sometimes significantly. There are at least two reasons for this. First, the equations are envelope curves for use in design rather than best-fit lines to experimental data. Second, the equations do not account for the slower rate of scour in cohesive soils. Thus, using more accurate hydraulic inputs does not necessarily improve scour predictions. In fact, the predictions would be even more conservative (higher) if larger flow velocity magnitude and/or flow angle of attack are computed by the 2D model, even though the results from the 2D model may be more accurate. The benefits of using a 2D flow model in bridge design become apparent only when it is used in conjunction with more accurate methodologies for scour prediction. For example, this study found that the predicted pier scour depth was very sensitive to the value of the soil critical shear stress.

A sensitivity analysis showed that the density of topographic data in the floodplain can be reduced considerably without significantly affecting the results of the 2D model. However, up-to-date bathymetric data, especially in the vicinity of the bridge, are crucial because the position of the thalweg is important for determining the velocity distribution at the bridge. The flow measurements at the SD 13 Bridge were conducted in 1993. The 2D model was created using bathymetric data collected in 2009. Changes in the channel cross sections at the bridge site between 1993 and 2009 might have contributed to the observed differences between the computed and measured flow velocities at the bridge. In addition, detailed flow data were lacking at the bridge site to vigorously validate a 2D model for predicting compound channel flow for meandering streams.

6.3 Hydraulic and Scour Analysis, SD 37 Bridges Over James River Near Mitchell, South Dakota

This site is ideal for testing 2D river model and studying the site characteristics that produce complex hydraulic conditions in a compound channel. The USGS has measured flow velocities and bed elevations in the main channel by using an ADCP during a 25-year event in 2001. The measurements covered a large area through the bridge opening and extending upstream and downstream of the northbound bridge.

Furthermore, bathymetry data for the main channel and high resolution LiDAR data for the floodplains are available from the same time period. A 2D flow model created using the LiDAR data reproduced all the main features in the flow measurements, including the concentrated flows on the right side of the channel between the upstream bend and bridge crossing and along the downstream meander loop. The observed concentrated flows were not predicted by HEC-RAS. Furthermore, numerical results from the 2D model provided insights into the effect of channel meandering, geomorphic setting of the river valley, floodplain alignment, and floodplain vegetation on the flow distribution and flow exchange between the main channel and floodplain. Although these hydraulic and geomorphic factors may not be fully understood by the engineer before conducting the flow analysis, the complex site geometries and severity of flow contraction at the bridge crossings should have suggested a 2D flow model for this site. Moreover, ineffective flow areas in a 1D model will be extremely difficult to define for the skewed bridges and meandering channel.

Due to the severity of flow contraction at the SD 37 bridges, the site has a large potential for scour. However, the observed scour depths produced by the flood of March 2011, which was a 100-year event, were small. The benefits of the 2D model become apparent in predicting live-bed contraction scour where the results are very sensitive to the discharge ratio in the upstream un-contracted section and the contracted section at the bridge crossing. The 1D model apportioned more flow to the floodplains in the approach flow and, consequently, significantly over-predicted the live-bed contraction scour depth. The 2D model provided more accurate information on the partition of flow between the main channel and floodplains along the meander. Away from the bridge crossings, the main channel normally carries about 20% of the total flow during a 100-year event. However, the 2D model indicated that bed shear stress in the upstream meander loop would be below the critical shear stress. Consequently, live-bed scour would not occur. Live-bed conditions would develop in the main channel after the upstream meander loop, but the discharge ratio is much closer to unity, thus significantly reducing the predicted scour depth. The 2D model also provided more accurate information on flow velocity and flow depth in the contracted section. When this information was used with the results of soil erodibility tests to predict clear-water contraction scour, the results showed that by taking into account the very slow rate of scour of the high plasticity clay, the predicted final scour depth for a 100-year event was only a few feet, which is many times smaller than the equilibrium scour depth. The latter would have grossly over-estimated the potential for contraction scour at this bridge site.

6.4 Two-Dimensional Model Construction

The 2D models for the case studies were created in SMS using the depth-averaged model FESWMS. SMS is a comprehensive graphical user environment for 1D and 2D surface water model construction. SMS provides the pre- and post-processing tools for importing and manipulating topographic and bathymetric data, grid generation, and visualization of results. The step-by-step procedure for constructing a 2D flow model in SMS for the two bridge sites studied is described in Larson (2010) and Rossell (2012). SMS provides an applications guide that demonstrates various aspects of the software. However, in a real-life situation, individual case is not always so straightforward. Larson (2010) and Rossell (2011) carefully documented the procedures they used and the modeling issues they encountered in creating a working model. These two documents should be consulted by new users who want to create an effective 2D river model in SMS.

The basic procedure for creating a 2D flow model in SMS consists of the following major steps. First, an aerial photograph of the study area and the topographic and bathymetric data are imported into SMS. Then, feature arcs are drawn on the background image to create an outline of the main channel and floodplain. Different material regions are then delineated and material properties are assigned to the individual domains. Next, a computational mesh is generated from the conceptual model and ground elevations are interpolated to the mesh. The final step before running the model is to assign values to

specific model parameters and to define the inflow and outflow boundary conditions. In Larson (2010), the following tools in SMS are demonstrated for the SD 13 Bridge:

- Selecting coordinate system and numerical model
- Creating and importing a geo-referenced background image
- Importing survey data
- Creating feature arcs and feature points to fill gaps in sparse data
- Using hydraulic bridges at the upstream and downstream boundaries
- Creating polygons and specifying material types
- Creating and refining 2D mesh
- Defining boundary conditions
- Inserting a weir structure
- Defining model parameters
- Running a model from a coldstart and using hotstart and spindown to revise the solution to satisfy the final flow boundary conditions. In a coldstart simulation, the flow velocities are zero and the water surface elevation is constant. The solution obtained is used to perform a hotstart, typically with incremental changes in the boundary conditions that are closer to the desired boundary conditions. Spindown is the series of "Runs" that generates solutions progressively closer to the desired answer.
- Creating observation arcs and observation points for plotting and comparison of modeling results with field measurements

Rossell (2012) discussed the following additional issues encountered in creating a 2D flow model for the SD 37 bridges:

- Using feature arcs and patch type mesh to create a uniform mesh in the main channel
- Minimizing problems with wetting and drying along the water edge in areas of high elevation gradients such as the roadway embankment and valley walls
- Using refine points to create larger, more uniform mesh elements in the overbank areas to reduce computation time and errors
- Creating roadway embankment using a scatter data set
- Inserting bridge piers into a 2D model
- Identifying and turning off unstable model elements during computation

7. IMPLEMETATION RECOMMENDATIONS

The findings of this research project may be used to improve hydraulic analysis of compound channel flows around highway structures. It is anticipated that only a small number of structures in South Dakota would require a 2D flow analysis. Additional surveys to collect bathymetry and topography data on structures requiring 2D flow analysis would be required, as well as flow measurements to validate the model. Training of design engineers in 2D flow modeling would also be required. SDDOT also needs to identify the design criteria for which the results of 2D flow analysis will be used for. The implementation recommendations presented below outline the tasks that will need to be accomplished by SDDOT in order to successfully use 2D flow models in hydraulic analysis and evaluating scour at bridges.

1. DEVELOP A FORMAL DECISION PROCESS FOR SELECTING HYDRAULIC MODELS

It is recommended that SDDOT develop a formal decision process for selecting 1D or 2D flow model for hydraulic analysis. The decision matrix in Gosselin et al. (2006) can be customized to meet the specific needs in South Dakota. The matrix would establish criteria involving site conditions (e.g., river bends, asymmetric floodplains), design considerations (e.g., evaluation of scour, ice loading) and other project related considerations (e.g., time constraints, data availability); assign weights to each of the decision criteria; and score the two alternatives (1D or 2D model) for each of the decision criteria. An example of application of the decision matrix can be found in Gosselin et al. (2006) for a bridge replacement project.

2. COORDINATE WITH OTHER AGENCIES IN THE STATE TO COLLECT LIDAR DATA FOR SOUTH DAKOTA

Lack of bathymetry and topography data was cited as one of the barriers in using a 2D flow model. NED data are available from the USGS. The data sets are of coarse resolution and may contain out-of-date information, so they should be carefully checked before being used for creating a hydraulic model. High-resolution LiDAR data should be used wherever available to reduce the effort invested in field surveying on the ground. LiDAR data have been acquired for the James River basin and part of eastern South Dakota. It is recommended that SDDOT coordinates with other agencies in the state to collect LiDAR data for the entire state and ensure that the data are processed and made available to the users in a timely manner.

3. CONDUCT TRAINING WORKSHOPS ON BRIDGE HYDRAULICS, HYDRAULIC MODELING, BRIDGE SCOUR, AND OTHER DESIGN TOOLS

Modeler experience was cited as one of the barriers in using 2D flow models. Training courses on SMS and other hydraulic models are regularly offered by vendors and professional organizations. Attending a training course will be the first step in learning these design tools. It is recommended that SDDOT establishes a continuing education program for engineers. The program may include in-house training (e.g., brown-bag lunch events), custom on-site training (e.g., NHI courses), off-site continuing education training (e.g., ASCE continuing education courses), and online education. To successfully implement a training program, training goals should be set to meet identified needs.

4. CONDUCT ADDITIONAL CASE STUDIES TO PROVIDE THE KNOWLEDGE BASE FOR DEVELOPMENT OF IMPROVED DESIGN GUIDELINES

The decision matrix for selecting 1D or 2D models requires the engineer to identify the site conditions in which a 2D flow model may produce substantial improvements in hydraulic analysis compared with a 1D model. Gosselin et al. (2006) have compared modeling results from 1D and 2D models for a wide range of idealized site conditions. Although the study has provided useful guidelines to the engineer, the geometries used in their test cases are highly simplified compared with the field conditions at most bridge sites. The effects of many site characteristics on bridge hydraulics are still not well understood. It is recommended that SDDOT conducts additional case studies that would combine detailed field data with 2D flow modeling to establish the knowledge base for hydraulic analysis of bridge waterways. The case studies can be conducted in conjunction with personnel training. An important criterion for selecting study sites will be the availability of flow data for validating a 2D model.

Other important factors in the decision process for selecting hydraulic models are the improvements that would be achieved in the final design if a 2D flow model is used for hydraulic analysis instead of a 1D model. Using a more advanced hydraulic model by itself does not necessarily improve design and/or reduce costs. In evaluating scour at bridges, for example, the uncertainty in scour analysis often outweighs the uncertainty in the hydraulic analysis, therefore design requirements (e.g., scour calculations, stream stabilization) is an important factor in selecting hydraulic models. Implementation of the following recommendations would improve the results of scour analysis:

1. MEASURE SOIL ERODIBILITY WHEN EVALUATING SCOUR AT BRIDGES

Accounting for the time rate of scour may significantly reduce the design scour depth for bridge sites with extremely erosion-resistant cohesive materials. In future design of bridge foundations, it is recommended that SDDOT collects thin wall tube samples at the foundation level during subsurface exploration and tests the samples to determine the soil erodibility. For extremely erosion resistant bed materials, the measured soil erosion function should be used to obtain realistic estimates of scour depth, thus eliminating the need to apply an empirical reduction factor to the scour predictions obtained using current methods developed for non-cohesive soils. SDDOT may consider collecting thin wall tube samples in different soil types across South Dakota and testing the samples to develop generalized relationships for erosion rate of cohesive soils.

2. COLLECT FLOW AND SCOUR DATA AT SELECTED BRIDGE SITES IN SOUTH DAKOTA

It is recommended that SDDOT initiates a research project to collect flow and scour data at selected bridge sites during high flow events. The measured data can be used for additional case studies or to conduct a general assessment of methods for evaluating scour at bridges. An assessment of published scour-prediction equations was last conducted in South Dakota by Niehus (1996) using real-time scour measurements collected at selected bridge sites during the flooding events in 1991 to 1993. The current state of practice has advanced substantially since the early 1990s, in light of the completion of several recent NCHRP projects, including *Project 24-15(2) Abutment Scour in Cohesive Materials* (Briaud et al. 2009), *Project 24-27(01) Evaluation of Bridge Scour Research: Pier Scour Processes and Predictions* (Ettema et al. 2011), *Project 24-27(02) Evaluation of Bridge-Scour Research: Abutment and Contraction Scour Processes and Prediction* (Sturm et al. 2011), *Project 24-27(03) Evaluation of Bridge Scour Research: Geomorphic Processes and Prediction* (Zevenbergen et al. 2011), and the recent revision of HEC-18 (Arneson et al. 2012) and HEC-20 (Lagasse et al. 2012).

3. CONDUCT RESEARCH TO UNDERSTAND THE TIME EFFECT OF SCOUR AND SIMULATION OF DESIGN FLOOD(S) FOR EVALUATING SCOUR AT BRIDGES

The new edition of HEC-18 (Arneson et al. 2012) provides alternative methods to evaluate bridge scour in cohesive soils. The new methods take into account the time rate of scour but will require the input of a constructed hydrograph. The effects of the temporal structure of floods and soil erodibility on scour depth are currently poorly understood. In particular, it is unclear whether determining a design scour depth will require the generation of long-term continuous hydrograph with its inherent high uncertainty, or if a series of design floods will suffice. It is recommended that SDDOT initiates a research project to investigate the estimation of hydrographs for use in long-term scour predictions. The research is also relevant for hydrologic design of highway structures in small watersheds, which often do not have adequate stream flow records.

REFERENCES

Annandale G. W. (2006). *Scour Technology, Mechanics and Engineering Practice*, McGraw Hill.

Arneson, L. A., Zevenbergen, L. W., Legasse, P. F., and Clopper, P. E. (2012). "Evaluating scour at bridges." Fifth Edition, Hydraulic Engineering Circular No. 18, Federal Highway Administration, Washington, D. C.

Briaud, J.-L. (2008). "Case histories in soil and rock erosion: Woodrow Wilson Bridge, Brazos River Meander, Normandy Cliffs, and New Orleans Levees." *Journal of Geotechnical and Geoenvironmental Engineering*, 134(10), 1425-1447.

Briaud, J.-L., Chen, H. C., Chang, K. A., Oh, S. J., and Chen. X. (2009). "Abutment scour in cohesive materials." *Final Report for NCHRP Project 24-15(2)*, Transportation Research Board, Washington, D. C.

Briaud, J.-L., Chen, H. C., Kwak, K. W., Han, S. W., and Ting, F. C. K. (2001a). "Multiflood and multilayer method for scour rate prediction at bridge piers." *J. Geotechnical and Geoenvionmental Engineering.*, ASCE, 127(2), 114-125.

Briaud, J.-L., Chen, H. C., Li, Y., and Nurtjahyo, P. (2004). "SRICOS-EFA method for complex piers in fine-grained soils." *J. Geotechnical and Geoenvironmenal Engineering*, ASCE, 130(11), 1180-1191.

Briaud, J.-L., Chen, H.-C., Li, Y., Nurtjahyo, P., and Wang, J. (2005). "SRICOS-EFA method for contraction scour in fine-grained soils." *Journal of Geotechnical and Geoenvironmental Engineering*, 131(10), 1283-1294.

Briaud, J.-L., Ting, F. C. K., Chen, H. C., Gudavalli, R., Perugu, S., and Wei, G. S. (1999). "SRICOS: Prediction of scour rate in cohesive soils at bridge piers." *J. Geotechnical and Geoenvionmental Engineering*, ASCE, 125(4), 237-246.

Briaud, J.-L., Ting, F. C. K., Chen, H. C., Cao, Y., Han, S. W., and Kwak, K. W. (2001b). "Erosion function apparatus for scour rate predictions." *J. Geotechnical and Geoenvironmental Engineering*, ASCE, 127(2), 105-113.

Ettema, R., Constantinescu, G., and Melville, B. (2011). "Evaluation of bridge scour research: pier scour processes and predictions." Final Report for NCHRP Project 24-27(01), Transportation Research Board, Washington D. C.

Ettema, R., Yoon, B., Nakato, T., and Muste, M. (2004). "A review of scour conditions and scour-estimation difficulties for bridge abutments." *KSCE Journal of Civil Engineering*, Korean Society of Civil Engineers, 8(6), 643-650.

FESWMS-2DH (2017). Finite-element surface-water modeling system for two-dimensional flow in the horizontal plane, US Geological Survey. https://water.usgs.gov/software/FESWMS-2DH/.

Gosselin, M., Sheppard, D. M., and McLemore, S. (2006). "Criteria for selecting hydraulic models." Final Report for NCHRP Project 24-24, Transportation Research Board, Washington, D. C.

Güven O., Melville, J. G., and Curry, J. E. (2002). "Analysis of clear-water scour at bridge contractions in cohesive soils." TRB Paper No. 02-2127, Transportation Research Record, National Research Council, Washington D. C.

Harris, D. T. (2005). "Numerical model evaluations of cumulative contraction scour at a bridge site with cohesive soils." M.S. thesis, Department of Civil Engineering, Auburn University, Auburn, Alabama.

HEC-RAS (2017). Hydrologic Engineering Center's River Analysis System, US Army Corps of Engineers. http://www.hec.usace.army.mil/software/hec-ras/.

Lagasse, P. F., Zevenbergen, L. W., Spitz, W. J., and Arneson, L. A. (2012). "Stream stability at highway structures." Fourth Edition, *Hydraulic Engineering Circular No. 20*, Federal Highway Administration, Washington, D. C.

Larsen, R. J. (2010). "Two-dimensional flow modeling of the Big Sioux River at the Highway 13 Bridge near Flandreau, South Dakota." M.S. thesis, Department of Civil and Environmental Engineering, South Dakota State University, Brookings, SD.

Larsen, R. J., Ting, F. C. K., and Jones, A. L. (2011). "Flow velocity and pier scour prediction in a compound channel: Big Sioux River Bridge at Flandreau, South Dakota." *Journal of Hydraulic Engineering*, 137(5), 595-605.

Munson, B. R., Young, D. F., Okiishi, T. H., and Huebsch, W. W. (2009). *Fundamentals of Fluid Mechanics*, Sixth Edition, John Wiley & Sons.

Niehus, C. A. (1996). "Scour assessments and sediment-transport simulation for selected bridge sites in South Dakota." USGS Water-Resources Investigations Report 96-4075.

Rossell, R. P. (2012). "Two-dimensional flow modeling of the James River at the State Route 37 bridge crossing north of Mitchell." M.S. thesis, Department of Civil and Environmental Engineering, South Dakota State University, Brookings, SD.

Sando, S. K., Driscoll, D. G., and Parrett, C. (2008). "Peak-flow frequency estimates based on data through water year 2001 for selected streamflow-gaging stations in South Dakota." *Scientific Investigations Report 2008-5104*, U.S. Geological Survey.

Sturm, T. W., Ettema, R., and Melville, B. W. (2011). "Evaluation of bridge-scour research: abutment and contraction scour processes and prediction." Final Report for NCHRP Project 24-27(02), Transportation Research Board, Washington D. C.

Sturm, T., Sotiropoulos, F., Landers, M., Gotvald, T., Lee, S., Ge, L., Navarro, R., and Escauriaza, C. (2004). "Laboratory and 3D numerical modeling with field monitoring of regional bridge scour in Georgia." Final Report for Georgia Department of Transportation Research Project No. 2002.

Ting, F. C. K., Briaud, J.-L, Chen, H. C., Gudavalli, R., Perugu, S., and Wei, G. S. (2001). "Flume tests for scour in clay at circular piers." *Journal of Hydraulic Engineering*, ASCE, 127(11), 969-978.

Ting, F. C. K., Jones, A. L., and Larsen, R. J. (2010). "Evaluation of SRICOS method on cohesive soils in South Dakota." MPC Report No. 08-195, Mountain-Plains Consortium, North Dakota State University, Fargo, ND.

Trammell, M. A. (2004). “Laboratory apparatus and methodology for determining water erosion rates of erodible rock and cohesive sediments.” M.S. thesis, University of Florida, Gainesville, Florida.

U.S. National Geodetic Survey (1986). *Geodetic glossary*, National Ocean Service, National Oceanic and Atmospheric Administration, Rockville, MD.

Wagner, C. R. (2007). “Simulation of water-surface elevations and velocity distributions at the U.S. Highway 13 Bridge over the Tar River at Greenville, North Carolina, using one- and two-dimensional steady-state hydraulic models.” Scientific Investigations Report 2007-5263, U.S. Geological Survey.

Wagner, C. R., Mueller, D. S., Parola, A. C., Hagerty, D. J., and Benedict, S. T. (2006). “Scour at contracted bridges.” Final Report for NCHRP Project 24-14, Transportation Research Board, Washington, D.C.

Zevenbergen, L. W., Thorne, C. R., Spitz, W. J., and Huang, X. (2011). “Evaluation of bridge scour research: geomorphic processes and predictions.” Final Report for NCHRP Project 24-27(03), Transportation Research Board, Washington, D. C.